AFRL-RY-WP-TR-2013-0188

LADAR AND OPTICAL COMMUNICATIONS INSTITUTE (LOCI)

Joseph W. Haus and Paul F. McManamon

University of Dayton

DECEMBER 2013
Final Report

AIR FORCE RESEARCH LABORATORY
SENSORS DIRECTORATE
WRIGHT-PATTERSON AIR FORCE BASE, OH 45433-7320
AIR FORCE MATERIEL COMMAND
UNITED STATES AIR FORCE

NOTICE AND SIGNATURE PAGE

Using Government drawings, specifications, or other data included in this document for any purpose other than Government procurement does not in any way obligate the U.S. Government. The fact that the Government formulated or supplied the drawings, specifications, or other data does not license the holder or any other person or corporation; or convey any rights or permission to manufacture, use, or sell any patented invention that may relate to them.

This report was cleared for public release by the USAF 88th Air Base Wing (88 ABW) Public Affairs Office and is available to the general public, including foreign nationals. Copies may be obtained from the Defense Technical Information Center (DTIC) (http://www.dtic.mil).

AFRL-RY-WP-TR-2013-0188 HAS BEEN REVIEWED AND IS APPROVED FOR PUBLICATION IN ACCORDANCE WITH ASSIGNED DISTRIBUTION STATEMENT.

//SIGNED//

TIMOTHY M. FINEGAN, Program Manager
LADAR Technology Branch
Multispectral Sensing and Detection Division

//SIGNED//

BRIAN D. EWERT, Chief
LADAR Technology Branch
Multispectral Sensing and Detection Division

//SIGNED//

TRACY W. JOHNSTON, Chief
Multispectral Sensing and Detection Division
Sensors Directorate

This report is published in the interest of scientific and technical information exchange, and its publication does not constitute the Government's approval or disapproval of its ideas or findings.

*Disseminated copies will show "//signature//" stamped or typed above the signature blocks.

REPORT DOCUMENTATION PAGE

Form Approved
OMB No. 0704-0188

1. REPORT DATE *(DD-MM-YY)*	2. REPORT TYPE	3. DATES COVERED *(From - To)*
December 2013	Final	3 October 2006 – 3 August 2013

4. TITLE AND SUBTITLE
LADAR AND OPTICAL COMMUNICATIONS INSTITUTE (LOCI)

5a. CONTRACT NUMBER
FA8650-06-2-1081

5b. GRANT NUMBER

5c. PROGRAM ELEMENT NUMBER
62204F

6. AUTHOR(S)
Joseph W. Haus and Paul F. McManamon

5d. PROJECT NUMBER
2003

5e. TASK NUMBER
11

5f. WORK UNIT NUMBER
Y05L

7. PERFORMING ORGANIZATION NAME(S) AND ADDRESS(ES)
University of Dayton
Electro-Optics Program
300 College Park
Dayton, OH 45469-2951

8. PERFORMING ORGANIZATION REPORT NUMBER

9. SPONSORING/MONITORING AGENCY NAME(S) AND ADDRESS(ES)
Air Force Research Laboratory
Sensors Directorate
Wright-Patterson Air Force Base, OH 45433-7320
Air Force Materiel Command
United States Air Force

10. SPONSORING/MONITORING AGENCY ACRONYM(S)
AFRL/RYMM

11. SPONSORING/MONITORING AGENCY REPORT NUMBER(S)
AFRL-RY-WP-TR-2013-0188

12. DISTRIBUTION/AVAILABILITY STATEMENT
Approved for public release; distribution unlimited.

13. SUPPLEMENTARY NOTES
PAO Case Number 88ABW-2013-5098, Clearance Date 3 December 2013. Report contains color. This material is based on research sponsored by Air Force Research Laboratory under agreement FA8650-06-2-1081. The U.S. Government is authorized to reproduce and distribute reprints for Governmental purposes notwithstanding any copyright notation thereon. The views and conclusions contained herein are those of the authors and should not be interpreted as necessarily representing the official policies or endorsements, either expressed or implied, of Air Force Research Laboratory or the U.S. Government.

14. ABSTRACT
This report is an assessment of the accomplishments on AFRL projects and student trainings activities for the LADAR and Optical Communications Institute (LOCI) cooperative agreement. The report covers the activities and accomplishments of LOCI over the years spanning from October 2006 to August 2013.

15. SUBJECT TERMS
coherent laser radar, multi-aperture imaging, synthetic-aperture laser radar, 3D digital holography, sparse frequency LADAR

16. SECURITY CLASSIFICATION OF:			17. LIMITATION OF ABSTRACT:	18. NUMBER OF PAGES	19a. NAME OF RESPONSIBLE PERSON (Monitor)
a. REPORT	b. ABSTRACT	c. THIS PAGE			Timothy M. Finegan
Unclassified	Unclassified	Unclassified	SAR	128	19b. TELEPHONE NUMBER *(Include Area Code)* N/A

Table of Contents

List of Figures

Figure **Page**

List of Tables

Table **Page**

1.0 Summary

LOCI was established in 2006 as a facility where government, industry and academic researchers and engineers could work together to solve projects of interest to the LADAR community outside the fence. The facility was leveraged over $2.5 million in funds from the State of Ohio through Third Frontier via the Institute for the Development and Commercialization of Advanced Sensors technology (IDCAST). Initially the facility was 10,000 sq. ft. of space with five laboratories and a range hall. Another space of 5,000 sq. ft. with an indoor range hall and an outdoor range over 7 km was added once the WBI LOCI Chair, Prof. M. Vorontsov was hired.

LOCI established a management team with Prof. Joseph Haus as the Director and later Dr. Paul McManamon was hired for technical leadership and strategic planning. Mr. Nicholas Miller was hired to manage research equipment and the labs and assist on the testbed research project, as well as conduct his own research. A Senior Research Engineer position was advertised and filled by Dr. Igor Anisomov with a goal to build a multi-aperture testbed. LOCI was strengthened by six industry partners that helped to establish an endowment for the WBI LOCI Chair and they advised LOCI management on future actions and directions for LOCI.

A number of metrics were identified by the industry, government and academia panel that wrote the Strategic Plan. They are chosen as a measure its progress and impact. Metrics include: publications, citations and invited talks measure the community recognition of excellent research; collaborators to partner on research projects based on LOCI's expertise; partnerships forged with other institutions to succeed at a larger goal; and companies come to further their own projects.

LOCI One main outcome of special interest to LOCI's sponsors was training students who could enter the aerospace workforce. In six years 30 students studied electro-optics and seven were hired directly by AFRL for workforce refreshment; two others are working in DoD government positions in other states and six are working in aerospace companies. In other words 50% are working in the field. This metric exceeds our expectations.

Other highlights of LOCI's actions include the **8** patent disclosures, **48** refereed published papers, **23** invited talks at conferences and **43** contributed talks at conferences. LOCI hired the WBI LOCI chair within three years of its establishment and it reached the goal of six Industry Partners within three years.

LOCI's industry projects included two with Lockheed-Martin and a collaborative project with four Industry Partners (Raytheon, Lockheed-Martin, Textron, Northrop-Grumman). Other research projects were conducted in LOCI with Optonicus, MZA, UtopiaCompression and Defense Engineering Corp among others. LOCI has projects in its labs with Dr. Rita Peterson (AFRL/RY) on nonlinear optics and lasers for mid-wave and long wave IR applications and a project with Dr. Adam Cooney (AFRL/RY) on Terahertz generation for non-destructive testing.

The sum of these activities demonstrates an interest in LOCI capabilities and LOCI research that leads to solutions for industry and government. Government and industry are coming to LOCI to work with government and academia in a collaborative environment and to pursue research to solve problems of interest to them.

Professor Vorontsov was hired in 2009 with a world-class record of research accomplishment in areas of adaptive optics and laser beam propagation in teh atmosphere. He rapidly established a strong research group and expand funding to other Air Force and DoD groups. His rapid expansion was assisted by $1.5 million in funds from the Ohio Third Frontier. He started a company called Optonicus that has added employees as they have successfully competed for projects. Prof. Vorontsov has also competed for and won an Air Force MURI project by put together a world-class team of researchers to study deep turbulence and quantify a new approach to understanding beam propagation through the atmosphere.

The testbed project lasted for three years and culminated in an innovative final design. During the project adjustments were made in the leadership to keep it on track. The LOCI group successfully designed, built, and final tested the design with seven sub-apertures. The design evolved through several iterations to achieve the final system. We worked with MZA to capture a set of images under different conditions, including adding phase plates to simulate atmospheric turbulence effects.

The research topics conducted by LOCI in partnership with AFRL included several using spatial and temporal heterodyne technique. This was a major theme for LOCI research with ten students whose theses were projects related to this theme. LOCI contributed to basic research that would help to develop sparse aperture or synthetic aperture images with resolution exceeding the sub-aperture size limitations. LOCI looked at extended versions of the technology to include multiple transmitters, as well as receivers and LOCI researchers examined techniques to improve the post-processing time for sharpness metrics. Other projects included studies of turbulence and its effect on beams propagating through the atmosphere; studies of speckle statistics to determine target identification, beam steering, LADAR signal foliage penetration, nonlinear optics and sensing or signal detection.

2.0 Introduction

The Air Force Research Laboratory, (AFRL), let this co-operative agreement to the University of Dayton, (UD), in 2006 to develop a center of excellence in the areas of Laser Detection and Ranging (LADAR) and free space optical communications. UD then established a Board of Governors including representatives from 6 major companies. Those companies are: Raytheon, Lockheed Martin, Textron, BAE Systems, Boeing, and Northrop Grumman. Each Partner company has contributed funds to endow a LADAR and Optical Communications Institute (LOCI) chair. Dr. Mikhail Vorontsov was selected to be that chair. He started work at the University of Dayton August 2009. He has specialized in free space laser communications, the effects of the atmosphere on active optical systems, and in phasing multiple lasers at a distance. He wrote a seminal paper showing experimentally the lack of a correct theory on deep turbulence, and has since been awarded a Multidisciplinary University Research Initiative (MURI) on deep turbulence by the Air Force Office of Scientific Research (AFOSR). His work and activities since joining UD are summarized in this report.

Twenty nine US national graduate students have graduated from UD and one is expected to finish by December 2013 under the LOCI umbrella, fulfilling one of the main objectives of this contract, namely workforce refreshment. At this time seven of the 29 work for AFRL, or for AFRL as base support contractors. At least nine additional graduates work for contractors who support the Department of Defense (DOD) in other cities. Based upon guidance from the Air Force the technical areas of aperture synthesis and stretch processing were emphasized in picking graduate student thesis and dissertations topics. These technical areas are discussed in detail with references given to recent work in some cases and an assessment of the research area.

Our initial technical research area was devoted to multi-aperture synthesis. Several students performed tabletop experiments and we developed extensive computational simulation capabilities to process the images using image sharpening metrics. This report also gives a complete report on the Innovative Multi-Aperture Gimbal-less Electro-optical, (IMAGE), testbed in Appendix A. We designed, built and tested a multi-aperture testbed and worked with a company (MZA) to capture and process multi-aperture images. The LOCI compact range was developed to allow quantitative scaled measurements of synthesizing high resolution images inserting known phase screens to simulate atmospheric effects at specific simulated distances from the pupil plane. The IMAGE testbed is a system for testing aperture synthesis concepts and trying new optical components, such as steering the field of view to off axis locations. A second technical area that was emphasized, but to a lower degree, was Linear Frequency Modulation (LFM) and stretch processing techniques that enable higher range resolution approaches while at the same time propagating energetic waveforms. The stretch processing technique also minimizes detector bandwidth. A third area discussed is mid IR laser technology development. A number of graduate students worked in that technical area. Significant facilities have been developed to support the center. These include an International Traffic in Arms (ITAR) qualified facility, a compact range for indoor testing of concepts, and a 7 Km outdoor range.

LOCI's academic achievements during the seven year period are certainly noteworthy. By many metrics LOCI has established itself as a truly prodigious research organization. In the seven years there are: 8 patent disclosures filed, 48 refereed publications, 23 invited conference presentations and 43 contributed conference presentations. The metrics are listed in section 4.14 of this report. The faculty and students were active members of the optics community and able to regularly attend the most important conferences in the field around the world.

2.1 Educational Development

The Electro-Optics Program (EOP) was established in 1983 offering an M.S. degree in Electro-Optics. A Ph.D. degree in Electro-Optics was added in 1994. The core courses consist of six optics courses and three labs. The program is structured as a hands-on educational experience for the students. The core courses form the foundation for optics courses taken as technical electives, or as advanced courses in the subject. We have designed a set of four courses as a LADAR concentration offered to our graduate students. These four courses will provide the basis for a LADAR certificate. The courses are: Statistical Optics, Free Space Optical Communications, Introduction to LADAR Systems, and Image Processing. All of these courses have been offered at least one time. Altogether there are 30 optics courses offered through the University of Dayton Program. In addition, through the Dayton Area graduate Studies Institute, (DAGSI), program, any course offered at Wright State University or Air Force Institute of Technology (AFIT) can also be taken for graduate credit. AFIT also has a large number of graduate level courses in electro-optics.

The LADAR certificate entailed a set of four classes, as mentioned above. The Image processing class is a regular course taught in the Electrical and Computer Engineering Department. The other three courses are taught in EOP. Dr. Watson taught the Statistical optics course for two cycles and he structured the course to deal with issues that were important to LOCI students studying coherent LADAR problems including radiometry, speckle noise, Carrier to Noise Ratio (CNR) and Signal to Noise Ratio (SNR) issues. Dr. Haus taught the Free Space Optical Communications course for several years with emphasis on optical beam propagation through turbulence. Students learned about applications of turbulence theory to free space optical communications and to LADAR systems. All students wrote a final paper and made a 15 minute PowerPoint presentation on their topic for the entire class. The Introduction to LADAR Systems course was co-taught by Drs. McManamon and Watson. They covered many aspects of LADAR system designs following the light from the source through the aperture and turbulent channel to the target and then back through the system again.

Dr. Haus hosted a Special Weekly Journal Club during the academic year to give students an opportunity for further professional growth. This was designed for peer interactions within the group. It was generally an informal meeting facilitated by Dr. Haus conducted during lunch hours. At the beginning of the academic year LOCI students were assigned topics and journals to scan for interesting articles. The Journal Club progressed in a two week cycle. In one week each student gave a brief synopsis of the articles they found that could be of interest to the entire group. Then the students chose two topics that could be expanded on for a full presentation in the following week. In the second week the students with the chosen topics were asked to expand the description and give a PowerPoint presentation on their article. All of the students gave two or three talks during the academic year.

Another experience to build students professionally is through EOP Seminars; they are a regular activity during the academic year and all students are expected to attend. An attendance list was taken and attendance was a condition of their contract. The seminars expose students to new topics and help them to think critically about a topic and they are encouraged to ask questions. If we could coordinate with the Journal Club ahead

of time students were exposed to a topic with a PowerPoint presentation and could enrich their seminar experience.

Dr. McManamon gave a week long short course in laser radar in June of 2011at Georgia Tech Research Institute (GTRI), in conjunction with Dr. Gary Kamerman. In the summer of 2013 LOCI will offer two one week short courses. One will be an Introduction to LADAR, taught by Drs. McManamon and Watson. It will be modeled after the similar 3 credit hour course taught last spring. The second one week short course will be Digital Holography, taught by Drs. Partha Banerjee and Georges Nehmetallah. Two Additional short courses will be offered next summer; one on Nonlinear Optics by Dr. Peter Powers and another on Nanofabrication by Dr. Andrew Sarangan.

The University of Dayton has three rooms outfitted for distance learning and has extensive experience delivering distance courses to companies. The EOP is developing distance learning courses for broadcast across the country and we have a strategy for initiating short courses. The introduction to LADAR course taught by Dr. McManamon and Dr. Watson started experimenting with distance learning. Dr. McManamon gave one lecture from the west coast, and he also arranged for Dr. Maurice Halmos at Raytheon to teach one lecture from his office on the west coast. Dr. McManamon listened in from the west coast on a guest lecture by Mr. Nick Miller, and one of Dr. McManamon's lectures had a student listening in from a remote location. We have tried different hardware for distance learning, and are continuing to experiment. As might be expected cost is a major barrier to the best equipment.

All LOCI students paid by AFRL attended weekly meetings. The format for the meetings the meetings varied over the years and the venue went from a conference room at AFRL to the LOCI conference room and back again. The presentations went in around the room giving each student a chance to present results for the past week. If problems were encountered the discussion between the student and the mentors would concentrate on how to resolve the issues.

3.0 Methods, Assumptions, and Procedures

3.1 LOCI Facilities

Figure 1 shows the facilities developed on the 5th floor of College Park Center. LOCI has 10,000 square feet of ITAR restricted space. This area contains 5 laboratories, a 100 foot long range hall for our multi-aperture test bed, 5 offices for personnel, and cubicle space for 12 students. In addition there is 5,000 square feet of space on the right side of Figure 1 that contains Dr Mikhail Vorontsov's Intelligent Optics laboratory facilities. Prof. Vorontsov's area includes 5 labs and a 100 foot range hall for deep turbulence simulations and target tracking studies. In between there are offices laboratories, and a class room, for the EO program.

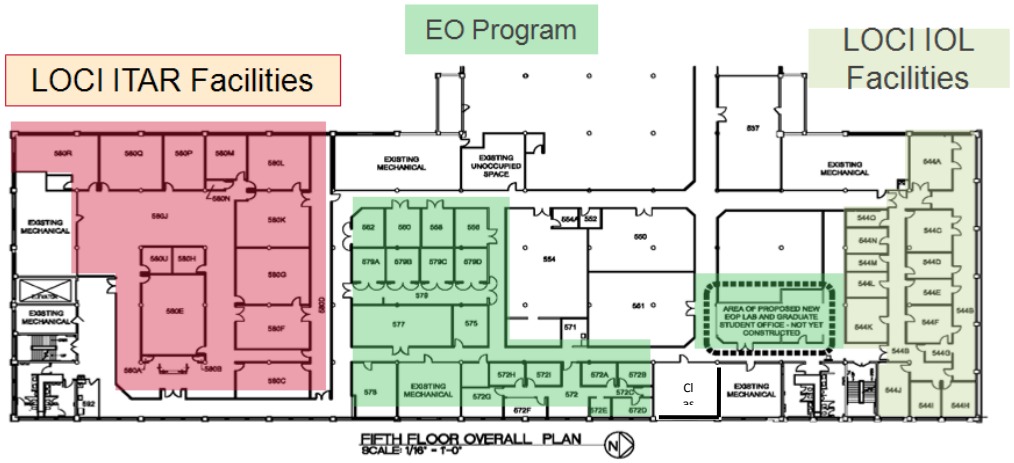

Figure 1: LOCI and UD EOP Facilities

Additional facilities are available in the physics building, including a 600 square foot clean room and many fabrication tools for nanoscale materials and devices. LOCI received more than $2.5 million from the State of Ohio for infrastructure and its commercialization activities. In the 100 foot long LOCI range hall we have the compact range. It makes use of a 24 inch (61 cm) mirror that the University of Dayton has had around for decades, and was put to good use. The mirror is shown in Figure 2.

Figure 2: 24 inch (~61 cm) Mirror Used in Compact Range

Figure 3 shows a conceptual diagram of the compact range. The compact range is a demagnifying telescope. It allows us to scale a long range, such as 7 Km, into a much more compact distance, such as the shown 4.75 meters. It also allows us to place reasonable size phase screens at specific simulated distances. The demagnification ratio of the telescope squared is the ratio of the simulated range reduction (7,000 meters divided by 38.4

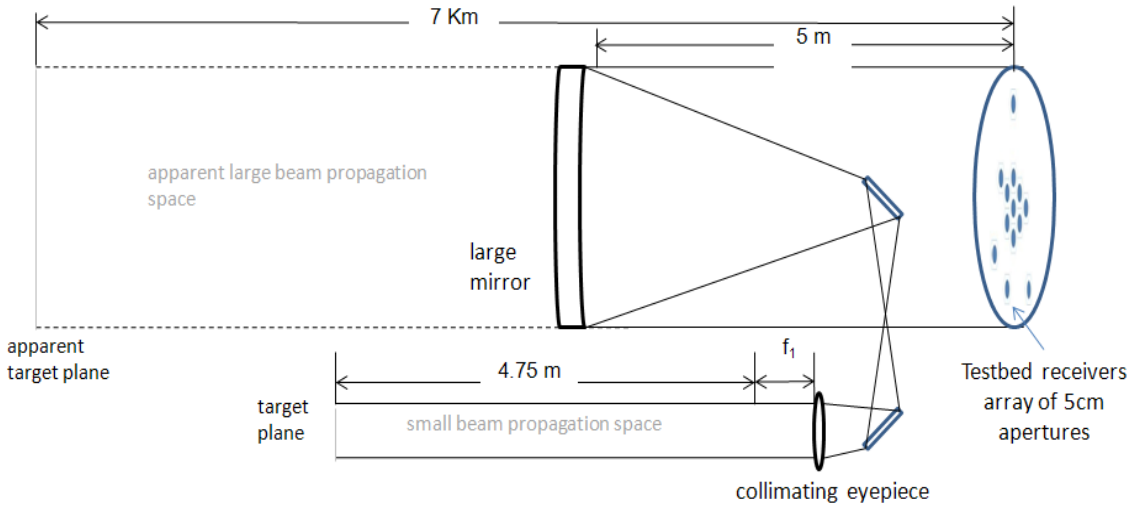

Figure 3: Conceptual Diagram of the Compact Range

squared is 4.75 meters). The pupil plane size of the image in the compact space is reduced by the magnification, but then the angular divergence is increased by the same factor of the magnification. Multiple magnification ratios have been used in the compact range, depending on the experiment being conducted. Changing the eye piece in the telescope changes the magnification, so it is a straight forward and easy to change magnification.

The atmospheric turbulence test bed consists of a 7 Km optical path that extends from the roof of the VA Medical Center (VAMC) to the fifth floor of the UD's College Park Center. It is shown conceptually in Figure 4.

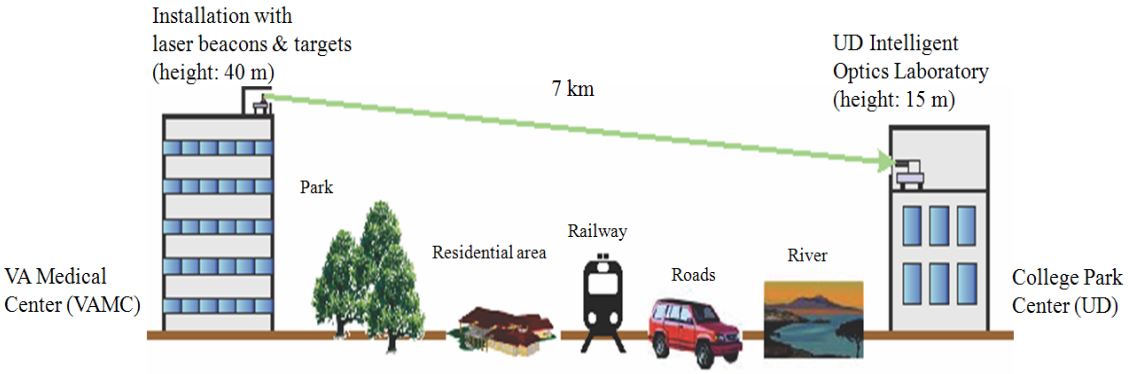

Figure 4: Conceptual Diagram of the UD 7 km Range

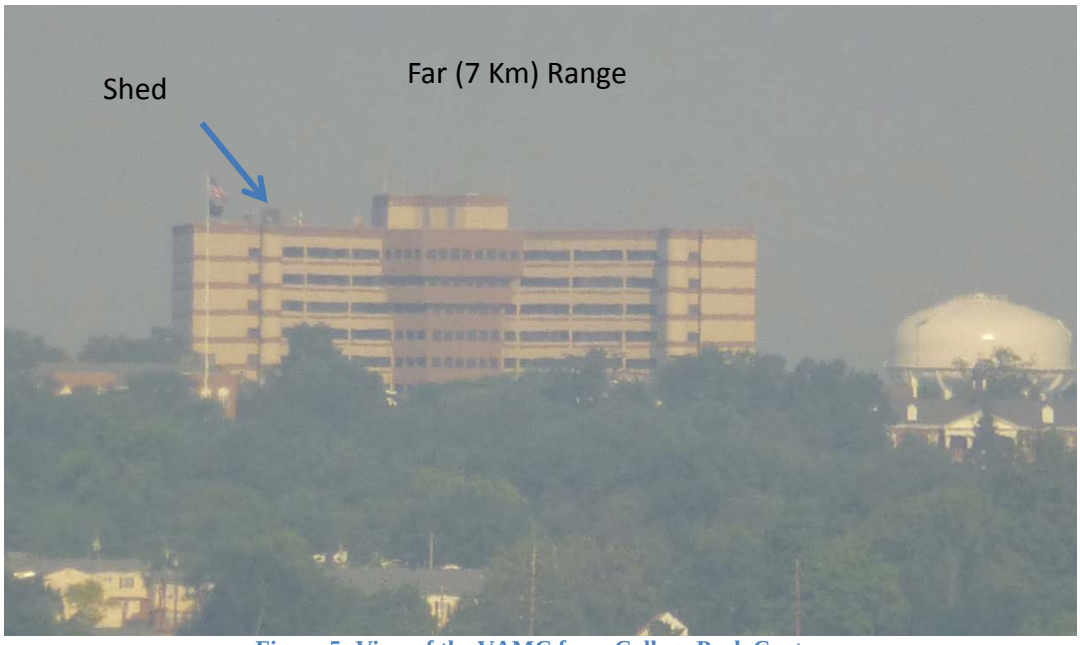

Figure 5: View of the VAMC from College Park Center

Figure 5 shows the view of the VA hospital from College park center. Note the shed on the roof. Figure 6 shows a close up view of the shed on top of the VA center. This shed allows the University to have instrumentation on both ends of the 7 Km path.

Figure 6: Shed on the Roof of the VAMC

In order assist calibration there is also a corner cube on the roof of the Marriott. The Marriott is 650 - 700 meters from College Park Center.

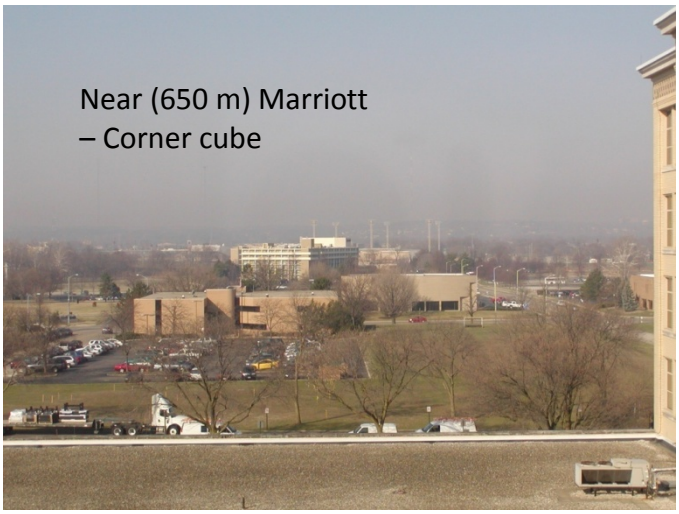

Figure 7: View of the Marriott from College Park Center

Three small companies moved their offices to CPC and work closely with LOCI on developing projects. Optonicus is a startup founded by Dr. Vorontsov to commercialize photonic components developed for free space optical communications applications. It has been highly successful in developing products and winning contracts that are within the expertise of the company staff. The staff has continually grown in the past 4 years. UtopiaCompression and Defense Engineering Corp. have offices in LOCI. They work on imaging applications for Wide Area Surveillance (WAS) and the Sense and Avoid (SAA) project for UAS applications and there are other DoD projects that draw on the Electro-Optics staff expertise. LOCI has three ongoing projects with these companies.

It should be noted that there are other faculty and staff who are capable researchers and have contributed to the LOCI mission. More details will be given about Dr. Mikhail Vorontsov in Section 4.13. Here we will briefly mention a few EO faculty who have built world-class laboratories and with these resources they have made tremendous research contributions.

Dr. Peter Powers has a nonlinear optics laboratory equipped with femtosecond and nanosecond laser to study parametric down-conversion using engineered nonlinear crystals. He is a star Team member of Dr. Ken Schepler's group in AFRL/RY and has mentored many students who have gotten EO degrees in that field over the past fifteen years. With his femtosecond laser he has the capability to generate THz waves for imaging and to carry out laser micromachining studies. His nanosecond lasers are capable of high peak power parametric down-conversion. He has worked with Dr. Haus and visitors to build specialty high-power, fiber lasers as compact sources for applications in remote sensing, LADAR and THz generation.

Dr. Andrew Sarangan established his NanoFabrication facility with State of Ohio funds in 2003. This is in the physics building, and it not part of LOCI, but is a valuable asset for the Electro-Optics Program. The equipment in this facility represents more than $5 million dollars of investment. The fabrication lab at UD has class 1000 and class 100 clean room facilities with extensive fabrication facilities. Especially he has sputtering and

electron-beam deposition capabilities, as well as Plasma Enhanced Chemical Vapor Deposition. He can etch materials for MEMS applications using his Inductively Coupled Plasma tool. His Lab/Cleanroom resides in the basement of the physics building and next to the NEST Lab where SEM and TEM characterization tools are available. He collaborates with groups in AFRL/RY.

The Nanocharacterization Lab of Prof. Qiwen Zhan has made new optical analysis tools with resolution below 50 nm (about $\lambda/10$). His lab studies beam forming, imaging, and information propagation with inhomogeneous polarization states. He also works closely with groups at AFRL/RX.

The Holography and Optical Signal Processing Lab (Partha Banerjee) also in the College Park Center at the University of Dayton has extensive facilities in optical processing and 3D imaging. It specializes in digital holography, holographic interferometry and holographic tomography for applications in 3D visualization of water droplets and 3D surface deformation characterization. Dr. Banerjee's Lab also has an active research program that works closely on photorefractive materials with AFRL/RX. The program collaborates with several outside groups, such as Prof. Nikolai Kuhktarev at Alabama A&M, an HBCU.

4.0 Results and Discussions

4.1 Aperture Synthesis

Aperture synthesis has been a major emphasis area for LOCI. By aperture synthesis we mean high resolution imaging either from an array of sub-apertures, or from one or more moving apertures. The high resolution image is synthesized from either many simultaneous sub-aperture samples of the received field, or from a lesser number of sub-apertures that sequentially sample the received field. Wikipedia defines aperture synthesis as "a type of interferometry that mixes signals from a collection of telescopes to produce images having the same angular resolution as an instrument the size of the entire collection."[1] In addition to developing the IMAGE testbed for this technical area we have had 9 theses in this technical area. As described earlier we also have developed appropriate test facilities.

The concept of a Phased Array of Phased arrays set of sub-apertures to develop a high resolution image has significant promise.[2,3]. In order to synthesize a high resolution image from multiple sub-apertures, or moving sub-apertures with sequential images, we need to measure, or estimate, the pupil plane field captured by each sub-aperture. Once the pupil plane field is known in each sub-aperture it is possible to Fourier transform the complete pupil plane field of the array of sub-aperture samples and obtain a high resolution image. Detectors do not respond fast enough to directly measure an optical field. A typical optical signal is about 1.5 μm in wavelength, or about 200 THz. Two hundred THz is orders of magnitude beyond the response capability of even the fasted detectors. Most imagers, even active imagers, are therefore direct detection systems, measuring only the intensity of the received field.

Three general methods of measuring, or estimating, the field in the array of pupil planes from multiple apertures are discussed. They are temporal heterodyne, spatial heterodyne, and wavefront sensing. Our graduate students have focused on spatial heterodyne, but we will place that in context by briefly discussing all 3 approaches. One graduate student used a single temporal heterodyne detector in conjunction with spatial heterodyne. To measure the intensity and the phase we usually make use of a local oscillator beat against the return signal in an active imager. In temporal heterodyne the local oscillator is co-aligned with the return signal, but is offset in frequency so you can tell from the return Doppler shift if an object is moving toward or away from you.[4] A high bandwidth detector in the GHz range with current state of the art is usually required to measure the temporal beat frequency between the local oscillator and the return signal. This of course depends on the amount of LO frequency offset and the Doppler shift of the return signal. Range to the target is measured by measuring time for the return and dividing the round trip distance by the speed of light essentially in a vacuum in order to measure distance. In temporal heterodyne since the piston phase of the return signal is measured it is possible to measure the difference in piston phase between one sub-aperture and the next. In spatial heterodyne the local oscillator is at the same frequency, but is offset in angle, to develop spatial fringes across either the return pupil or image plane.[5] The spatial variation in phase across a receive object can be measured by the spacing of the fringes. Low bandwidth framing detector array cameras can measure

spatial phase variation, but you will need sufficient spatial resolution in the detector array to see the fringes. Spatial heterodyne is a form of digital holography. In spatial heterodyne piston phase is not measured, so the piston phase shift between sub-apertures is usually estimated using a hill climbing algorithm (using an image metric which is optimized to enhance image sharpness). Spatial heterodyne requires narrow line width lasers so the spatial fringes will be visible. Another issue for spatial heterodyne, or wavefront sensing, is the measurement must take place in a short enough time so the atmosphere does not change during a measurement. This is not an issue in temporal heterodyne because measurements are in the nanosecond range anyway, but spatial heterodyne uses low bandwidth framing cameras. Measurements should be accomplished in a period on the order of a millisecond in order to freeze the atmosphere.. Framing cameras can be gated shorter than that. With short gate times it is useful to have pulsed illumination source for spatial heterodyne.

It is also possible to measure spatial phase variation in a sub-aperture using a wavefront sensor, such as a Shack Hartman sensor. A wavefront sensor does not directly measure phase. It measures the optical path difference, OPD, variation across an aperture. This is equivalent to measuring phase at a given wavelength. Thus direct detection sensors using a wavefront sensor can effectively measure spatial phase variations without requiring an LO, or the narrow bandwidth lasers used for spatial heterodyne.

4.2 Temporal Heterodyne

This is the more common form of heterodyne, used in most coherent LADARs.[4] Assume a point source of light in the far field, the equation of the complex field for a spherical wave at a distance, r, from a source is:

$$E\left(\vec{r},t\right)=Ae^{j\phi}e^{jkr}e^{-j\omega t}, \tag{1}$$

where A is the real amplitude, φ is an arbitrary phase term, k is the wave vector ($k = 2\pi/\lambda$), and $\omega = 2\pi c/\lambda$. Since it is a spherical wave it does not matter what direction the light leaves the point. All that matters is distance. An image of course can be made up of multiple point sources. We also could consider a plane wave, in which case r would be replaced by z, the distance from some plane wave reference plane. An LO can be a plane wave or can have curvature. The LO has to be matched to the return signal or we will develop high frequency spatial fringes as the LO diverges from the return signal in angle. For temporal heterodyne we use an LO that is frequency offset, but co-aligned with the return signal, so there will be no spatial fringes if we match the LO properly. We have a beat frequency of $\Delta\omega = \omega - \omega_0$, where the signal does not have a subscript and the subscript 0 is used for the LO. The beat frequency will usually be chosen higher than any expected Doppler shift, so it is unambiguous which direction the velocity of the object is, toward or away from the sensor. The Doppler shift is given by:

$$\Delta\nu = \frac{2v}{\lambda} \quad . \tag{2}$$

For a 1.5 μm laser the Doppler shift for several velocities is given in Table 1.

Velocity (m/sec)	Frequency
0.001	1.33×10^{3}
1	1.33×10^{6}
200	2.67×10^{8}
8000	1.07×10^{10}

Table 1: Doppler Shift for a 1.5 μm laser.

The 8000 m/sec could represent an orbiting object in low earth orbit. 200 m/sec could be a nominal aircraft. Also, range resolution is inversely proportional to bandwidth, so a 500 MHz bandwidth has a .3 meter range resolution, 1 GHz has .15 meter, etc. One very nice feature is that if the LO is stable then a phase shift at the beat frequency, sometime called the IF frequency, directly correlates with the same phase shift of the carrier frequency. This allows a direct measurement of piston phase of the carrier.

4.3 Spatial Heterodyne

The major advantage for spatial heterodyne is the ability to use low bandwidth framing cameras. These are available is relatively large formats. Visible cameras have very large formats, certainly well into the megapixel regime. At 1.5 μm camera formats are smaller, but still substantial. 256 x 320 is a relatively small format. 512 x 640 is a very common FPA format. Megapixel cameras are becoming available. Because we are relying on spatial variation in the beat between the return signal and the LO we need spatial sampling. We can consider a simple case of a plane wave signal (something viewed far away), and a plane wave LO in the pupil plane. The temporal part of the beat frequency does not matter in this case. We have both the LO and the return signal at the same frequency, except for velocity considerations, which we will initially ignore. One graduate student project addressed velocity variations when using spatial heterodyne.

$$E\left(\vec{r},t\right) * E\left(\vec{r_0},t\right) \propto e^{jkr} e^{-jkr_0} \tag{3}$$

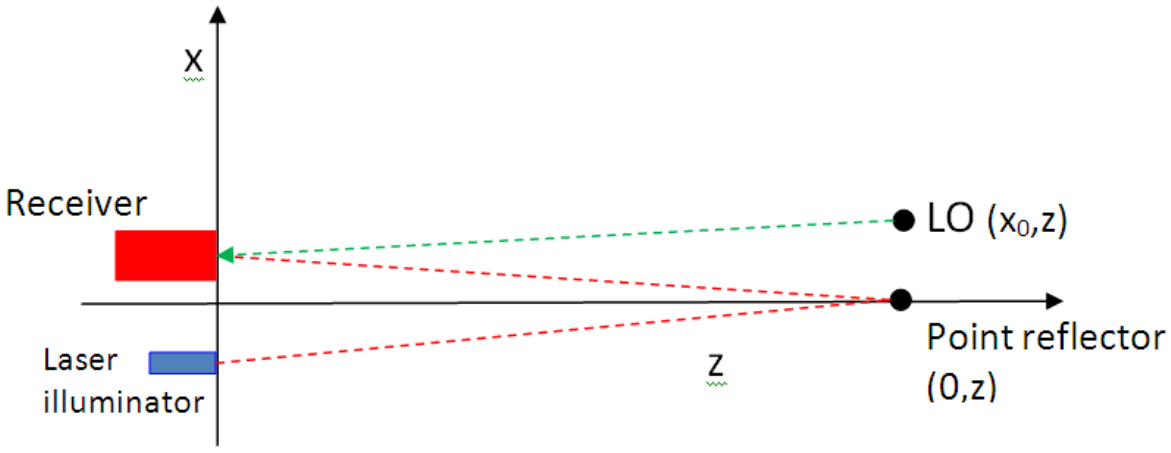

Figure 8: Illustration of the Spatial Heterodyne Geometry

We assume scattering off of a point reflector, and the LO is emitted at a point the same distance from the aperture as the point reflector, but offset slightly in x so it hits the detector array at a different angle. For simplicity let r=z, meaning the point reflector is on axis to the detector array (0,z). The LO is displaced slightly in the x direction (x,z), as shown in figure 8. We will calculate the spatial variation in x based on the interference between the LO and the return signal. Let us define the distance from the point reflector to the receiver to be r_0. To get exactly the right curvature we should put the LO the same distance from the center of the imager as the point reflector is, so if the LO is emitted as a point radiator slightly to the side it would have to be slightly closer in the z direction, but this is a minor change which we will ignore. We also assume that z is significantly larger than the x displacements. The two distances are:

$$r = \sqrt{z^2 + x^2} \approx z + \frac{x^2}{2z} \tag{4}$$

and

$$r_0 = \sqrt{z^2 + (x - x_0)^2} \approx z + \frac{(x - x_0)^2}{2z} \tag{5}$$

$$E\left(\vec{r},t\right) * E\left(\vec{r_0},t\right) \propto e^{jkr} e^{jkr_0} \approx e^{jk\left[\frac{xx_0}{z} - \frac{x_0^2}{2z}\right]} \tag{6}$$

Only one term oscillates in x. the other term is a constant since x_0 is a constant. We can see the oscillation is a product of x times x_0, so the farther off zero we place the LO the more rapid the oscillation in spatial frequency. As we get farther off axis the fringes oscillate more rapidly. We have to size the detector sampling to see these fringes.

The history of spatial heterodyne imaging began in May 1948 when Gabor demonstrated and published the first hologram[6]. The method described in the paper, which is sometimes termed as a Gabor hologram, is an in-line hologram. This means that there were multiple image elements stacked on each other. Though there were ways to get the image to show up clearly, his discovery was to be used for improving resolution for electron microscopes. Light sources did not have the needed coherence for optical holography. It was not until after Theodore Maiman constructed the first working laser in 1960, and the invention of the visible CW He-Ne by A.D. White and J.D. Rigden in 1962, that holography could be made practical[7, 8]. E. N. Leith and J. Upatniek took the concepts of holography and expanded them[9,10,11]. They developed a method that used an off-axis reference beam instead of Gabor's in-line approach. The off-axis reference beam made it so the images were not all stacked on top of each other as they were with Gabor's holograms. There are several different names that refer to these holograms: Leith-Upatnieks hologram, offset-reference hologram, off-axis holography, and spatial heterodyne. In 1967, J. W. Goodman and R. W. Lawrence created the first digital capture and reconstruction of a hologram[12]. In 1971 T. S. Huang wrote "Digital

Holography" His contribution brought holography into the computer age[13]. In his paper, he brought together the ideas of manipulating optical data and creating holograms using computers. Huang's paper is a summary of the work of the time, for which he gives many references. This early work, and the advances in computing since, has paved the way for modern digital holography (spatial heterodyne).

With the birth of the He-Ne laser at 633 nm, by White and Rigden, another phenomenon was observed. J. D. Rigden and E. I. Gordon wrote the first paper on laser speckle[14]. The coherence of the laser was good for holography but it was bad when creating the image of a diffuse object. Object roughness causes interference patterns in the images which take the form of patches of light and dark areas. This speckle noise is enough to bring the signal to noise ratio down to 1. S. Lowenthal and H. Arsenualt determined that the average transfer function for the coherent imaging is the transfer function for incoherent imaging[15]. This means that, with enough coherent images, coherent images can be averaged together to get an image without speckle noise.

To average the coherent images, the camera must look through the same atmosphere, however a new speckle realization is required for each sample. A speckle realization is a new interference sample of the target. A method for sharpening images was discussed by R. A. Muller, and A. Buffington, in 1974[16]. They discuss several sharpening metrics that can be used and give general results for several of the sharpening metrics from their computer simulations, but their work was for incoherent light. R. G. Paxman and J.C. Marron wrote a paper in 1988 that shows that the image sharpness metrics can be used with coherent speckled data[17]. These sharpening metrics allow for digital manipulation of the images to get rid of phase aberrations in the images. This allows for the averaging of the images.

One of the early spatial heterodyne papers for gaining the higher resolutions was written about by J. C. Marron and R. L. Kendrick[5]. In this method, they used many of the digital holography techniques mentioned earlier to build higher resolution images using several smaller apertures. Numerous other papers have been published as spatial heterodyne has been more thoroughly explored.[18,19]

The IMAGE testbed was developed by LOCI as a research tool in support of multiple sub-aperture based EO systems. It has been structured so far to use spatial heterodyne in either a pupil plane or image plane imaging modality. The IMAGE testbed has been, and will be, used to test phasing algorithms that provide the full diffraction limited resolution associated with array dimensions, to test required spatial sampling issues, to test phasing approaches that also involve array motion, and to provide a means of testing components associated with multi-sub-aperture based imaging. This can be accomplished even in the presence of a turbulent atmosphere. Two fixed phase screens have been used in some tests to date.[20] A secondary purpose of the testbed is to support imaging for aim point selection and maintenance for directed energy weapon development using a similar architecture for Acquisition, Pointing, and Tracking, and for the weapon itself. Another secondary purpose is to develop novel free space laser communication systems.

The sub-aperture unit in the IMAGE testebed was designed with an imaging approach of spatial heterodyne, but with the potential to implement other sub-aperture combining approaches at a later time. Both image and pupil plane imaging have been implemented. A single sub-aperture for the spatial heterodyne approach is shown in Figure 9.[21]

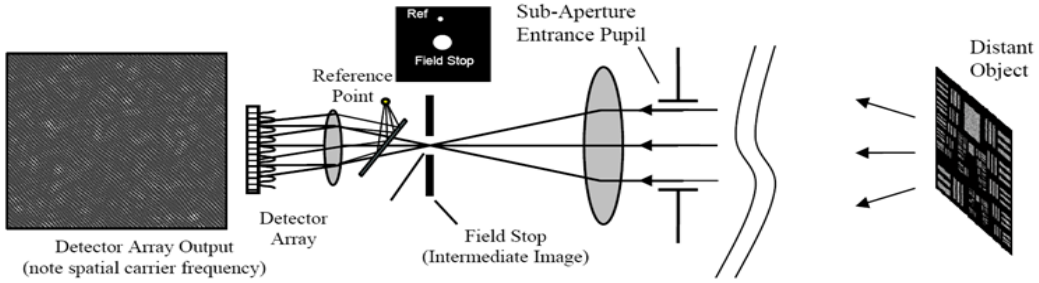

Figure 9: Sub-Aperture of the Spatial Heterodyne Imaging Approach from Ref.(5)

Spatial heterodyne captures a pupil plane image for each sub-aperture. A low bandwidth imaging detector array can be used in each sub-aperture for spatial heterodyne. Each pupil plane image contains both image information and spatial phase variation.

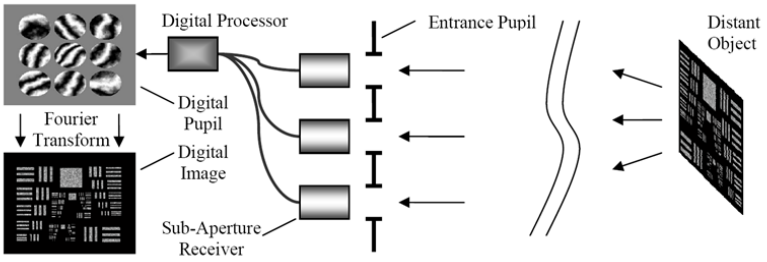

Figure 10: Multiple Sub-Aperture Spatial Heterodyne Imaging from Ref.(5)

The pupil plane image from each detector is Fourier transformed into the image plane and then sharpened using a sharpness metric. In order to sharpen each pupil plane image each sub-aperture must have sufficient signal to noise. False sharp images, such as a point must be avoided. The sharpened pupil plane images from each sub-aperture are transformed back into the pupil plane and used to assemble a more complete pupil plane image. The phase distortion in each sub-aperture image can be judged based upon the difference between the captured image and the sharpened image. This phase distortion can be used to place the sub-aperture pupil plane images in the correct locations. Real geometry can aid in this placement, as a reality check. Piston phase information between sub-apertures must be estimated, using a sharpness metric. An image such as shown in Figure 11 is generated by Fourier transforming the phase adjusted mosaic of pupil plane images from the individual sub-aperture pupil plane images.

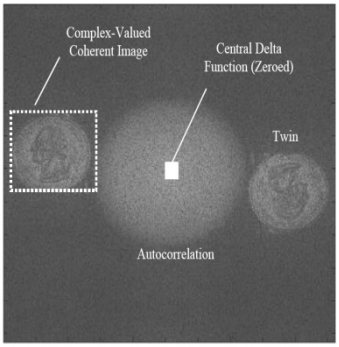

Figure 11: Spatial Heterodyne Image

4.4 3D Imaging Using Spatial Heterodyne

Optical scanning holography (OSH), as developed by Poon et al. is a highly sophisticated technology, with numerous facets and applications. OSH is a distinct electronic or digital holographic technique. Real-time holographic recording of a three-dimensional (3D) object can be acquired by using two-dimensional active optical heterodyne scanning. Synthetic-aperture optics is an equally appropriate term and has been also been widely used.

Conventionally, digital holography (DH) offers a convenient way of reconstructing the 3D object using numerical reconstruction techniques. In the last decade, DH with its two variations, digital holographic interferometry (DHI) and digital holographic microscopy (DHM), have become the method of choice for various metrological applications. These applications range from deformation detection, visualization and quantization as well as surface profilometry in 3D. An important issue in is the recovery of the phase of the object which relates to its depth information. Dr Partha Banerjee and his students have worked on DH and DHI for several applications, viz. the determination of aircraft attitudes using DHI, exact 3D profiling of water droplets in rain showers using digital holographic tomography (DHT), and determination of 3D deformations during impact. Holographic microscopy is also being pursued by for monitoring semiconductor wafer fabrication. Banerjee's work on water droplet holography recently won the Army Small Business Innovative Research (SBIR) Phase II Achievement Award for 2011. The basic objective in DH is to reconstruct the 3D shape of the object. The depth information is in the phase of the recorded hologram, and can be retrieved in a variety of ways. In one method, the recorded (intensity) hologram in a photo-detector array is inverse Fresnel transformed to yield the 3D image of the object (and the twin image). The real image and its twin can be effectively spatially separated using off-axis holography and its digital reconstruction, or what is also referred to as "spatial heterodyning". LOCI has been active in this field as well.

While depth information is in the unwrapped phase of the reconstructed image, depths of the order of microns are easily decipherable using a single optical wavelength, which is also in the order of microns. Larger depths demand a multi-wavelength approach, where the unwrapped phases of the reconstructed images are subtracted to yield the depth information. Subtraction of phases is also expected to reduce the effect of coherent noise or speckle, especially if multiple exposures at each frequency are recorded

and averaged before subtraction. The range resolution for a two-wavelength recording and reconstruction can be expressed in terms of an effective "beat" or "synthetic" wavelength. Hence by suitably choosing the two wavelengths, 3D objects with arbitrary depths can be reconstructed. The method can be generalized by using both spatial and temporal heterodyning using reference waves (aka local oscillators or LOs) offset at different angles and with different wavelengths, in which case the objects and the twin images, when individually reconstructed, are positioned in different locations, as illustrated in Figure 11.

4.5 Wavefront Sensing

There are many approaches to sense the wavefront across an aperture. A Shack Hartman wavefront sensor is a common method. A Shack Hartman wavefront sensor is shown in Figure 12, taken from Wikipedia[22,23,24]. When a wave enters any of the lenslets at an angle it will

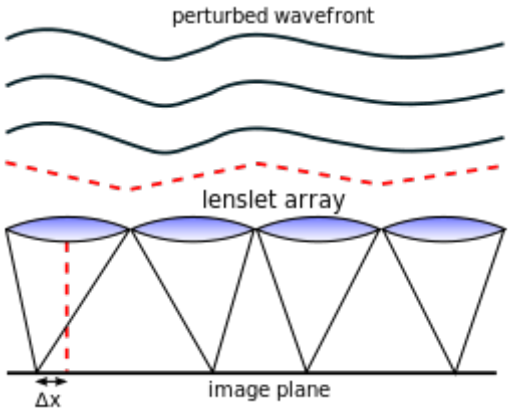

Figure 12: Illustration of a Shack Hartman Wavefront Sensor

result in the focal spot being moved to the left or right. This provides a measure of the wavefront tilt at any given location. Of course the wavefront tilt is only measured on the order of the size of the lenslets. A Shack Hartman sensor will not have the same spatial resolution in measuring wavefront variation as spatial heterodyne, but you do not need a local oscillator, or a narrow band laser. For moderate spatial variation in phase this could be an interesting method of measuring spatial phase variation. One issue with broadband lasers is that phase only makes sense over a narrowband, so the pupil plane field across multiple sub-apertures will need to be described as a set of narrowband fields. While we have not yet explored this space we feel comparing this method of measuring spatial phase variation against spatial heterodyne will be interesting research.

Below is a table showing the graduate work performed by LOCI in the Aperture Synthesis technical area. The aperture synthesis technical area has had more student projects than other technical area. We note that Jeff Kraczek was also supported for one year by a grant from Lockheed-Martin and a second year he was supported by UD funds.

Last name	First Name	Year of Graduation	Degree	Advisor	Title of Thesis or Dissertation
Miller	Nick	2007	M.S.	Brad Duncan	Optical Sparse Aperture Imaging
Stafford	Jason	2009	M.S.	Brad Duncan	Perturbation Analysis and Experimental Demonstration of Holographic Aperture LADAR Systems
Stokes	Andy	2009	M.S.	Brad Duncan	Improving Mid-Frequency Contrast in Sparse Aperture Optical Imaging Systems Based Upon the Golay-N Family of Arrays
Kraczek	Jeff	2011	M.S.	Paul McManamon	An Evaluation of the Effects of the Ability to Measure Piston on Multi-aperture Spatial Heterodyne Systems
Bobb	Ross	2012	M.S.	Matt Dierking	Doppler Shift Analysis for a Holographic Aperture LADAR System
Venable	Sam	2012	M.S.	Brad Duncan	Demonstrated Resolution Enhancement Capability of a Stripmap Holographic Aperture LADAR System
Crotty	Maureen	2012 projected	M.S.	Ed Watson	Conformal Aperture Imaging Techniques
Wu	Gui Min	2012 projected	M.S.	Paul McManamon	Wavefront Control with Beam Steering Device in a Multi-Aperture Imager
Whitfield	Erica	2012 projected	M.S.	Partha Banerjee	Holographic Imaging

Table 2: Aperture Synthesis Related Theses and Dissertations

An abstract for each of these theses or dissertations is included along with a quad chart in Section 4.12 which describes graduate student projects. These projects cover a variety of subject areas. All of them rely on spatial heterodyne. Some of them use moving sub-apertures. Some compensate for aberrations. Some consider signal to noise issues. We have a variety of efforts in the aperture synthesis area.

4.6 Linear Frequency Modulation Processing

In contrast to our sparse aperture imaging research using slow frame rate cameras and multiple sub-apertures the stretch temporal heterodyne processing uses a single, high bandwidth photodiode to capture a return signal, or return signals, from a target. For single detectors the high resolution image is constructed by scanning the field of view. The stretch processing techniques developed here are applicable to single detector, or to an array of high bandwidth detectors. For simplicity we are using a single detector. In order to accurately measure range we need high bandwidth in our signals, but the higher the bandwidth the more expensive the detectors and read out circuits. We would like to measure very high resolution without buying detectors that have bandwidth equivalent to the desired range resolution. At some point we cannot buy high enough bandwidth detectors at any cost. We therefore explore techniques in which the LO frequency is varied to minimize the required detector bandwidth to obtain a certain range resolution. We did not buy the widest possible bandwidth detectors for this work, but the techniques developed to expand the effective bandwidth are applicable to higher bandwidth detectors as well.

4.7 Sparse Frequency Signals: Theory and Simulations

The extension of coherent sparse aperture concepts to the temporal domain was conceived as a LOCI project in the spring of 2007. The first student to work on the project was Robert Chimenti. Robert began in the summer of 2007 and he was tasked with using multiple signals as a method to improve the range resolution. Range resolution, ΔR, is inversely proportional to the total signal bandwidth B_T

$$\Delta R = c / 2B_T . \tag{7}$$

The constant c is the speed of light in vacuum. The total bandwidth is segmented into N pieces that are not overlapping and may not be contiguous with one another, as illustrated in Figure 13.

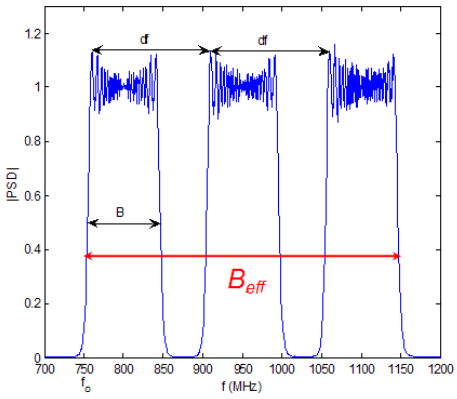

Figure 13: N=3 Segmented Bandwidths after Ref.(1)

(The frequency shift, df, and bandwidth, B, for all segments is identical)

For N segments each with a bandwidth, B, Chimenti et al.[25] determined that the effective bandwidth is

$$B_{eff} = B + (N-1)df . \tag{8}$$

The total bandwidth is now improved by introducing a number of sources that are launched at the same time. A general schematic of the system is shown in Figure 14 for N sources. One source signal is chosen as the Local Oscillator (LO) and mixed with the return signals from the target. The heterodyne signal from the photodiode is processed using Fourier transform techniques to extract the in-phase (I) and in-quadrature (Q) time series of the complex signal.

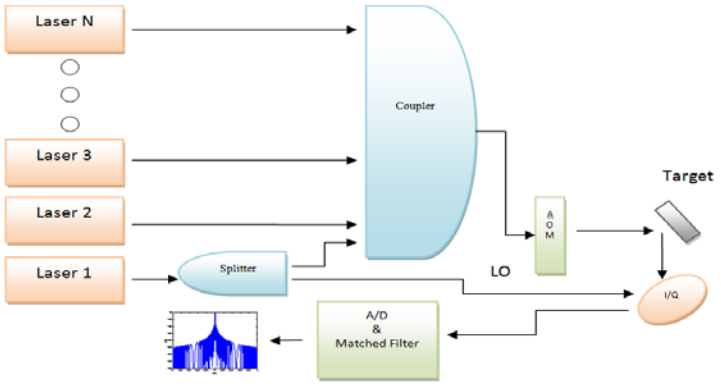

Figure 14: Sparse Frequency Signal Optical Design

(N frequency offset laser sources are multiplexed using a coupler and linearly frequency chirped using an acousto-optic modulator. One laser signal is picked off to mix with the N signals as the Local Oscillator (LO).)

The return signal is match filter processed by forming the autocorrelation function of the signal, u(t)[26]:

$$\chi(\tau,0)=\int_{-\infty}^{\infty}u(t)u^{*}(t+\tau)dt \tag{9}$$

The autocorrelation function is s special case of the more general ambiguity function defined as:

$$\chi(\tau,\nu)=\int_{-\infty}^{\infty}u(t)u^{*}(t+\tau)e^{i2\pi\nu t}dt \tag{10}$$

The velocity uncertainty of the object can be extracted by the frequency spectrum, υ, of autocorrelation function. For a stationary target the Doppler frequency is $\upsilon=0$. The complex signal corresponding to the N laser source system depicted in Figure 14 is defined as

$$u(t)\Big|_0^T=\tilde{A}\tilde{A}_{LO}^{*}\sum_{n=1}^{N}e^{i\left(2\pi(f_o+(n-1)df)t+\frac{1}{2}\beta t^2\right)}, \tag{11}$$

Where the pulse duration is T, df is the frequency offset for each source, and β is the chirp parameter defined as $\beta=2\pi B/T$. The parameter f_0 is a common frequency offset due to the AOM. It is retained because the LO does not have this frequency offset and therefore it placed a limit on digitizing the signal bandwidth for our experiments.
For $N=2$ the following expression for the autocorrelation function is derived[27]

$$|\chi(\tau,0)|=I\times I_{LO}\left|\begin{array}{l}\operatorname{sinc}(B\tau)e^{-i2\pi\left(f_o+\frac{B}{2}\right)\tau}\left(1+e^{-i2\pi df\tau}\right)\\ +\dfrac{B-df}{B}\left[\delta\left(\tau+\dfrac{Tdf}{B}\right)+\delta\left(\tau-\dfrac{Tdf}{B}\right)\right]e^{-i\frac{2\pi^2 df}{B}(df+2f_o)\tau}\\ \otimes\begin{cases}\operatorname{sinc}((B-df)\tau)e^{-i2\pi\left(f_o+\frac{B+df}{2}\right)\tau}, & if\ df\le B\\ 0, & if\ df>B\end{cases}\end{array}\right| \tag{12}$$

On the top line in Eq. (12) the *sinc* function is the autocorrelation of the single source; the following term on the first line is an interference contribution that narrows the central lobe as *df* increases. The delta functions on the second line produce two symmetric side peaks that are "ghost" or after-image copies of the autocorrelation function. The convolution shows that the after-image contributions widen as *df* increases. The autocorrelation function for *N=2* is plotted in Figure 15 as a function of τ and *df*. Note the central peak and the two strong side peaks, which broader and disappear at *df=B*. The central line narrows as the *df* increases, but for *df* > *B* side lobes grow.

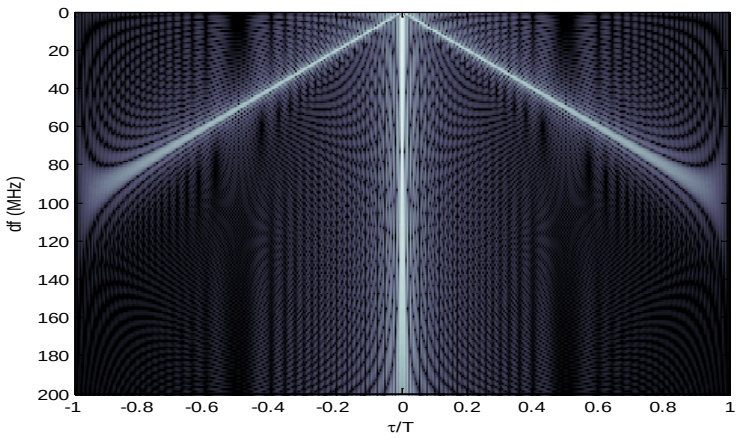

Figure 15: Magnitude of the Autocorrelation Function for B=100 MHz. After Ref.(3)

The price to pay for *df* > *B* is an increase in the side lobe amplitudes. This is best demonstrated by studying the results in Figure 16 comparing three sparse frequency signals with a single frequency signal. The Peak-to-side-lobe ratio (PSLR) is the ratio of the highest side-lobe peak to the height of the central peak. On the right side for a single frequency LFM signal the PSLR is constant for all bandwidths. On the left hand side the bandwidth is set to B=100 MHz; the PLSR first decreases as *df* is increased and the largest value around -15 dB is reached when *df=B*. Thereafter the PSLR increases and for *df*= 2B the PSLR is about -3.8 dB. It continues to increase so that the side lobes can be confused with a signal lobe. The range resolution on the other hand, which is based on the central lobe width, continues to improve as *df* is increased.

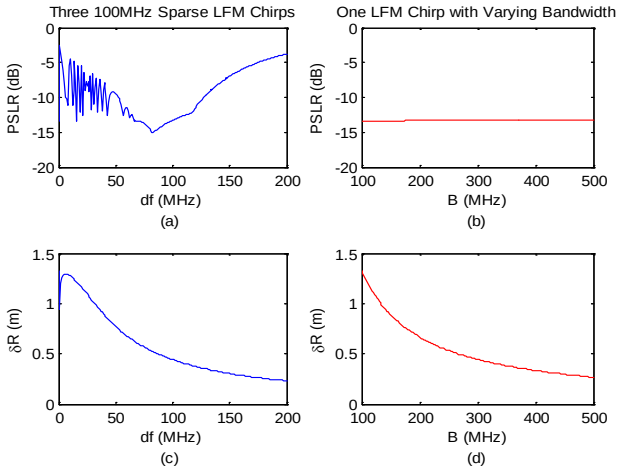

Figure 16: Comparison of a Single LFM Chip to Three 100MHz LFM Chirps

(Comparison of a superposition of three 100MHz LFM chirp signal to a single LFM chirp signal: (a) PSLR of sparse frequency LFM chirped signal, (b) PSLR of continues LFM chirp signal, (c) Range resolution of sparse frequency LFM chirped signal, (d) Range.)

4.8 Sparse Frequency – Linear Frequency Modulation Experiments

The SF-LFM experiments were performed after the theory and simulations had been completed. After the equipment was ordered there was a delay in delivering the pieces, but once the laboratory was in place the experiments were completed quite fast.
The schematic of the elementary experiment is shown in Figure 17. A highly Stable Laser Diode (HSLD) system was purchased from Innovation Photonic Solutions. The two diodes were frequency stabilized for hours and could be tuned to within about 1 MHz accuracy from 0 to over 1 GHz. We used polarization preserving fibers to split and combine the beams as shown. A Brimrose Acousto-optic modulator (AOM) was used to chirp the signal. Due to problems with the Variable Frequency (VF) driver electronics we were only able to achieve about B=37 MHz bandwidth. The frequency offset of the AOM was 750 MHz. As shown the VF driver was driver by a sawtooth wave form; since the VF driver delivered a triangularly response shaped function our bandwidth was severely limited. The signals were mixed in photodiodes (Thorlabs BW 6.5 GHz) and the PD output was passed to an Acqiris two channel digitizer each capable of 4 GSamples/s.

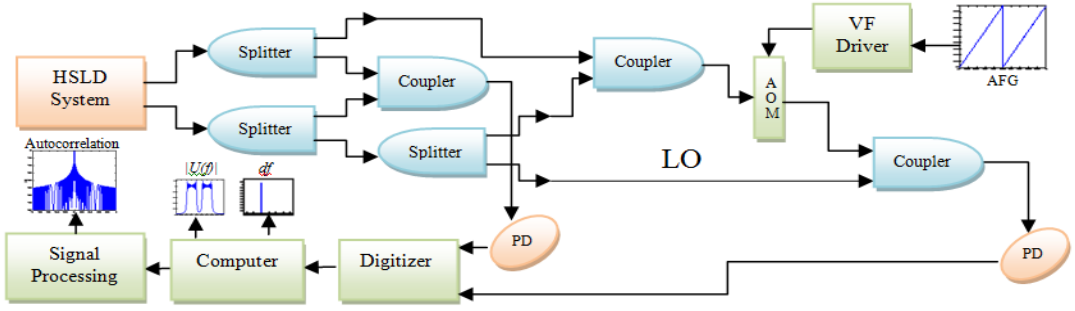

Figure 17: A schematic of the Experimental Setup with no Delay or Multiple Targets

An example of experimental results is shown in Figure 17[28]. The agreement between the theory and experiment was very satisfying. Resolution improvement of about a factor of

three was achieved with a PLSR around -3.8 dB and corresponding to an effective bandwidth of ~100 MHz.

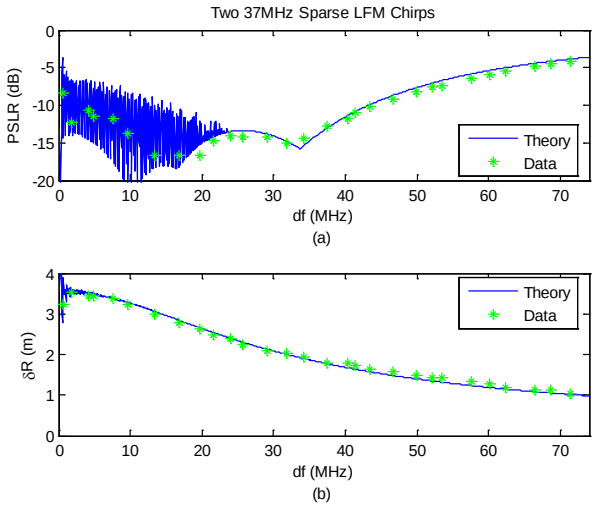

Figure 18: Comparison of Experimental Data and Modeling with Modified Waveform

(Range Resolution (a) and PSLR (b) for a 4μs LFM chirp with a 37MHz bandwidth)

4.9 Doppler Measurements

Eric Bailey undertook the measurement of Doppler shifts due to motion and identifying multiple targets with different velocities using the multiple frequency extension. The phase of successive signals returned from one or more targets was matched filter processed and the radial velocities of the targets were calculated. The ambiguity function is rewritten to include the possibility of signal attenuation and distortion:

$$\chi(\tau,\nu)=\int_{-\infty}^{\infty}u_{mf}(t)u_s^*(t+\tau)\exp(-i2\pi\nu t)dt\,. \tag{13}$$

The matched filter and signal for a two chirp SF-LFM signal is represented as

$$u_{mf}(t)=1/\sqrt{2T}\,\mathrm{Rect}(t/T)\left(A_1\exp\left[i\left(2\pi f_0 t+\tfrac{1}{2}\beta t^2\right)\right]+A_2\exp\left\{i\left[2\pi\left(f_0+df\right)t+\tfrac{1}{2}\beta t^2\right]\right\}\right), \tag{14}$$

where T is the signal time duration, A_1 and A_2 are the complex amplitudes of the matched filter, f_0 is the frequency offset due to the acousto-optic modulator. The rectangular function is defined as:

$$\mathrm{Re}\,ct(x)=\begin{cases}1\,, & |x|<1/2\\ 1/2\,, & |x|=1/2\\ 0\,, & |x|>1/2\end{cases}. \tag{15}$$

For a signal frequency bandwidth B, the signal chirp coefficient, β, is the slope of the LFM pulse; it is defined by $\beta=2\pi B/T$, and df is the offset frequency between the two laser sources. The time delayed return signal is then recorded and defined by:

$$u_s(t) = 1/\sqrt{2T}\ \mathrm{Rect}\left[(t-t_1)/T\right]\begin{pmatrix} A_3 \exp\left\{i\left[2\pi f_0(t-t_1) + \tfrac{1}{2}\beta(t-t_1)^2\right]\right\} + \\ A_4 \exp\left\{i\left[2\pi(f_0+df)(t-t_1) + \tfrac{1}{2}\beta(t-t_1)^2\right]\right\} \end{pmatrix}, \quad (16)$$

where the parameters are the same as defined after Eq. (3) with the following additions: the A's are the respective complex amplitudes of the return signal and signal t_1 is time delay of the signal related to the target range, R, by $t_1 = 2R/c$.

Substituting Eqs. (8) and (10) into Eq. (7) yields the following ambiguity function

$$\chi(\tau,\nu) = \alpha \exp\left[-i(2\pi f_0 + \pi df - \pi\nu)(\tau - t_1)\right]\left[1-(\tau-t_1)/T\right]\times \\ \begin{Bmatrix} \cos\left[\pi df(\tau-t_1)\right]\mathrm{sinc}\left[(\tfrac{1}{2}\beta\tau - \tfrac{1}{2}\beta t_1 + \pi\nu)(T+\tau-t_1)\right] + \\ \tfrac{1}{2}\exp(-i\Delta\phi)\mathrm{sinc}\left[(\pi df + \tfrac{1}{2}\beta\tau - \tfrac{1}{2}\beta t_1 + \pi\nu)(T+\tau-t_1)\right] + \\ \tfrac{1}{2}\exp(i\Delta\phi)\mathrm{sinc}\left[(-\pi df + \tfrac{1}{2}\beta\tau - \tfrac{1}{2}\beta t_1 + \pi\nu)(T+\tau-t_1)\right] \end{Bmatrix}, \quad (17)$$

Where $\Delta\phi$ is the phase difference between A_1 and A_2. The assumptions used to arrive at Eq. (17) are: the magnitudes of the complex amplitudes are equalized and normalized to 1, ie: $|A_\alpha| = 1$. Due to equal changes in optical path length (OPL), there is a relationship between the complex amplitudes that is $A_3^* = \alpha A_1^*$ and $A_4^* = \alpha A_2^*$ where α is, in general, an overall amplitude and phase change that is proportional to the OPL.

The parameters f_0, df, $\Delta\phi$, and ν remain constant over multiple measurement instances; then the only term α changes between successive measurements. The form of this parameter is chosen as purely a phase change:

$$\alpha = \exp(-i\phi). \quad (18)$$

The phase change between two successive pulses is then:

$$\delta\phi = \phi_1 - \phi_2. \quad (19)$$

The relationship between ϕ_1 and ϕ_2 are related to the change in OPL and given as a function of velocity:

$$\phi_2 = \phi_1 + 4\pi\nu\Delta t / \lambda_{Carrier}, \quad (20)$$

where ν is the velocity of the target, Δt is the time delay between the two pulses, and $\lambda_{Carrier}$ is the carrier wavelength. Likewise, from phase change one can back out the velocity to be:

$$\nu = \delta\phi/(2\pi)\times\lambda_{Carrier}/(2\Delta t). \quad (21)$$

Selected results from Bailey's thesis are shown in Figure 19. For the image on the left hand side two data sets are shown for single targets one stationary and the other moving. The right side image is the return phase shift for two distant targets, one is stationary (red points) and the other is moving (black points). The measured velocities were on the order of 1-10 mm/s. For measurements every microsecond and allowing for a phase sampling of say $\pi/4$ radians as the maximum change for unambiguous phase measurements, the maximum velocity measured by this technique would be about 0.2 m/s. This could be adapted for vibration measurements, but would not be an approach for target velocities of most vehicles.

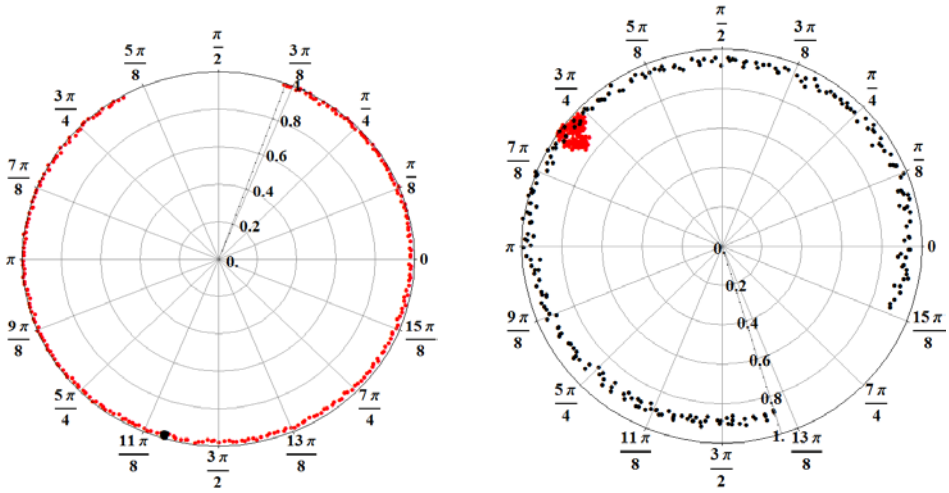

Figure 19: Experimental Results for Single Target (Left) and Multiple Targets (Right)

(Left: Single target results. The moving target phase data is plotted in red. The stationary target data is plotted in black. Right: Multiple targets with a close stationary target (red data points) and a distance moving target (black data points).)

4.10 Extension to Stretch Processing

LFM Radar concept was introduced as a rich phenomenology for accurately measuring target range and velocity[29]. Indeed this technology was adapted to the optical regime and there are many examples of LFM LADAR already found in the literature [30-38].

Perhaps the most popular form of LFM LADAR is when both the signal and the LO are linearly ramped. This reduces the required bandwidth and processing the delayed echo signal with a chirped LO produce a beat signal that is directly related to the target range[30]. The performance of these systems depends on the pulse time duration and frequency ramp, and linearity of the optical frequency sweep[31]. Optical frequency sweeps of several GHz have been reported[32, 33]. Sub-millimeter resolution, optical bandwidths of hundreds of GHz are required and to achieve this an algorithmic stitching approach was used by Vasileyev [33] to increase the effective bandwidth of resulting in 500 µm range resolution. The philosophy of their approach is similar to that adopted in our earlier papers [25,27,28]. It is also noteworthy that a frequency chirp bandwidth of almost 5 THz was also demonstrated using a self-heterodyne technique by Piracha et al.[34,35]. This list is by no means exhaustive with many other significant contributions made on the topic.

The stretch processing concept is illustrated in Figure 20. In the optical domain the LO (blue line) and the signal (green line) have different frequencies because the return signal was delayed by a time t_1. The photodiode detects the interference between the LO and signal and the output is an RF signal with frequency *df*, which can be directly related to the time delay t_1.

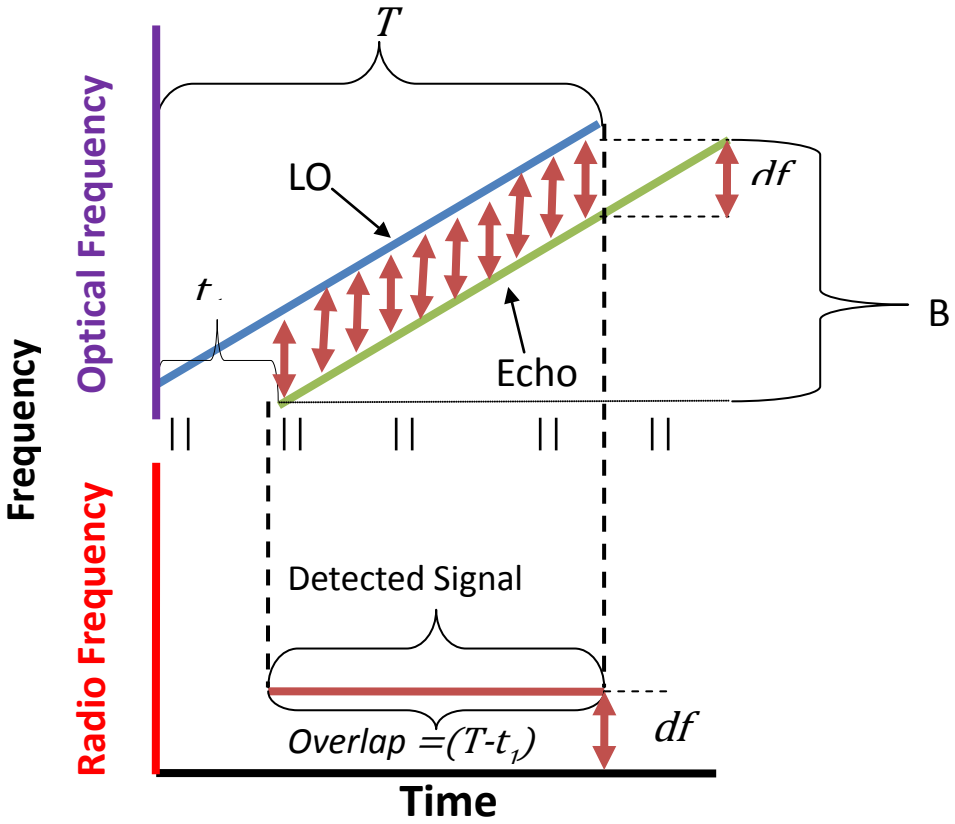

Figure 20: The Optical and RF Domains of Stretch Frequency Processing

Robert Brown's thesis introduced a new multi-frequency Stretched Processing (MFSP) technique by using two frequency chirped pulses and beat with a single LO on each of them. The essence of his technique is shown in Figure 21. The distinction from Figure 20 is that now two signal waves are delayed and interfered on the photodiode with a chirped LO. As a result two beat frequencies are observed.

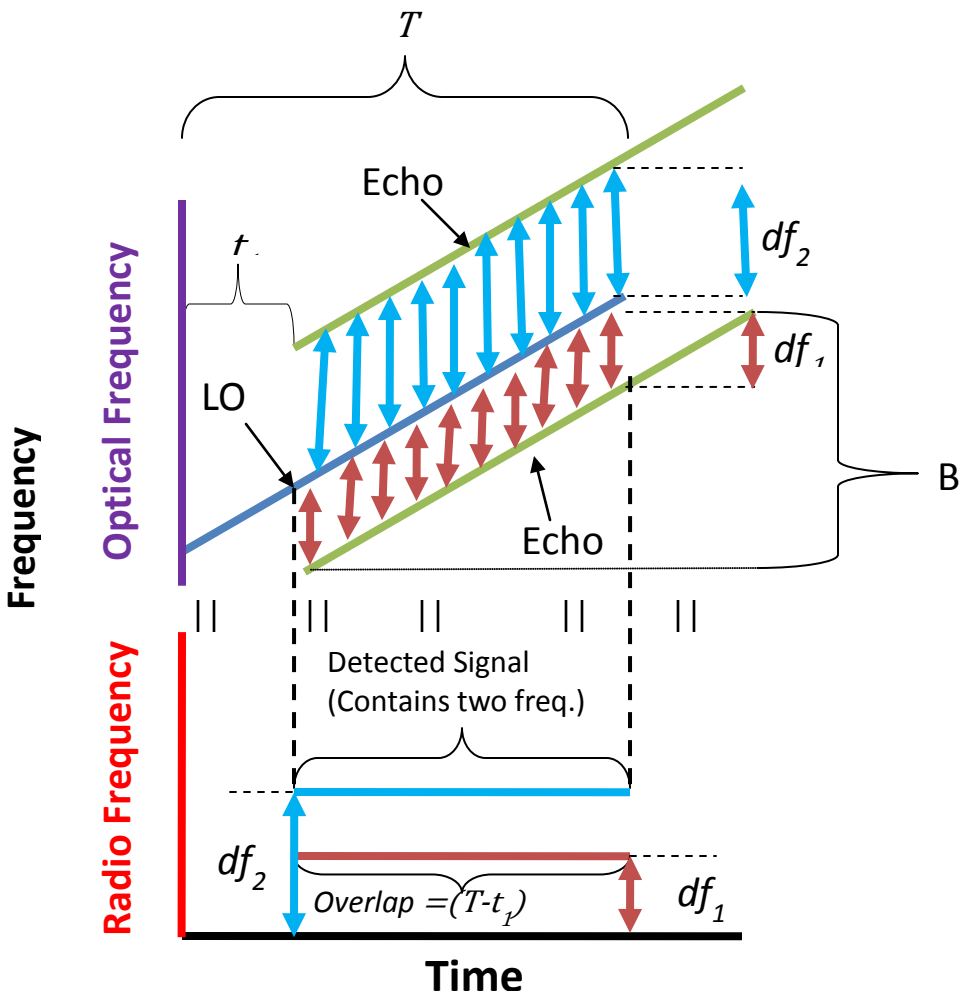

Figure 21: Multi-frequency Stretched Processing (MFSP) Illustrated with Two Signals.

(The LO has two offset frequencies (df1,df2) that are measured as RF frequencies. The analysis of these signals gives the range to the target.)

To determine the improvement in range resolution the signals needed a post processing algorithm. The measured time series of the two signals was Fourier transformed to extract the frequency spectra of each signal and them each segment was inverse Fourier transformed to the time domain where the relative phase between each segment could be determined. Finally the two time series were stitched together and the autocorrelation function of the composite signal was measured. Results are illustrated in Figure 22. The upper frequency and lower frequency band data alone each yield a broader autocorrelation function. When the two are stitched together with the relative phase corrected between tem, the result is an autocorrelation with about 2 times improved in the range resolution. In Brown's experiments the bandwidth was low and the final range resolution corresponds to 24 m. The effective bandwidth was about 6 MHz for this experiment. Table 3 summarizes the theses and dissertations provided in the stretch processing technical area.

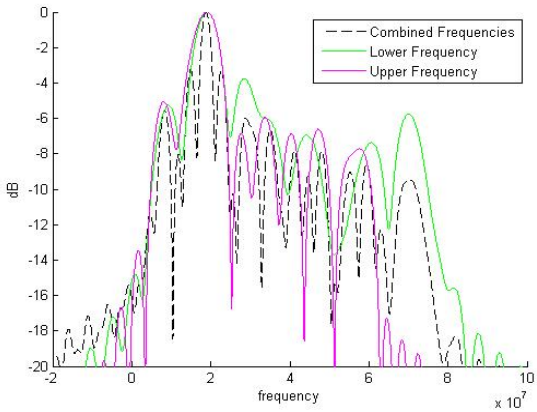

Figure 22: Autocorrelation Function for the MFSP Data

Last name	First Name	Year of Graduation	Degree	Advisor	Thesis Title
Chimenti	Robert	2009	M.S.	Peter Powers	Sparse Frequency Linearly Frequency Modulated Laser Radar Signal Generation, Detection, and Processing
Bailey	Eric	2010	M.S.	Peter Powers	Sparse Frequency, Linearly Frequency Modulated Laser Radar Signal Modeling and Doppler Processing
Brown	Robert	2011	M.S.	Joe Haus	Stretch Processing of Simultaneous, Segmented Bandwidth Linear Frequency Modulation in Coherent LADAR

Table 3: Stretch Processing Oriented Student Projects

4.11 IR and THz Laser Theses and Dissertations

Laser sources that can cover important wavelength bands in several atmospheric transmission windows are not widely available with the pulse energies and wavelength agility required to defeat potential threats. As a result the Air Force has a significant Air Force interest in developing MWIR and LWIR lasers to solve the technical hurdles. For non-destructive testing and evaluation purposes AFRL has an interest in pursuing THz technology, as well. Brian Dolasinski has been working in LOCI with a laser setup and also performing experiments at AFRL. Table 4 shows theses in this technical area.

Last name	First Name	Year of Graduation	Degree	Advisor	Title of Thesis or Dissertation
Evans	Jonathon	2010	M.S.	Peter Powers	Rapid Beam switching of an ND-YAG Laser using domain Engineered Prisms in 5 MOL% Magnesium-Oxide Doped Congruent Lithium Niobate
Feaver	Ryan	2011	M.S.	Peter Powers	Longwave-IR Optical Parametric Oscillator in Orientation Patterned Gallium Arsenide
Phelps	Charles	2011	M.S.	Peter Powers	Diode-Pumped 2Micron Q-Switched TM: YAG Microchip Laser
Voratovic	Dayen	2011	M.S.	Peter Powers	Generation and Detection of Coherent Pulse Trains in Periodically Poled Lithium Niobate through Optical Parametric Amplification
Dolasinski	Brian	2013 projected	Ph.D.	Peter Powers	THz Generation by Difference Frequency Generation in a DAST Crystal
McDaniel	Sean	2012	M.S.	Peter Powers	Seeded, Gain-Switched Chromium doped Zinc Selenide Amplifier

Table 4: MWIR Laser Oriented Student Projects

The work on laser sources was supported through other AFRL funds, Industry Partner Grants and internal funds from EOP. Four of the students (Evans, Feaver, Phelps and McDaniel) in Table 4 worked in the IR Counter Measures group of Drs. Ken Schepler and Rita Peterson. They were paid directly from Base funds usually in a Coop status. In addition Lockheed Martin sponsored some work on seeding of a laser which could be done in the Mid IR region. LOCI research efforts in developing infrared sources have focused on supporting laser radar and remote sensing applications. Dr. Peter Powers' group has addressed MWIR laser technology by developing nonlinear optics based frequency converters as well as direct laser sources. The nonlinear frequency conversion efforts looked at ways to use widespread commercially available lasers as pump sources, which are subsequently frequency converted to a particular wavelength of

interest. This work centered on using the engineered crystals periodically poled lithium niobate and orientation patterned gallium arsenide to quasi-phase match the nonlinear interaction for highly flexible and efficient frequency conversion. Efforts in this area were primarily accomplished through the work of graduate students Ryan Feaver, Brian Dolasinski, Dayen Voratovic, and Jonathon Evans. While Dayen Voratovic converted a ~1 μm pump to ~1.5 μm with the idler of ~3.5 μm. If a narrow line seed laser was available then the idler and signal wavelengths could have been switched. In a parallel effort, graduate students Charles Phelps and Sean McDaniel worked on laser sources that directly operate at wavelengths of importance in the infrared. Their projects centered on developing a 2 μm thulium doped YAG microchip laser and on a 2.5 μm gain-switched chromium-doped zinc selenide master-oscillator power amplifier system. Both projects focused on not only generating lasers at specific wavelengths, but also on using system architectures that allows for the lasers to be deployed in harsh environments.

4.12 Summary Description of Student Projects

This section summarizes information about students' research topics with an abstract for the work, the committee, and if available, a quad chart describing the thesis or dissertation. US national students doing graduate work under the LOCI co-operative agreement are listed in Tables 5 and 6. Table 5 lists the students who were in the program from its inception to 2011. In Table 6 the students graduated in 2012 or are continuing students.

The Tables show that one of the objectives of the co-operative agreement is being realized. Namely, the training of U.S. citizen's in fields that are relevant to future warfighter capabilities. Over time a larger number of faculty and staff advisors have become involved in the training of students and our course offerings have expanded, as well. Looking over the table we see Dr. Peter Powers has advised, or is advising , 8 students, Dr. Brad Duncan 6 students, Dr Ed Watson and Dr. Haus advised 3 students each, Dr. Mikhail Vorontsov and Dr. Paul McManamon have advised 2 students, and Dr. Andrew Sarangan, Dr Partha Banerjee, and Dr Matt Dierking have advised 1 student. This shows the kind of diversity we are achieving and moreover, UD EOP has recognized the value of having AFRL personnel as primary technical advisors for the students. UD has given Drs. Dierking and Watson Graduate faculty status, which means they can Chair Ph.D. committees.

LOCI recognizes that we have some areas of weakness, such as signal and image processing. We have tried to fill these areas by tapping into the expertise of Electrical and Computer Engineering faculty, such as Drs Vijay Asari, Keigo Hirakawa and Russell Hardie. We have also sought to partner with Dr. James Fienup at the University of Rochester, a noted expert in the field and we work with companies, such as MZA on projects. We have the capability to work on processing oriented topics.

Student theses and dissertations are now available online through OhioLink. When available the URL link to the website has been listed.

Last name	First Name	Graduation Year	Degree	Advisor	Thesis or Dissertation Title
Greiner	Michael	2007	M.S.	Brad Duncan	Monte Carlo Simulation of Tree Canopy Scattering and Propagation
Miller	Nicholas	2007	M.S.	Brad Duncan	Optical Sparse Aperture Imaging
Chimenti	Robert	2009	M.S.	Peter Powers	Sparse Frequency Linearly Frequency Modulated Laser Radar Signal Generation, Detection, and Processing
Drain	Katharine	2009	M.S.	Qiwen Zhan	Novel Optical Components for Non-Mechanical Beam Steering
Stafford	Jason	2009	M.S.	Brad Duncan	Perturbation Analysis and Experimental Demonstration of Holographic Aperture LADAR Systems
Stokes	Andrew	2009	M.S.	Brad Duncan	Improving Mid-Frequency Contrast in Sparse Aperture Optical Imaging Systems Based Upon the Golay-N Family of Arrays
Bailey	Eric	2010	M.S.	Peter Powers	Sparse Frequency, Linearly Frequency Modulated Laser Radar Signal Modeling and Doppler Processing
Cordray	Jared	2010	M.S.	Ed Watson	Investigation of Liquid Crystal Spatial Light Modulators to Simulate Speckle Fields
Evans	Jonathon	2010	M.S.	Peter Powers	Rapid Beamswitching of an ND-YAG Laser using domain Engineered Prisms in 5 MOL% Magnesium-Oxide Doped Congruent Lithium Niobate
Greiner	Michael	2010	Ph.D.	Brad Duncan	Effects of Multiple Photon Scattering in Deciduous Tree Canopies
Brown	Robert	2011	M.S.	Joe Haus	Stretch Processing of Simultaneous, Segmented Bandwidth Linear Frequency Modulation in Coherent LADAR
Conrad	Dallis	2011	M.S.	Ed Watson	Speckle Statistics of Articulating Objects
Duran	Josh	2011	M.S.	Andrew Sarangen	Ion Implementation Study of Be in InSb for Protodiode Fabrication
Feaver	Ryan	2011	M.S.	Peter Powers	Longwave-IR Optical Parametric Oscillator in Orientation Patterned Galliaum Arsenide
Kraczek	Jeffrey	2011	M.S.	Paul McManamon	An Evaluation of the Effects of the Ability to Measure Piston on Multi-aperture Spatial Heterodyne Systems
Phelps	Charles	2011	M.S.	Peter Powers	Diode-Pumped 2Micron Q-Switched TM: YAG Microchip Laser
Reierson	Joseph	2011	M.S.	Mikhail Vorontsov	Analysis of Atmospheric Turbulence Effects on Laser Beam Propagation using Multi-wavelength Laser Beacons
Voratovic	Dayen	2011	M.S.	Peter Powers	Generation and Detection of Coherent Pulse Trains in Periodically Poled Lithium Niobate through Optical Parametric Amplification

Table 5: US National Graduate Students Sponsored Through 2011

LOCI 2007 Graduates

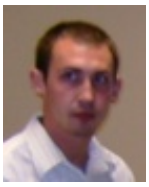

Michael Greiner
Degree: Master of Science (M.S.), University of Dayton, Electro-Optics, 2007

Title: **Monte Carlo Simulation of Tree Canopy Scattering and Propagation**

Abstract: The objective of his research was to investigate the physical and optical properties of tree canopies in order to develop an improved foliage penetration model. This project was broken into two separate segments: experimental and simulation. The experimental portion presents his investigations into the optical scattering properties of both maple and cottonwood leaves in the near-infrared wavelength regime. The bidirectional scattering distribution function (BSDF) describes the fractions of light reflected by and transmitted through a leaf for a given set of illumination and observation angles. Experiments were performed to measure the BSDF of each species at a discrete set of illumination and observation angles. He then modeled the BSDF's in such a way that other researchers may interpolate their values for scattering in any direction under illumination at any angle.

In the modeling segment of the research he created a Monte Carlo algorithm for tracking the propagation of photons through a canopy consisting of many randomly distributed leaves. He used several different methods for modeling the individual scatterers based on the experimental results: ideal Lambertian, Lambertian-Rayleigh, and the interpolated data model. The output coordinates of the photons were saved and used quantify the temporal, spatial, and angular dispersion experienced by an incident pencil beam through a foliated forest canopy. The results of each leaf model were then compared such that an optimum method was determined.

Committee/Advisors:

Bradley D. Duncan, PhD (Committee Chair)
Matthew P. Dierking (Committee Member)
Joseph W. Haus, PhD (Committee Member)

Nicholas J. Miller
Degree: Master of Science (M.S.), University of Dayton, Electro-Optics, 2007

Title: **Optical Sparse Aperture Imaging**

Abstract: The resolution of a conventional diffraction limited imaging system is proportional to its pupil diameter. A primary goal of sparse aperture imaging is to enhance resolution while minimizing the total light

collection area, the latter being desirable, in part, because of the cost of large, monolithic apertures. Performance metrics are defined and used to evaluate several sparse aperture arrays constructed from multiple, identical, circular sub-apertures. Sub-aperture piston and/or tilt effects on image quality are also considered. Based on the observed qualitative behavior of simple linear arrays, we select arrays with compact nonredundant autocorrelations first described by Golay. We vary both the number of sub-apertures and their relative spacings to arrive at an optimal array. We report the results of an experiment in which we synthesized an image from multiple sub-aperture pupil fields by masking a large lens with a Golay array. For this experiment, we imaged a slant edge feature on a resolution target in order to measure MTF. We note the contrast reduction inherent in images formed through sparse arrays and demonstrate the use of a Wiener-Helstrom filter to restore contrast in our experimental images. Finally, we describe a method to synthesize images from multiple sub-aperture focal plane intensity images using a phase retrieval algorithm to obtain estimates of sub-aperture pupil fields. Experimental results of synthesizing an image of a point object from multiple sub-aperture images are presented and weaknesses of the phase retrieval method for this application are discussed.

Committee/Advisors:

Bradley D. Duncan, PhD (Committee Chair)
Joseph W. Haus, PhD (Committee Member)
Matthew P. Dierking (Committee Member)

LOCI 2009 Graduates

Robert Chimenti

Degree: Master of Science (M.S.), University of Dayton, Electro-Optics, 2009

Title: **Sparse Frequency Linearly Frequency Modulated Laser Radar Signal Generation, Detection, and Processing**

Abstract: Linearly frequency modulated (LFM) laser radar (LADAR) signals allow for an increase in signal bandwidth without the need to utilize temporally shortened laser pulses. This allows for the measurement of both range and velocity, without the sacrifice of signal to noise ratio. While LFM signals are easily generated in the radio-frequency (RF) domain the ability to produce large linear chirps in the optical domain is limited by device constraints. To overcome this issue we have proposed a unique method of increasing the effective bandwidth of a LFM LADAR signal by superimposing two or more sparse frequency signals which are then linearly chirped using a conventional modulator. Both numerical and analytical models have been developed which show the viability of these types of signals. An experiment was conducted to verify the results of the modeling using two frequency offset locked lasers, whose outputs were detected using heterodyne techniques and post processed to extract the range resolution and peak to sidelobe ratio of the matched filter output. Finally a target at range was simulated by the use of a fiber optic delay line and detected and compressed through coherent on receive processing.

Committee/Advisors:

Peter E. Powers, PhD (Committee Chair)
Matthew P. Dierking (Committee Member)
Joseph W. Haus, PhD (Committee Member)

Sparse Frequency LFM Ladar Signals

Robert V. Chimenti, Matthew P. Dierking, Peter E. Powers, Joseph W. Haus

Goal

To Increase the total bandwidth of a LFM ladar signal without the need for large modulation bandwidth, through the use of segmented bandwidth in order to improve range resolution.

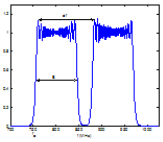

Technical Approach

Superposition of two lasers with controllable frequency offsets coupled into the same AO modulator. This will insure that both lines get he same modulation and that the resulting modulation noise is correlated between the two lines.

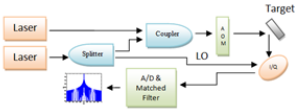

Major Issues

- Tuning the difference frequency between two locked lasers in real time by 1MHz increments. We plan to overcome this issue by isolating the two lasers in micro-Kelvin ovens, and temperature tuning difference frequency between the two lines.
- Interference between the two chirps in the frequency domain introduces additional ambiguity peaks in the matched filter output when the difference frequency is less then the modulation bandwidth.

I graduated from Rowan University in 2007 with a B.S. in Physics and a minor in Mathematics, and from Peirce College in 2006 with a B.S. in Business Administration with a concentration in Management. I am currently finishing my M.S. in Electro-Optics at the University of Dayton . Before coming to the LOCI I worked for two and a half years at Light Age Inc. where I worked with alexandrite and Nd:YAG lasers systems for various medical, industrial, and scientific applications.

Expected Outcomes

We expect to be able to produce large range resolution with out the need for extremely large bandwidth AO modulators

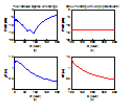

We expect the peak-to-sidelobe ratio will be the best when the difference frequency is just slightly less then the modulator bandwidth

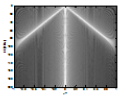

Katharine Drain

Degree: Master of Science (M.S.), University of Dayton, Electro-Optics, 2009

Title: **Novel Optical Components for Non-Mechanical Beam Steering**

Abstract: Non-mechanical beam steering can be accomplished by various devices/techniques such as a liquid crystal spatial light modulator or a parabolic mirror combined with a Goos-Hänchen focal plane shifter. For this application, a suitable transmit/receive (Tx/Rx) switch that isolates the transmitter from the receiver of the system is required. For a liquid crystal spatial light modulator, beam steering occurs when the incident beam is linearly polarized at a prescribed orientation. Previous Tx/Rx switches utilized a circularly polarized beam in conjunction with a polarization beam splitter, which proved to be a lossy solution. By using a two-dimensional reflection type liquid crystal spatial light modulator with a large aperture Faraday rotator, it is possible to develop a more efficient Tx/Rx switch for non-mechanical beam steering, which can be applied to laser scanning imaging systems. In the first section of this thesis, I will present the proposed design of such a switch along with demonstrating the experimental results at a 1.064μm operation wavelength for steering angles up to 2°. Also, the characterization of the Faraday rotator was addressed in terms of its allowable field of view and imaging quality. For the second portion of this thesis, electronic electro-optic beam steering techniques will be discussed for faster scanning speeds, larger steering angles, and higher efficiency than liquid crystal spatial light modulators. In particular, calculations for the theoretical and experimental steering angles at various translational distances of a parabolic mirror are shown. Finally, the theory behind utilizing the Goos-Hänchen effect as a focal plane shifter will be presented.

Committee/Advisors:

Qiwen Zhan, PhD (Committee Chair)
Joseph W. Haus, PhD (Committee Member)
Robert Nelson, PhD (Committee Member)
Edward A. Watson, PhD (Committee Member)

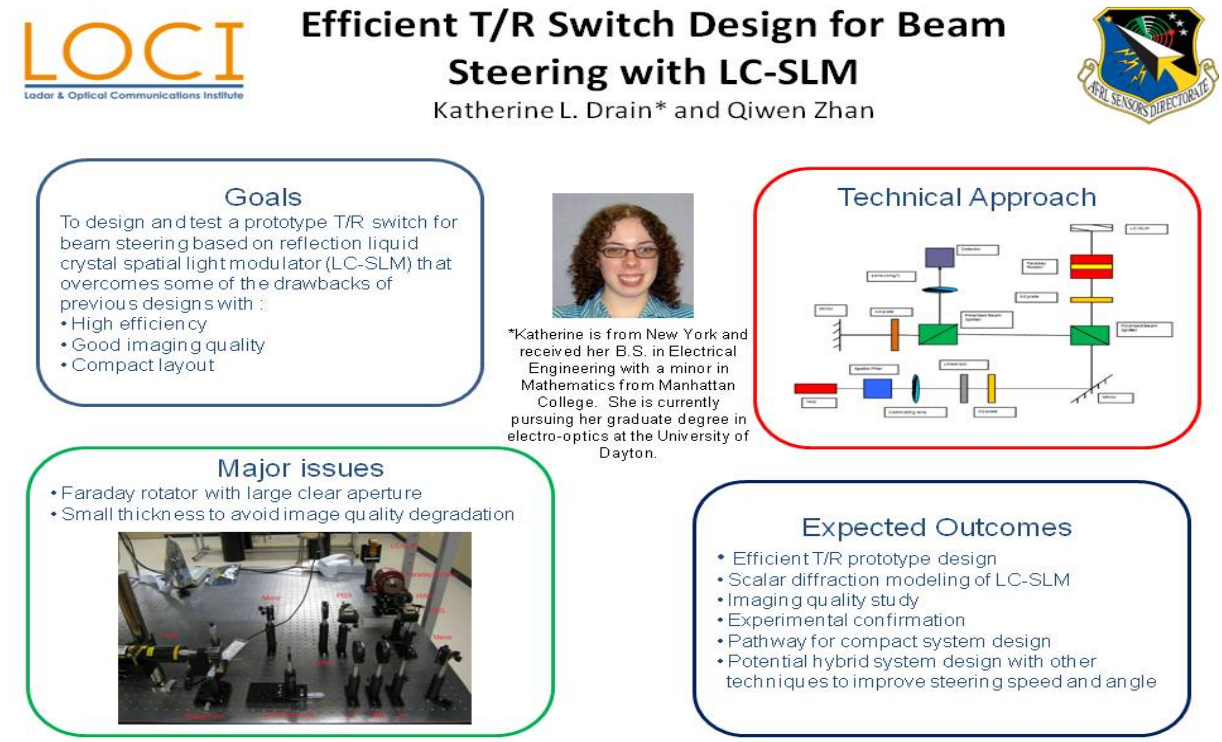

Jason Stafford

Degree: Master of Science (M.S.), University of Dayton, Electro-Optics, 2009.

Title: **Perturbation Analysis and Experimental Demonstration of Holographic Aperture LADAR Systems**

Abstract: Synthetic aperture radar (SAR) and its cousin in the optical regime, synthetic aperture LADAR (SAL) have been employed to overcome limited resolution in long range remote sensing. Both methods typically use a single antenna or detector acting as a point receiver and take advantage of platform motion to collect multiple coherent shots in order to synthesize a larger cross-range receiving aperture. Holographic aperture LADAR (HAL) is a recent variant of SAL that uses a translating imaging sensor instead of a point detector to allow for angle-angle imaging and increased longitudinal cross-range resolution. Here, we will focus on a perturbation analysis and experimental verification of the stripmap HAL transformation. Since the HAL transform requires precise knowledge of the data collection sites, real world application of this technique is difficult. Both laser pulse jitter and system platform vibration will negatively affect the efficacy of the HAL process. In an effort to characterize the impact of these factors on a HAL system's performance, several image quality metrics and a numerical model are developed. The results of this perturbation analysis will be used in the laboratory work to

follow, where we demonstrate and confirm some of the theoretical predictions for the stripmap HAL method. The previous theoretical work assumed prior access to multiple pupil plane field segments and focused upon the development of the required phase transformations. For the work described herein, an actual collection of field segments was created via off-axis digital holography. We then substantiate the HAL transformation's ability to precisely correct for the effects due to an off-axis transmitter and most importantly we confirm the capacity of the method to provide an increase in longitudinal cross-range resolution.

Committee/Advisors:

Bradley D. Duncan, PhD (Committee Chair)
Matthew P. Dierking, PhD (Committee Member)
Joseph W. Haus, PhD (Committee Member)

LOCI
Ladar & Optical Communications Institute

Perturbation analysis and demonstration of Holographic Aperture Ladar

Jason W. Stafford, Bradley D. Duncan, Matthew P. Dierking,

AFRL SENSORS DIRECTORATE

Goals

Characterize the effects of laser pulse jitter and platform positional uncertainty on HAL systems. Demonstrate the performance of a HAL system in the lab.

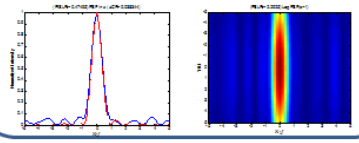

Technical Approach

Determine image quality metrics to assess impacts of uncertainty on final image. These address common concerns such as ghosting, SNR, resolution and wave front error. Implement Monte Carlo simulation of HAL system. Design and build HAL system.

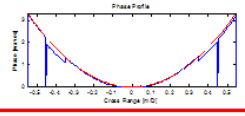

Major Issues

Since the HAL transform requires precise knowledge of data collection sites, positional uncertainty, especially piston , is a major concern. These problems are compounded with the small scales of a bench top setup.

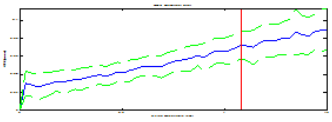

Expected Outcomes

Our model suggests that HAL systems are relatively robust under the effects of longitudinal positional uncertainty and pulse-to-pulse laser jitter; however, piston phase effects are still an obstacle to diffraction limited performance.

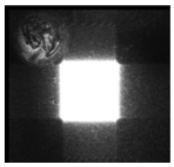

Andrew Stokes

Degree: Master of Science (M.S.), University of Dayton, Electro-Optics, 2009.

Title: **Improving Mid-Frequency Contrast in Sparse Aperture Optical Imaging Systems Based Upon the Golay-N Family of Arrays**

Abstract: Sparse aperture imaging systems are capable of producing high resolution images while maintaining a small overall light collection area compared to a fully filled aperture yielding the same resolution. This is advantageous for applications where size, volume, weight and/or cost are important. However, sparse aperture systems pay the penalty of reduced contrast at midband spatial frequencies. The focus of this work has been on increasing the midband contrast of sparse aperture imaging systems based on the Golay-*N* family of arrays. These arrays are of interest due to their compact, non-redundant autocorrelations. The modulation transfer function provides a quantitative measure of both the resolution and contrast of an imaging system and, along with an average relative midband contrast metric, will be used to compare perturbations to the Golay arrays. Numerical calculations have been performed to investigate the behavior of Golay-9 and -12 arrays into which autocorrelation redundancy has been introduced. An increase in midband average relative contrast of over 55% was experimentally verified for the Golay-9 array.

Committee/Advisors:

Bradley D. Duncan, PhD (Committee Chair)
Matthew P. Dierking, PhD (Committee Member)
Joseph W. Haus, PhD (Committee Member)

LOCI 2010 Graduates

Eric Bailey

Degree: Master of Science (M.S.), University of Dayton, Electro-Optics, 2010.

Title: **Sparse Frequency, Linearly Frequency Modulated Laser Radar Signal Modeling and Doppler Processing**

Abstract: Sparse frequency, linearly frequency modulated laser radar (LADAR) signals achieve improved range resolution comparable to a larger signal bandwidth. From basic radar/LADAR principles it is known that the bandwidth of a signal is inversely proportional to range resolution. Hence, the effective bandwidth of a LADAR signal using sparse frequency techniques is larger than the bandwidth of each modulated laser frequency. Previous experiments have validated range resolution and peak to sidelobe ratio derived from models utilizing two segmented bandwidths. This thesis discusses the modeling with three segmented bandwidths. The model is verified against an experimental setup using three frequency offset lasers. The two segmented bandwidth, sparse frequency LADAR signal is reexamined to include Doppler effects. The new modeling utilizes a coherent on receive setup allowing for phase information to be processed from the signal. The extracted phase information can be used to determine characteristics about a target, namely its speed and direction with respect to the receiver. This modeling was experimentally verified for cases where the target was next to the receiver, at a distance (simulated through a fiber delay line), and for multiple targets. As a final check of the modeling, the velocity determined from the phase information was compared against the velocity readout of a stage with a built in optical encoder.

Committee / Advisors

Peter E. Powers, PhD (Committee Chair)
Matthew P. Dierking, PhD (Committee Member)
Joseph W. Haus, PhD (Committee Member)

URL: http://rave.ohiolink.edu/etdc/view?acc_num=dayton1271937372

Jared Cordray

Degree: Master of Science (M.S.), University of Dayton, Electro-Optics, 2010.

Title: **Investigation of Liquid Crystal Spatial Light Modulators to Simulate Speckle Fields**

Abstract: We investigate liquid crystal spatial light modulators as a means to simulate the speckle fields produced by laser light scattering off of rough surfaces. Of primary interest was the ability of these devices to accurately simulate the statistical properties of speckle fields. Characterization of the liquid crystal spatial light modulators was performed and a look-up table was created that specified the required voltage for a desired phased on a pixel-by-pixel basis. A model was created to simulate the field leaving the device and the resulting irradiance distribution in the far field. The 2nd and 4th moments of the field at the observation plane were calculated to determine the mean irradiance and contrast of the speckle pattern. Two random phase distributions that create the speckle patterns were investigated. These distributions were uniform phase distribution and "wrapped" Gaussian phase distribution. It was found that the devices are unable to simulate spatially stationary irradiance and contrast. Experimental investigations showed good agreement with the theoretical data except where $\sigma < 0.1\pi$.

Committee / Advisors

Edward A. Watson, PhD (Committee Chair)
Joseph W. Haus, PhD (Committee Member)
Zhan Qiwen, PhD (Committee Member)

URL: http://rave.ohiolink.edu/etdc/view?acc_num=dayton1272472315

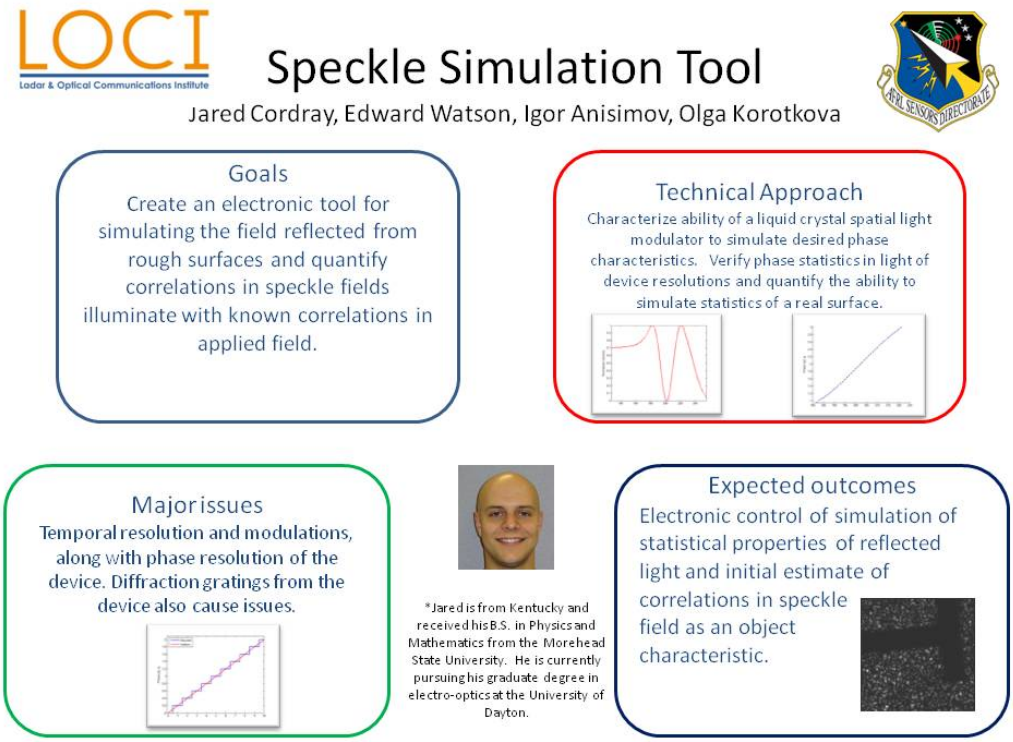

Jonathon Evans

Degree: Master of Science (M.S.), University of Dayton, Electro-Optics, 2010.

Title: **Rapid Beamswitching of an ND-YAG Laser using domain Engineered Prisms in 5 MOL% Magnesium-Oxide Doped Congruent Lithium Niobate**

Abstract: In this work, a novel electro-optic beam switch (EOBS) is designed, fabricated and demonstrated. The EOBS presented in this work is designed for a Nd:YAG laser operating at $\lambda = 1064$ nm and is demonstrated to achieve >750 μm of beam translation at switching rates of up to 3 Hz.

The EOBS consists of a series of electronically controlled prisms fabricated by ferroelectric domain inversion in an electro-optic crystal wafer. The prisms are arranged such that positive angular deflections are counterbalanced by subsequent negative angular deflections. The result is discrete beam translation with no angular deflection.

In this work, an algorithm for designing optimal beam translation geometries is developed. Five of the resulting geometric designs are then fabricated in 5 mol% magnesium oxide doped congruent lithium niobate (5%MgO:CLN). The performance of one particular geometry is modeled in detail and analyzed experimentally. The EOBS is used to demonstrate

wavelength tuning of a near-infrared laser system using a selectable optical parametric generation (OPG) grating.

Committee/Advisors:

Peter E. Powers, PhD (Committee Chair)
Andrew Sarangan, PhD (Committee Member)
Kenneth L. Schepler, PhD (Committee Member)

URL: http://rave.ohiolink.edu/etdc/view?acc_num=dayton1281366442

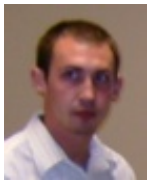

Michael Greiner

Degree: PhD, University of Dayton, 2010

Title: **Effects of Multiple Photon Scattering in Deciduous Tree Canopies**

Abstract: Detecting objects hidden beneath forest canopies has proven to be a difficult task for optical remote sensing systems. Rather than relying upon the existence of gaps between the leaves, our goal is to use the light that is scattered from the leaves to image through dense foliage. We develop a Monte Carlo canopy propagation model to simulate the scattering of light through a maple tree canopy. We measure several forest parameters, including the gap fraction and maximum leaf area density of a real test canopy and apply them to the model. We run the simulation for 80o illumination and report on the results in the ground and receiver planes. We then authenticate the validity of the model by illuminating a test forest at an 80^{o} angle, collecting data both on the canopy floor and in a monostatic receiver, and comparing the results to the simulation. Additionally, we examine the accuracy of the model in accounting for seasonal canopy variations and verify the simulation with experimental results. Lastly, we investigate methods for boosting the signal-to-noise ratio of detected photons and make SNR calculations for various illumination angles.

Committee/ Advisors:

Bradley D. Duncan, PhD (Committee Chair)
Matthew P. Dierking (Committee Member)
Joseph W. Haus, PhD (Committee Member)
Peter E. Powers, PhD (Committee Member)
Edward Watson, PhD (Committee Member)

LOCI 2011 Graduates

Robert Brown

Degree: Master of Science (M.S.), University of Dayton, Electro-Optics, 2011.

Title: **Stretch Processing of Simultaneous, Segmented Bandwidth Linear Frequency Modulation in Coherent LADAR**

Abstract: In stretch processing (SP) both the local oscillator (LO) and the transmitted signal are linearly frequency modulated (LFM). A heterodyne detection process is performed using the LO and the received echo signal, which create a detected signal at a single difference-frequency. The frequency is proportional to the distance the received echo signal travels relative to the LO signal, and the range resolution is inversely proportional to the bandwidth making large bandwidth LFM chirps favorable. However, it is difficult to maintain linearity over a lager bandwidth LFM chirp. On the other hand small bandwidth LFM chirps can be easily produced, so the idea of segmenting the transmitted pulse into multiple small non-overlapping frequency LFM chirps was conceived. The extended frequency bandwidth is recovered in post processing. This technique is called multi-frequency stretch processing (MFSP). The procedure outlined is a practical method to achieve greater range resolution using less expensive technology. Another advantage of this technique is the similar modulation noise on each LFM chirp. The multiple signals are processed using an algorithm developed for extracting the additional bandwidth information. The range resolution is related to the time span and bandwidth of the LFM pulses. For n transmitted LFM chirped signals the range resolution is nearly n times longer. Moreover the required detection bandwidth of the echo signal is lower than for other LFM processing systems without a chirped LO signal.

Committee / Advisors:

Joseph W. Haus, PhD (Committee Chair)
Matthew P. Dierking, PhD (Committee Chair)
Peter E. Powers, PhD (Committee Member)

URL: http://rave.ohiolink.edu/etdc/view?acc_num=dayton1304437012

Stretch Processing

Robert Brown, Matthew P. Dierking, Peter E. Powers, Joseph W. Haus

Goal

The goal of the stretch processing project is to determine whether or not stretch processing is a viable tool to achieve greater range resolution using two or more chirped signals.

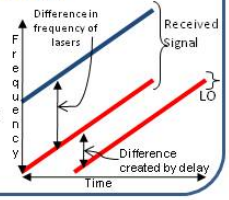

Technical Approach

Two lasers with controllable frequency offsets coupled into the same AO modulator. This will insure that both lines get the same modulation. The signal is split one line sent to a target and the other through a LPF leaving only the lower frequency signal. The filtered signal and the targets signal are combined to detect the offset frequencies.

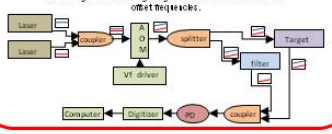

Major Issues

- Determining how to processes the additional bandwidth data to achieve the greatest range resolution.
- Extracting essential information and post processing the phase difference between the lasers to achieve higher range resolution.
- Do side lobes add ambiguity to the range data?
- Finding approaches to separate the additional laser lines from the LO signal.

I graduated from Western Carolina University in 2009 with my B.S. in Electrical Engineering and a minor in Mathematics. I am currently studying for my M.S. in Optic-Engineering at the University of Dayton.

Expected Outcomes

By using an effectively wider pulse width the frequency spectrum is narrower to achieve greater range resolution. We will use the stretch processing technique.

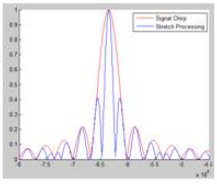

Dallis Conrad

Degree: Master of Science (M.S.), University of Dayton, Electro-Optics, 2011.

Title: **Speckle Statistics of Articulating Objects**

Abstract: This thesis documents research to determine if an articulating objects speckle can be used to identify properties of said object. Speckle is an interference phenomenon that is created by coherent light scattering off a rough surface, which creates various path lengths to the observation plane. It was thought that as an object articulates, the average speckle size would vary as time evolved. The average speckle size can be estimated though the speckle field correlation, which is documented to be dependent on two factors: the irradiance distribution of the object, and the correlation properties of the materials composing the target. The irradiance distribution describes the shape and motion of the illuminated object. Its contribution to an object's speckle pattern was first examined through MATLAB modeling, where those results were tested within laboratory experiments. The understanding of the contribution of the materials composing the object was investigated through recording the speckle pattern of various materials within the lab. The collected speckle irradiance distributions could then be used to determine the correlation properties of that material, which could then be compared to the other materials analyzed.

Committee / Advisors:

Edward A. Watson, PhD (Committee Chair)
Joseph W. Haus, PhD (Committee Member)
Partha Banerjee PhD (Committee Member)

URL: http://rave.ohiolink.edu/etdc/view?acc_num=dayton1320673424

Speckle Statistics of Articulating Objects

Dallis Conrad III, Edward Watson, and Joseph W. Haus

LOCI
Ladar & Optical Communications Institute

Goal

To discover if it is possible to identify and track an articulating target through its speckle field irradiance pattern. This will be accomplished though both lab experiments and MatLab modeling.

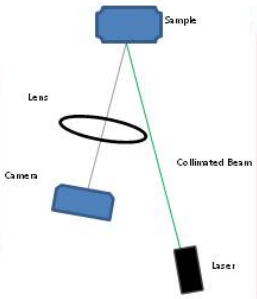

Technical Approach

Correlation on the surface of materials will produce variations in the far-field average speckle irradiance pattern. In the lab we use a 2f system to measure the scaled far-field pattern scattered off of samples of various materials.

Size and shape of the scattering object determine the size and shape of speckles in the far field. In MatLab we simulate a moving human with 52 delta functions whose relative positions change with time, producing a time-varying speckle shape. The effect of simple backgrounds will also be investigated

Major Challenges

Measurement of the average far field irradiance of the scattered speckle pattern.

Simple simulation of an articulating human based on data of a human walking.

Inclusion of the effects of background scatter that mixes with scatter from model human.

I graduated from Baldwin-Wallace College-Ohio 2009 with a B.S. in Physics and a minor in Mathematics. I am currently working on my M.S. in Electro-Optics at the University of Dayton

Expected Outcomes

Evaluation of the utility of measuring speckle patterns for human motion estimation.

Estimation of required system parameters to make such measurements in realistic scenarios.

Josh Duran

Degree: Master of Science (M.S.), University of Dayton, Electro-Optics, 2011.

Title: **Ion Implementation Study of Be in InSb for Protodiode Fabrication**

Abstract: InSb p-n junction detectors from bulk crystals are commonly utilized for mid-wave infrared (MWIR) focal-plane arrays (FPAs) because of their high quantum efficiency and well-established fabrication methods. The doping profiles of these detector structures are commonly defined by thermal diffusion techniques because it is an economical and repeatable fabrication process. The resulting impurity profiles have a characteristic shape determined by Fick's diffusion laws. In order to realize structures that are more complicated than simple PN junctions, like APDs, alternative methods of introducing and controlling impurities need to be developed, especially when high and low doping concentrations at specific depths beneath the surface are needed.

Another technique that could maintain similar cost effectiveness and repeatability as thermal diffusion while providing greater control over the doping profile is ion implantation. This is well-developed for silicon, but less developed for InSb. Accurate modeling of the doping profile shapes and depth are important for transitioning detector designs to properly functioning devices. SRIM modeling software is used to predict the doping profiles of implanted Be ions into n-type InSb substrates. To test the accuracy of this software, implantations of varying energy were performed. After implantation, the doping profiles of these samples were measured using secondary ion mass spectrometry (SIM.S.) before and after a rapid thermal anneal. It was found that Be ions do not diffuse within the repeatability tolerance of the SIM.S. measurement technique. The SIM.S. results also revealed a highly oxidized InSb surface. This oxidized surface should be considered during the fabrication process. Spreading resistance profile measurement is made on an annealed Be implanted sample. P on N carrier concentration is verified by this measurement which suggests successful activation during anneal.

A process for fabricating InSb photodiodes with ion implantation is developed and reported. The fabrication process has not been optimized for performance, but verification of functioning detectors is established with dark current and spectral response measurements. These measurements verify successful photodiode operation.

Committee / Advisors:

Andrew Sarangan, PhD (Committee Chair)
Thomas Nelson, PhD (Committee Member)

John Scheihing (Committee Member)
Qiwen Zhan, PhD (Committee Member)

URL: http://rave.ohiolink.edu/etdc/view?acc_num=dayton1310392650

Ryan Feaver

Degree: Master of Science (M.S.), University of Dayton, Electro-Optics, 2011.

Title: **Longwave-IR Optical Parametric Oscillator in Orientation Patterned Galliaum Arsenide**

Abstract: Coherent tunable laser sources in the long wave infrared (LWIR) spectral region are in high demand for military applications. Most lasers cannot produce outputs far into the infrared region, and therefore a conversion process is needed to achieve desired wavelengths. Quasi-phase matching is a technique that spatially modulates the nonlinear properties of a given material, periodically reversing the induced nonlinear polarization to ensure positive energy flow from the pump source to the converted fields, subject to conservation of energy and momentum. Through the use of optical parametric oscillation (OPO), and nonlinear quasi-phase matched orientation-patterned gallium arsenide (OPGaAs), producing LWIR wavelengths is possible. The OPGaAs OPO was pumped with a Q-switched 2.054μm Tm,Ho:YLF laser. As a precursor to the LWIR OPGaAs OPO, different resonator geometries were explored with a midwave (MWIR) OPGaAs OPO utilizing both SRO and DRO mirror sets. While thresholds increased with cavity length, the slope efficiencies remained relatively similar with the respective mirror set.
The LWIR OPGaAs OPO explored the performance using two separate cavity configurations, an SRO and an asymmetric cavity; and five different OPGaAs samples representing three different grating periods. The highest slope efficiency in the SRO LWIR cavity was found to be ~29%, with threshold values of ranging from ~45-90μJ. The slope efficiencies for the asymmetric cavity range from ~4-16% while experiencing higher thresholds of ~150-220μJ, lower overall output power, and increased cavity instability. At higher pump energies, rollover was observed in both cavity configurations. SNLO was used to model the OPO output in the hopes that it might provide some insight into this behavior. The theoretical performance plot fit the acquired data decently but failed to predict the behavior at the higher energies. Spectroscopic data were collected for both OPO signal and idler output, presenting good agreement with theoretical tuning curves.

Committee / Advisors:

Peter E. Powers, PhD (Committee Chair)
Rita Peterson, PhD (Committee Member)
Joseph W. Haus, PhD (Committee Member)

URL: http://rave.ohiolink.edu/etdc/view?acc_num=dayton1324048074

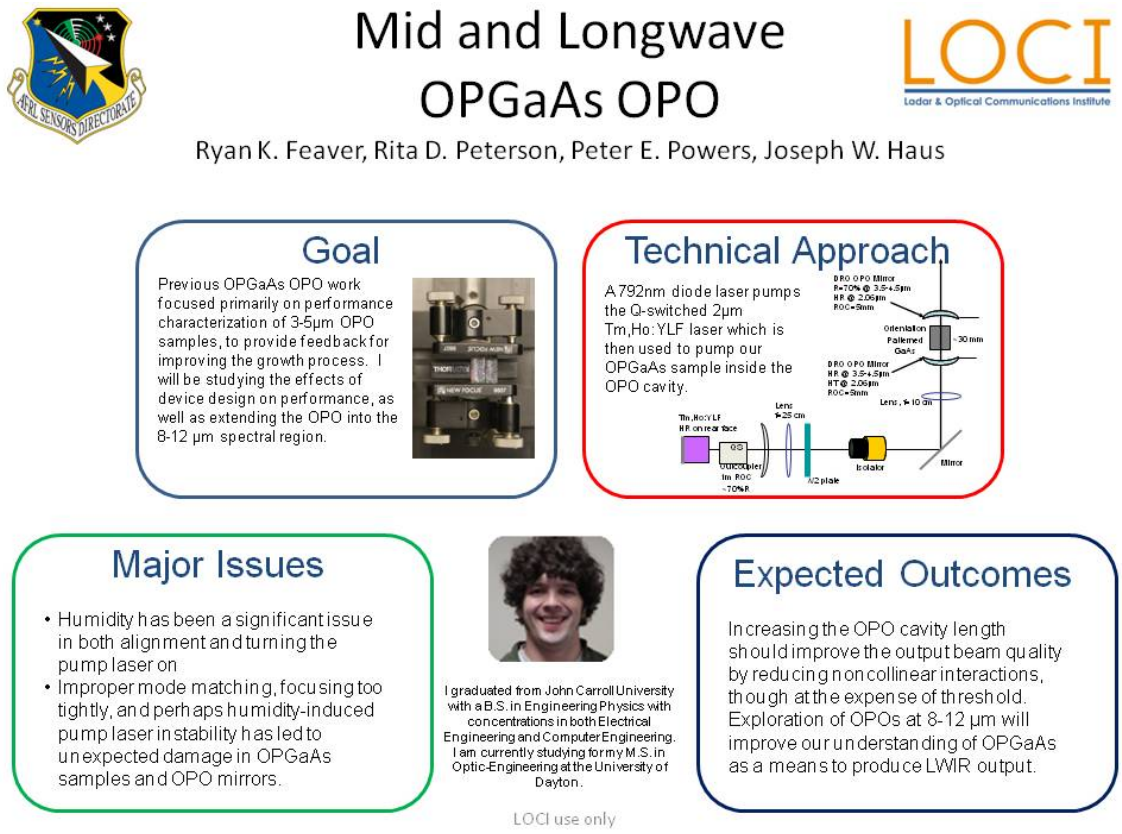

Jeff Kraczek

Degree: Master of Science (M.S.), University of Dayton, Electro-Optics, 2011.

Title: **An Evaluation of the Effects of the Ability to Measure Piston on Multi-aperture Spatial Heterodyne Systems**

Abstract: Multi-aperture imaging has been used to receive high resolution images from arrays of sub-apertures. The use of sub-aperture arrays allows for more compact optical systems and enables conformal aperture imaging. Images collected from these arrays are processed to obtain the high resolution image. A High resolution image is created from an accurate

representation of the pupil plane fields in each sub-aperture. Data processing to create an image is time consuming and computationally heavy. Compensating for the unknown piston phase error between the different sub-apertures is one of the more time consuming corrections required to process the image data into a single image.
Sub-aperture phasing simulations are used to explore the processing of multi-aperture arrays. The data is processed for several sub-aperture arrays, including 2 and 3 in-line sub-aperture arrays, and hex 7 and 19 sub-aperture arrays. A scheme is proposed for measuring the piston phases in each sub-aperture. It is shown through numerical simulations that a system that measures the piston phase could significantly reduce the processing time required to phase the images from a multi aperture system into a single high resolution image.

Committee / Advisors:

Paul F. McManamon, PhD (Committee Chair)
Joseph W. Haus, PhD (Committee member)
Joseph Marron, PhD (Committee member) (Lockheed Martin)

URL: http://rave.ohiolink.edu/etdc/view?acc_num=dayton1323284036

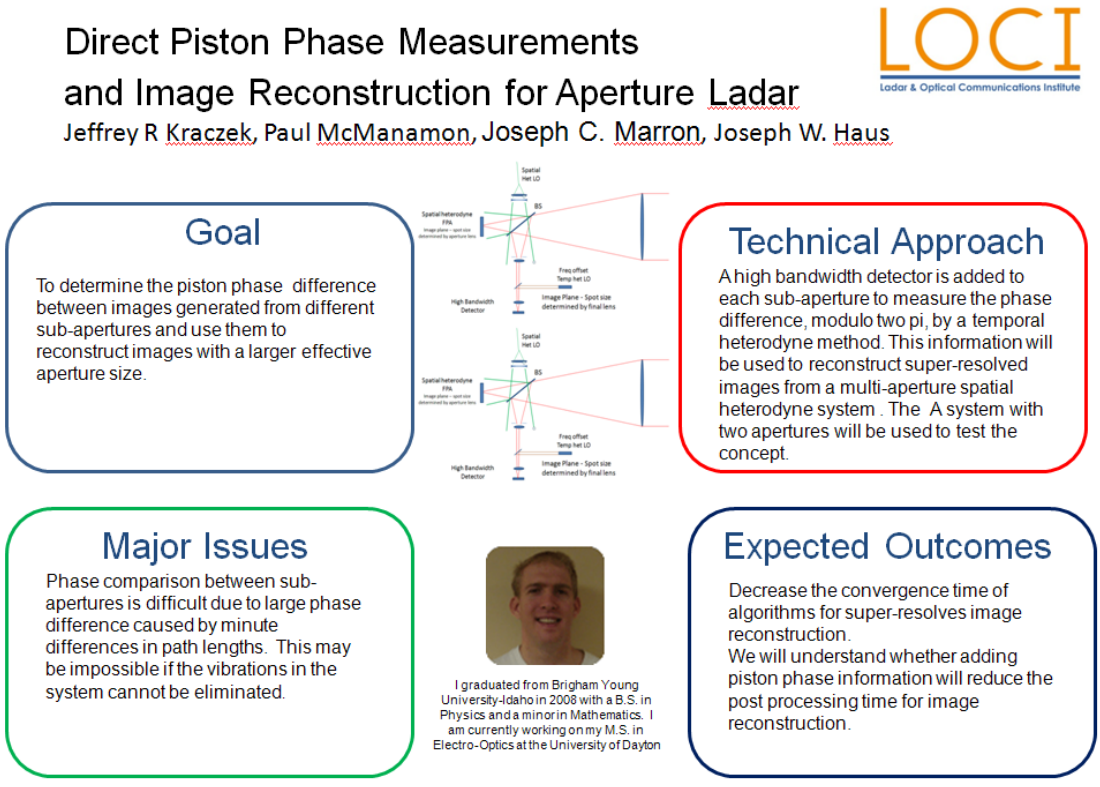

Charles Phelps

Degree: Master of Science (M.S.), University of Dayton, Electro-Optics, 2011.

Title: **Diode-Pumped 2Micron Q-Switched TM: YAG Microchip Laser**

Abstract: In this report we discuss the design, simulation, construction, and characterization of an actively Q-switched, diode-pumped solid state laser operating at 2 μm. The laser cavity has a "microchip" configuration and uses a 6% thulium-doped YAG crystal as the lasing medium. In continuous wave mode, we achieve output powers of up to 450 mW with a slope efficiency of 9.5%. Using an acousto-optic Q-switch, the laser was run in pulsed mode at an average power of 42 mW and a pulse rate of 1.66 kHz. Pulse duration was approximately 400 ns with a pulse energy of 25 μJ. The center wavelength was 2.019 μm with a linewidth of <0.045 nm. Additionally, a design is presented for replacing the active Q-switch with a chromium-doped zinc selenide crystal acting as a saturable absorber passive Q-switch. Finally, we will propose possible future modifications to the laser system design to improve its performance, ruggedness and compactness, and to broaden its functionality.

Committee / Advisors:

Peter E. Powers, PhD (Committee Chair)
Patrick Berry, PhD (Committee Member)
Kenneth Schepler, PhD (Committee Member)
Joseph W. Haus, PhD (Committee Member)

URL: http://rave.ohiolink.edu/etdc/view?acc_num=dayton1304695817

Joseph Reierson

Degree: Master of Science (M.S.), University of Dayton, Electro-Optics, 2011.

Title: **Analysis of Atmospheric Turbulence Effects on Laser Beam Propagation using Multi-wavelength Laser Beacons**

Abstract: Atmospheric turbulence affects optical systems that operate in various atmospheric conditions. The characteristics of the optical wave transmitted through atmospheric turbulence can undergo dramatic changes resulting in potential system performance degradation. Knowledge of atmospheric

turbulence effects would aid in the development of a wide class of atmospheric-optics systems including laser communication, directed energy, lidar, remote sensing, and active and passive imaging systems. In the classical atmospheric turbulence theory, the refractive index structure parameter is the key parameter known to describe the strength of the atmospheric turbulence and accurate measurement of this parameter represents an important task. The refractive index structure parameter can be difficult to measure, as it is influenced by many factors including path length, time of day, season, and microclimate conditions which cannot be applied universally and may change in a matter of minutes. To further complicate atmospheric turbulence characterization, the key assumptions of classical (Kolmogorov) turbulence theory, such as statistical homogeneity and isotropy of the refractive index random field, are not always satisfied. From this viewpoint, experimental analyses to determine the applicability of the Kolmogorov turbulence theory in different optical wave propagation conditions represent important tasks and can assist in the adequate evaluation of atmospheric turbulence effects on optical system performance and design. In this thesis, the applicability of the classical turbulence theory was verified through simultaneous intensity measurements (pupil- and focal-plane intensity distributions) from multi-wavelength laser beacons over a near-ground, near-horizontal, and seven-kilometer-long propagation path. These measurements allowed independent evaluation of the refractive index structure parameter for two different wavelengths (λ_1 = 532 nm, λ_2 = 1064 nm), and these results were compared to theoretical predictions. In addition, the turbulence-induced intensity scintillations were investigated across the projected laser beam footprint, and a numerical analysis of the propagation was compared to the experimental data. To obtain the intensity measurements, the optical setup included four sub-systems using fast-framing (~150 frames/second) cameras that were synchronized using previously developed control software; additional software was developed for data acquisition and processing. The conducted experiments in the turbulence conditions investigated here showed that the results of measurements and predictions based on the Kolmogorov turbulence theory are in reasonably good agreement but are particularly sensitive to the footprint position of the transmitted beacon. The atmospheric characterization technique using a multi-wavelength beacon provided a useful tool for examining the applicability of the Kolmogorov turbulence theory along this propagation path.

Committee / Advisors:

Mikhail A. Vorontsov, PhD (Committee Chair)
Joseph W. Haus, PhD (Committee Member)
Edward A. Watson, PhD (Committee Member)

URL: http://rave.ohiolink.edu/etdc/view?acc_num=dayton1324053129

Imaging through Deep Turbulence

Joseph L. Reierson, Mikhail A. Vorontsov, Joseph W. Haus

Goal

Characterize custom turbulence generators to investigate turbulent effects on intensity (coherent and incoherent) including their scalability and determine the limitations of extended atmospheric turbulence in this system.

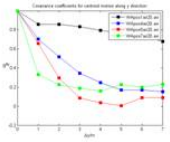

Technical Approach

Characterize each of seven turbulence generators along each of the seven range hall positions and then assess the cohesiveness between generators. Use both wide and narrow FOV scopes to capture images using as small an integration time as possible.

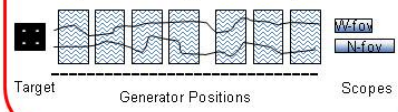

Major Issues

- The turbulence generators require manual assembly and custom modifications. These may or may not affect their characterization but care will be taken to prepare them in most nearly the same way as possible.
- Temperature gradients and accurate temperature measurements
- Characterizing data such that a given turbulence environment is repeatable.

I graduated from the University of North Dakota in 2009 with a B.S. in Electrical Engineering and a minor in Mathematics, I am currently pursuing a M.S. in Electro-Optics at the University of Dayton. During my undergraduate education, I was hired as a Co-op with Emerson Process Management where I spent approximately three months in each of Quality Control, Failure Analysis, and PlantWeb Marketing departments at the Rosemount division.

Expected Outcomes

We expect to be able to reproduce turbulence covariance coefficients among individual generators such that they can be combined to consistently model various turbulence environments.

We expect the results to follow computational simulations investigated by another student, and output particular Cn^2 values.

Dayen Voratovic

Degree: Master of Science (M.S.), University of Dayton, Electro-Optics, 2011.

Title: **Generation and Detection of Coherent Pulse Trains in Periodically Poled Lithium Niobate through Optical Parametric Amplification**

Abstract: This work reports on the generation, modulation, and detection of temporally coherent pulses in periodically-poled lithium niobate (PPLN) configured as an optical parametric amplifier (OPA). The OPA was pumped at 1 µm, by a 10 kHz, 1 ns, Nd:YAG laser. The cw seeding sources for the OPA were two separate 1550 nm lasers. One source had a short coherence length of 0.3 Km, the other a long coherence length of 95 Km. The generated pulse trains where phase modulated by using a set of mirrors on a single axis motorized stage. A 10 Km fiber optic delay line was used to simulate free space propagation. A homodyne, coherent optical detection system, utilizing the in-phase and quadrature components of the circularly polarized local oscillator, was built to detect the amplitude and phase modulated pulse trains. We report the detection of the modulated signal for the long coherence length source and the loss of the modulated signal for the short coherence length source, demonstrating that the OPA process can transfer the temporal coherence (or coherence length) of the input signal to the pulse-amplified signal

Committee / Advisors:

Peter E. Powers, PhD (Committee Chair)
Joseph W. Haus, PhD (Committee Member)
Matthew P. Dierking, PhD (Committee Member)

URL: http://rave.ohiolink.edu/etdc/view?acc_num=dayton1324406162

1.5 µm Pulsed OPA for LADAR Applications

Dayen Voratovic, Peter Powers, Joseph Haus, Matthew Dierking,
Tim Carrig, Joe Buck

Goal

Utilize a seeded OPA configuration to generate nanosecond pulses for Laser Remote Sensing applications in the 1.5 or 3.8 micron range.

Calculate Time-Bandwidth Product (TBP)

Observe and verify coherence between pulses

Technical Approach

Pulse coherence demonstrated by using a coherent homodyne detection split into and in-phase and quadrature channels.

Use the IQ detection to measure the velocity of a moving stage by measuring the pulse-to-pulse phase shift

Loss and regain coherence by inserting a 10 km delay line and switching to a very narrow linewidth seed source

Major Issues

Currently, regaining coherence using the 10 km delay is the major challenge. Only partial coherence is seen. Reasons could include,
-Delay line is non-PM fiber
- Fiber optic coupling between PM fibers is not correct
- Non-linear effects occurring inside the delay line

I graduated from University of Cincinnati in 2003 with a B.S. in Physics and a minor in Mathematics. Spent two years at Wright State University working on my Masters in Physics until 2005.

I am currently finishing my M.S. in Electro-Optics at the University of Dayton

Expected Outcomes

Previous research has shown that the amplified pulses have the seed bandwidth and beam profile.

I expect we will be able to show that the coherence / phase of the amplified pulses are dependent on the coherence / phase of the seed beam.

Last name	First Name	Graduation Year	Degree	Advisor	Thesis or Dissertation Title
Bobb	Ross	2012	M.S.	Matt Dierking	Doppler Shift Analysis for a Holographic Aperture LADAR System
Venable	Samuel	2012	M.S.	Brad Duncan	Demonstrated Resolution Enhancement Capability of a Stripmap Holographic Aperture LADAR System
Idehenre	Ighodalo	2013	M.S.	Joe Haus	Evanescent and Plasmonic Sensing Using Linear and Radial Polarization Modes in Tapered Microfibers
Crotty	Maureen	2013	M.S.	Ed Watson	Conformal Aperture Imaging Techniques
Dolasinski	Brian	2014 projected	Ph.D.	Peter Powers	THz Generation by Difference Frequency Generation in a DAST Crystal
Wu	Gui Min	2012	M.S.	Paul McManamon	Wavefront Control with Beam Steering Device in a Multi-Aperture Imager
Gatz	Micah	Left program	Ph.D.	Mikhail Vorontsov	Coherent Combining of Phased Array on an Extended Target Using Speckle Metric as Feedback
McDaniel	Sean	2012	M.S.	Peter Powers	Seeded, Gain-Switched Chromium doped Zinc Selenide Amplifier
Seidel	Aaron	Incomplete	M.S.	Joe Haus	Imaging and Strong Extended Turbulence
Whitfield	Erica	2012	M.S.	Partha Banerjee	Propagation of Gaussian Beams through a Modified von Karman Phase Screen

Table 6: US National Graduate Students Graduating after 2011

LOCI 2012 Graduates

Ross Bobb

Degree: Master of Science (M.S.), University of Dayton, Electro-Optics, 2012.

Title: **Doppler Shift Analysis for a Holographic Aperture LADAR System**

Abstract: Since the invention of the laser, laser radars (LADARs) have been investigated following the extensive development path of radar systems. LADAR systems have progressed from simple direct detect systems to more complicated synthetic aperture heterodyne systems. Developments in digital processing allowed a new type of synthetic aperture LADAR known as holographic aperture LADAR where the heterodyne detection of temporal synthetic aperture LADAR was combined with the holographic digital recording methods. Using holographic aperture LADAR increases cross-range resolution, but by using a low bandwidth spatial receiver array instead of a high bandwidth point receiver increases the system's Doppler effect vulnerability for each sub-aperture image. The Doppler frequency offsets are due to projected line of sight velocities across the target. In a broadside imaging configuration, one side of the target will appear to be approaching the target while the other appears to be receding. The projected line of sight velocity is zero at the center of the target (normal to the LOS), and has maximum values at the edges of the target field. This produces an approximately linear differential Doppler frequency shift across the target in the dimension of travel. This spatially dependent, sinusoidal signal is temporally integrated over the fixed integration time of the imaging array which maps the sinusoidal signal into a spatial sinc pattern across the target's image. Since the targets edges have the highest projected velocities, the sinc pattern appears as a loss in target information effectively reducing the field of view. Faster platform velocities and longer integration times produce larger compressions in the field of view. This paper describes the velocity and integration time required to limit the field of view reduction to a selected value. The first null in the cross sectional sinc pattern is assumed to be a good measure for the compression of the field of view. Analytic expressions and numerical simulations are developed for the impact of differential Doppler frequencies and then verified with laboratory experiments. Four integration times were analyzed in this experiment. Since the motion is relative, the target's velocity varied. The integration times were 0.25 ms, 0.5 ms, 0.75 ms, and 1.0 ms and the velocities varied between 0 and 14 cm/s. The results of this experiment were in good agreement with the theory and simulation and confirm that selection of faster effective integration times is required to limit data loss due to platform motion.

Committee / Advisors:

Matthew P. Dierking, PhD (Committee Chair)
Bradley D. Duncan, PhD (Committee Member)
Joseph W. Haus, PhD (Committee Member)
David J. Rabb, PhD (Committee Member)

URL: http://rave.ohiolink.edu/etdc/view?acc_num=dayton1334950140

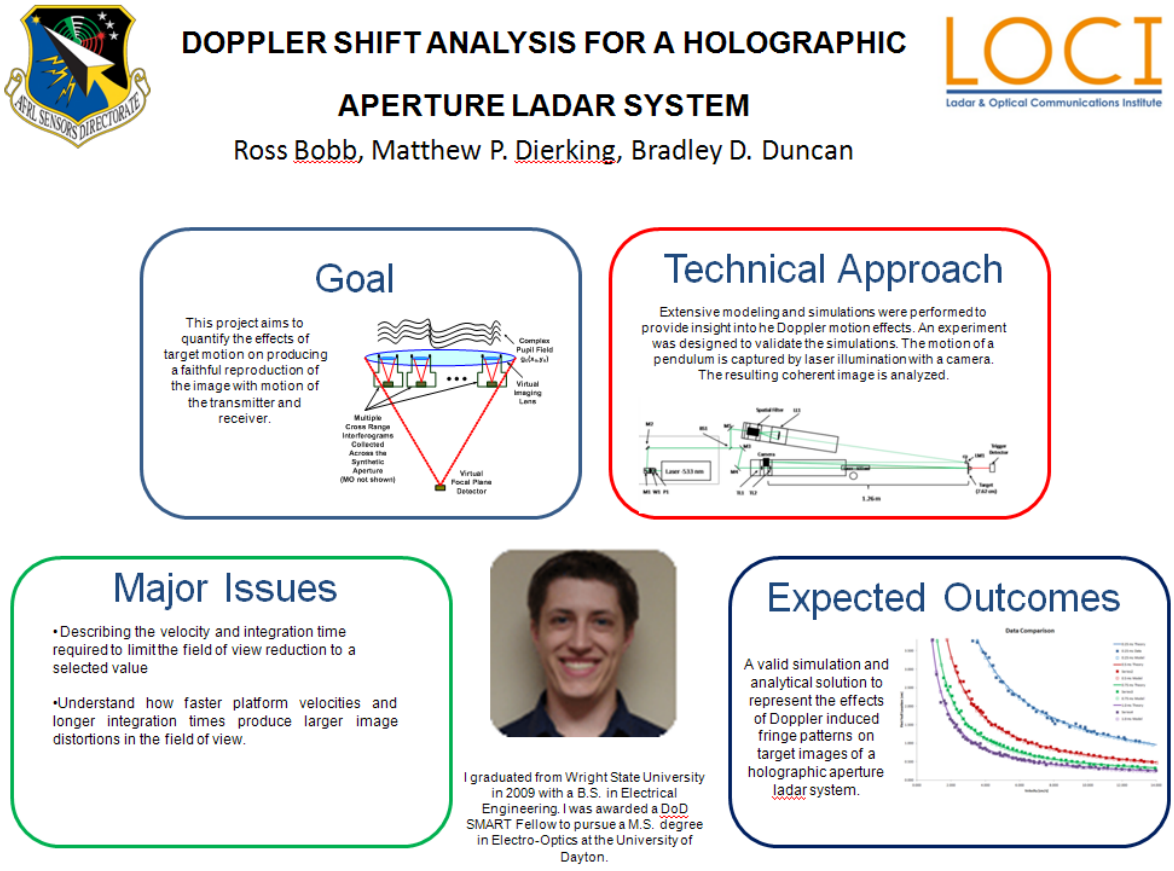

Samuel Venable

Degree: Master of Science (M.S.), University of Dayton, Electro-Optics, 2012.

Title: **Demonstrated Resolution Enhancement Capability of a Stripmap Holographic Aperture LADAR System**

Abstract: Holographic aperture LADAR (HAL) is a variant of synthetic aperture LADAR (SAL). The two processes are related in that they both seek to increase cross-range (i.e., the direction of the receiver translation) image resolution through the synthesis of a large effective aperture – which is in turn achieved via the translation of a receiver aperture and the subsequent coherent phasing and correlation of multiple received signals. However, while SAL imaging incorporates a translating point detector, HAL takes advantage of two-dimensional translating sensor arrays. For the research presented in this article, a side looking Stripmap HAL geometry was used to sequentially illuminate a set of Ronchi ruling targets. Prior to this, theoretical calculations were performed to determine the baseline, single sub-aperture resolution of our experimental, laboratory based system. Theoretical calculations were also performed to determine the ideal modulation transfer function (MTF) and expected cross-range HAL image sharpening ratio corresponding to the geometry of our apparatus. To verify our expectations, we first sequentially captured an over-sampled collection of pupil plane field segments for each Ronchi ruling. A HAL processing algorithm was then employed to phase correct and re-position the field segments after which they were properly aligned through a speckle field registration process. Relative piston and tilt phase errors were then removed prior to final synthetic image formation. By then taking the Fourier transform of the synthetic image intensity and examining the fundamental spatial frequency content, we were able to produce experimental modulation transfer function curves which we could then compare to our theoretical expectations. Our results show that we are able to achieve nearly diffraction limited results for image sharpening ratios as high as 6.43

Committee / Advisors:

Bradley D. Duncan, PhD (Committee Chair)
Matthew P. Dierking, PhD (Committee Member)
Joseph W. Haus, PhD (Committee Member)

URL: http://rave.ohiolink.edu/etdc/view?acc_num=dayton1333558737

Sensitivity of Holographic Aperture Ladar

Processing Methods to Return Signal Levels

Sam M. Venable, Matthew P. Dierking, Bradley D. Duncan

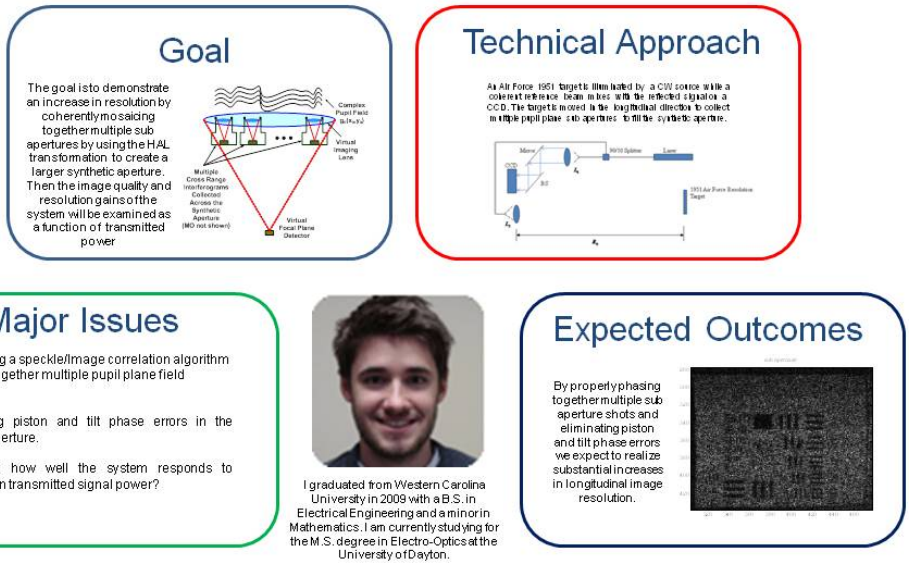

Erica Whitfield

Degree: Master of Science (M.S.), University of Dayton, Electro-Optics, 2012.

Title: **Propagation of Gaussian Beams through a Modified von Karman Phase Screen**

Abstract:

Gaussian beam propagation through discrete phase screens and an extended random media has been studied extensively over the last four decades. In this thesis, we numerically examine the effects of a discrete phase screen during Gaussian beam propagation on the scintillation index for a single beam and on the fringe visibility for the two transversely separated beams. We use the modified von Karman spectrum model to describe the phase screen statistics, utilizing the Fried parameter, inner scale and the outer scale. The scintillation index is analyzed as a function of the structure constant, phase screen location, the initial width of the Gaussian beam, etc. Similarly, the numerical simulations are extended using a pair of transversely separated Gaussian beams. We examine the interference of the beams and measure the fringe visibility at the target. We then correlate the scintillation index and the fringe visibility results and suggest the possible applications.

Committee / Advisors:

Partha Banerjee, PhD (Committee Chair)
Joseph W. Haus, PhD (Committee Member)
Dean Evans, PhD (Committee Member)

URL: http://rave.ohiolink.edu/etdc/view?acc_num=dayton1355513250

Gui Min Wu

Degree: Master of Science (M.S.), University of Dayton, Electro-Optics, 2012.

Title: **Wavefront Control with Beam Steering Device in a Multi-Aperture Imager**

Abstract:

A multi-aperture imaging system with a non-mechanical steering device replacing each lens sub-aperture was considered. Such setup allows for focusing and tracking of a target over a fine angle while preserving high resolution imaging in a compact system. An imaging system has the ability to add digitally focus for receiving. However, in the case of transmitting the focus must be provided by optical components. Even when receiving, at a short enough range it might be necessary to introduce optical corrections to avoid phase aliasing. To this end, the effects of implementing a real device such as the BNS Spatial Light Modulator (SLM), a reflective 512x512 pixels with 83.4% area fill factor steering device, on the multi aperture imaging system were investigated. The pixelated phase of the SLM, and the use of 2π resets to provide stepped blazed phase profiles for steering and stepped quadratic phase focusing, are modeled. Each pixel of the SLM is modeled by an array of 10x10 elements with 9 active and 1 inactive in both the x and y direction. As expected, and shown by the simulation results, the periodic reset of the quadratic phase bowl introduced phase grating modulations, which produces the so call "ghost image" around the center image. By only providing stepped blazed profile to steer, the simulation shows that with increasing phase steps within the blazed profile the diffraction efficiency increase but at the cost of decreased steering angles. The ability of the SLM to correct for aberrations and its limitation in correcting aberration is investigated. Further, the basic concept of conformal aperture, enabled by the multi-aperture, was investigated and simulated.

Committee / Advisors:

Paul McManamon, PhD (Committee Chair)
Joseph W. Haus, PhD (Committee Member)
Edward Watson, PhD (Committee Member)

URL: http://rave.ohiolink.edu/etdc/view?acc_num=dayton1355243952

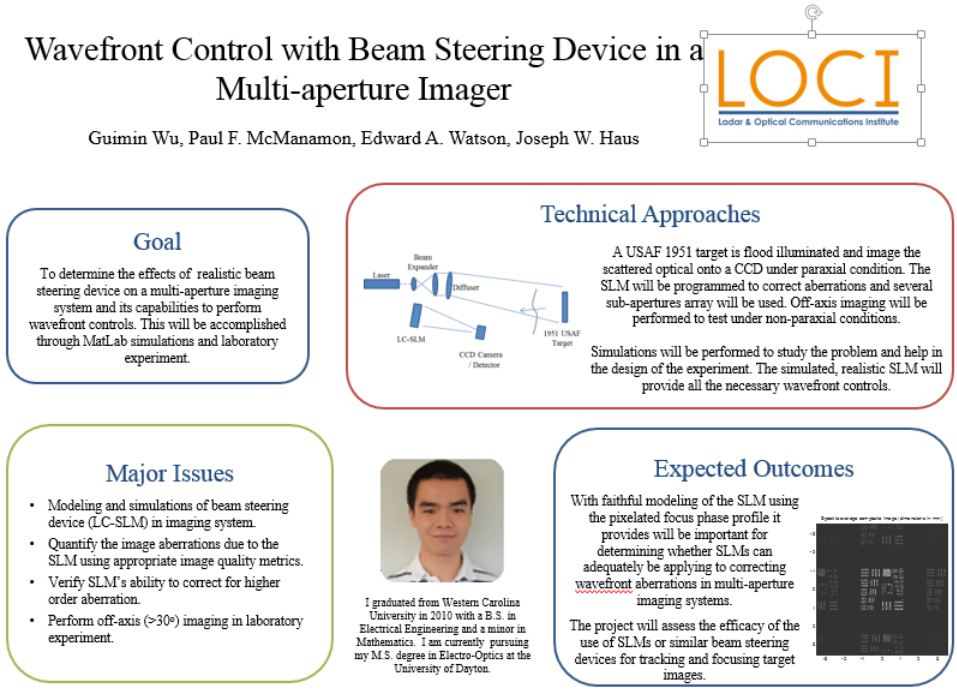

Sean McDaniel

Degree: Master of Science (M.S.), University of Dayton, Electro-Optics, 2012.

Title: **Seeded, Gain-Switched Chromium doped Zinc Selenide Amplifier**

Abstract:

Many scientific and military applications require pulsed laser sources with high peak power output which are tunable throughout the midwave infrared (mid-IR) spectral region. In this report we discuss the design, construction, and characterization of a gain-switched chromium-doped zinc selenide (Cr:ZnSe) amplifier pumped by a Q-switched holmium-doped yttrium aluminum garnate (Ho:YAG) laser and seeded by a free running continuous wave (CW) Cr:ZnSe laser.

The amplifier pump laser was constructed using a 0.5% Ho-doped, Brewster-cut YAG rod. In CW operation, powers of up to 3.68 W and a slope efficiency of 45% were obtained. In pulsed operation at 1 kHz pulse repetition frequency (PRF), pulse energies of 2.6 mJ per pulse were obtained with temporal pulse widths less than 100 ns. The output wavelength of the pump was 2.1 μm with a spectral width less than 1 nm.

The pulsed Ho:YAG laser was then used to gain-switch a Cr:ZnSe single-pass pulsed amplifier seeded with a CW Cr:ZnSe laser with a free-running wavelength of 2.4 μm and a spectral linewidth of 50 nm. The output of the gain-switched

amplifier yields a pulsed beam at the seed wavelength demonstrating high gain. By design, this source will follow the lasing wavelength of the seed beam allowing for tunability over the entire emission wavelength of Cr:ZnSe with proper seed design. The end result of this work was a versatile, pulsed mid-IR source.

Committee / Advisors:

Peter Powers, Dr. (Committee Chair)
Patrick Berry, Dr. (Committee Member)
Ken Schepler, Dr. (Committee Member)
Andrew Sarangan, Dr. (Committee Member)

URL: http://rave.ohiolink.edu/etdc/view?acc_num=dayton1343760359

LOCI 2013 Graduates or Later

Maureen Crotty

Degree: Master of Science (M.S.), University of Dayton, Electro-Optics, 2013.

Title: **Signal to Noise Ratio Effects on Aperture Synthesis for Digital Holographic LADAR**

Abstract:

The cross-range resolution of a laser radar (LADAR) system can be improved by synthesizing a large aperture from multiple smaller sub-apertures. This aperture synthesis requires a coherent combination of the sub-apertures; that is, the sub-apertures must be properly phased and placed with respect to each other. One method that has been demonstrated in the literature to coherently combine the sub-apertures is to cross-correlate the speckle patterns imaged in overlapping regions. This work investigates the effect of low signal to noise ratio (SNR) on an efficient speckle cross-correlation registration algorithm with sub-pixel accuracy. Specifically, the algorithms ability to estimate relative piston and tilt errors between sub-apertures at low signal levels is modeled and measured. The effects of these errors on image quality are examined using the modulation transfer function (MTF) as a metric. The results demonstrate that in the shot noise limit, with signal levels as low as about 0.02 signal photoelectrons per pixel in a typical CCD, the registration algorithm estimates relative piston and tilt accurately to within 0.1 radians of true piston and 0.1 waves of true tilt. If the sub-apertures are not accurately aligned in the synthetic aperture, then the image quality degrades as the number of sub-apertures increases. The effect on the MTF is similar to the effects due to defocus aberrations.

Committee / Advisors:

Edward Watson, PhD (Committee Chair)
Matthew P. Dierking, PhD (Committee Member)
David Rabb, PhD (Committee Member)

URL: http://rave.ohiolink.edu/etdc/view?acc_num=dayton1355245759

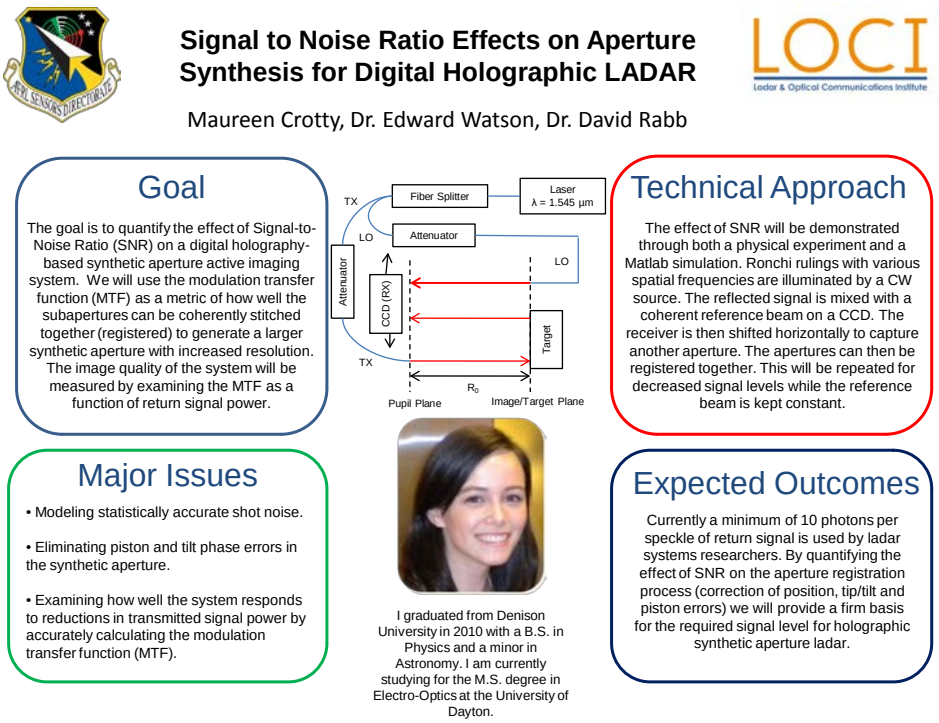

Ighodalo Idehenre

Degree: Master of Science (M.S.), University of Dayton, Electro-Optics, 2013.

Title: **Evanescent and Plasmonic Sensing using Linear and Radial Polarization Modes in Tapered Microfibers**
Abstract:

We present optical transmission results for biconic tapered optical fibers using a coupled mode theory (CMT) and perturbative analysis. In this area of research much of the theoretical and empirical studies on biconic fiber tapers for sensor applications have focused primarily on the behavior of the quasi-linear polarized hybrid modes ($HE_{1\ell}$; $EH_{1\ell}$).

In this thesis we begin by examining the properties of the quasi-linear polarized modes.

That is a prelude to our study of radial ($TM_{0\ell}$) and azimuthal ($TE_{0\ell}$) polarized modes in biconic tapered fibers. We performed a detailed comparison of hybrid, radial, and azimuthal mode behavior for tapered fibers down to various fiber waists radius. The comparison study was divided in to two parts. First we looked at the differences in design and optimization of the taper regions to retain the launched mode as the primary mode in the fiber. In other words our primary goal in designing an adiabatic tapers was to minimize the power exchange to higher order modes. To quickly obtain results for the fiber output, we modeled amplitude of the modes propagating in a tapered fiber as a set of coupled differential equations, and numerically solved the system of equations. We confirmed the efficacy of the model by comparing our simulations with experimental data. Coupled mode analysis of these types of tapers revealed that the radial/azimuthal require taper lengths on the order of tens of centimeters to suppress coupling energy to higher order modes. The taper lengths found for the radial/azimuthal modes was in contrast to the adiabatic coupling length of hybrid modes, which only required tens of millimeters. Our CMT approach was then successfully used to design non-adiabatic tapers, a necessity for standard, compact biconic sensors. The additional losses were quantified for our cases of non-adiabatic tapers, where short taper sections were fabricated in the lab. Initial experimental results comparing transmission for EH-HE modes are shown and compared with our simulations.

The second part of our study was to discover whether the tapered fibers and the waist region between the two tapers would be useful for sensing analytes near the fiber's surface. Our investigation of both hybrid and radial/azimuthal polarized modes revealed that the latter modes generally had more energy stored outside the fiber in the evanescent regime for the same fiber radius. This was especially true for small fiber radii. This means that fiber sensors designed using the TM-TE modes would have higher sensitivity than with the EH-HE modes.

At the cost of introducing propagation losses for the modes we added plasmonic nano-films on the surface of the waist region of the tapered fibers to draw the fields from the glass fiber into the evanescent regime outside the fiber. The mode shape changes were managed within the CMT of our earlier studies, but the losses were handled by applying perturbation using the reciprocity theorem. At longer wavelengths the field amplitude in the metal for radial polarization is suppressed (due to a boundary condition effect) and the mode can propagate farther along the fiber waist. At the same time the plasmonic nano-film creates more field energy extending into the evanescent region outside the fiber which improves the sensitivity of the tapered fibers as sensors. We find that the TM-TE modes have more energy displaced to the outside than the EH-HE modes, which makes them interesting candidates for future fiber sensor designs.

Committee / Advisors:

Joseph W. Haus, PhD (Committee Chair)
Peter E. Powers, PhD (Committee Member)
Karolyn Hansen, PhD (Committee Member)

URL: http://rave.ohiolink.edu/etdc/view?acc_num=dayton1367346795

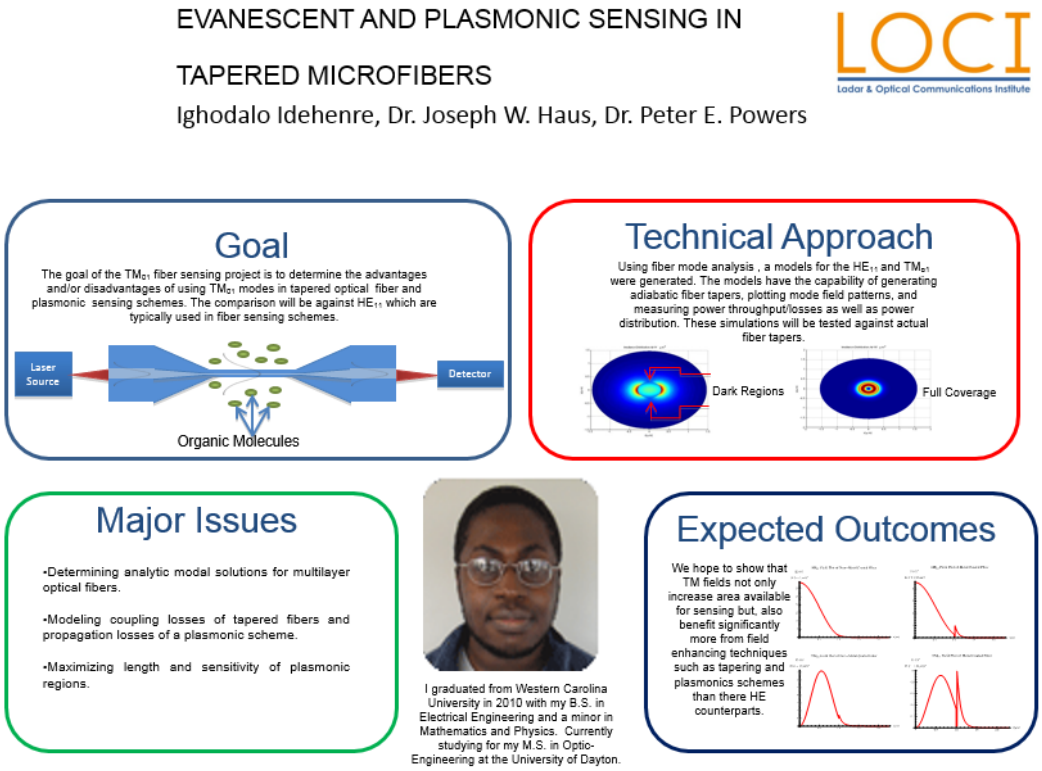

Benjamin Dapore

Degree: Master of Science (M.S.), University of Dayton, Electro-Optics, 2013.

Title: **Phase Noise Analysis of 3D Images from a two wavelength Coherent Imaging System**

Abstract:

Two wavelength coherent imaging is a technique that offers several advantages over conventional coherent imaging. A significant advantage examined in this thesis is the ability to extract 3D target relief information from the phase contrast image at a known difference frequency. However, phase noise detracts from the accuracy that the target can be faithfully identified. We therefore describe a method for developing a relation of phase noise relative to the correlation of the image planes corresponding to each wavelength. Being able to predict the phase

noise spectrum of a scene will help greatly in determining our ability to reconstruct the target relief.

We examine the validity of previously derived equations, and extend them to a general case, which allows for the calculation of a correlation of a complex image field which has content from many spatial frequencies. The correlation coefficient can be used to generate a probability density function which represents the overall phase noise of the system relative to the spatial frequency content. For a simple target the spatial frequency content is based on a single tilt angle for the target. We discuss both computer-based modeling that is compared to an analytic equation, as well as an experimental spatial heterodyne verification of the model. We further extend our theory by building scenes with complex objects, discussing whether the derived equations hold for multi-faceted surfaces.

Committee / Advisors:
Joseph W. Haus, PhD (Committee Chair)
Paul McManamon, PhD (Committee Member)
David Rabb, PhD (Committee Member)
Partha Banerjee, PhD (Committee Member)

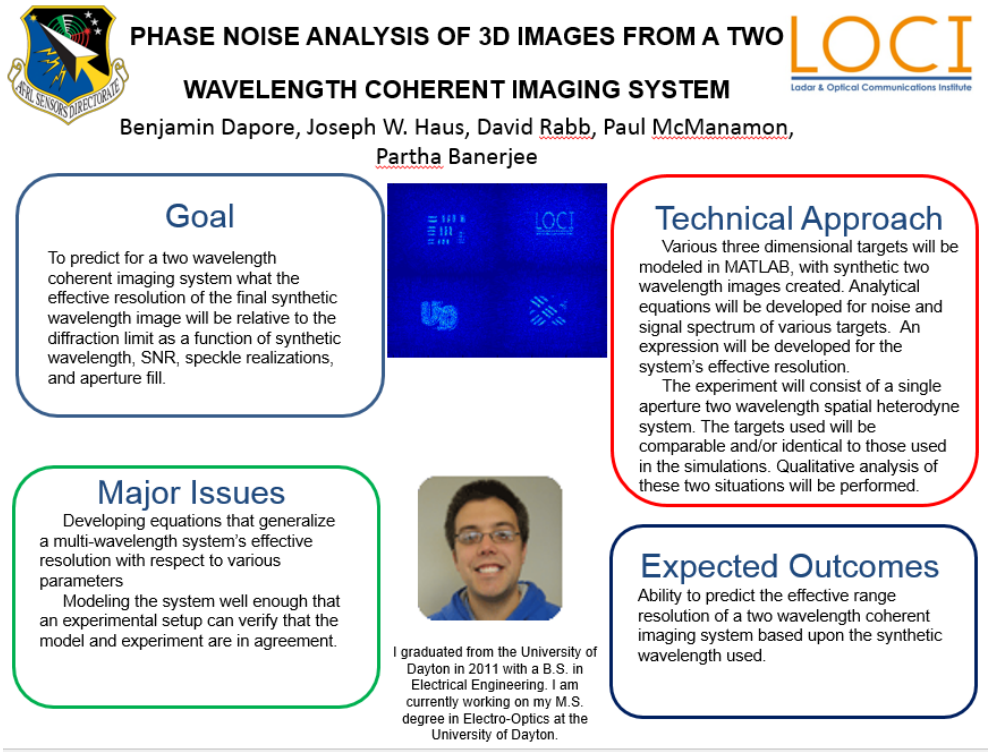

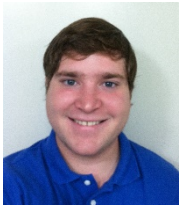

Cullen Bradley

Degree: Master of Science (M.S.), University of Dayton, Electro-Optics, 2013.

Title: **LADAR: A Mono-Static System for Sense and Avoid Applications**

Abstract:

In this thesis we study a laser radar, aka LADAR, system design to be mounted in an Unmanned Aircraft Systems (UAS) to prevent collisions with other aircraft. This system is called a Sense and Avoid technology and it is designed to anticipate future standards on flying the UAS in civil airspace that the U.S. Federal Aviation Administration (FAA) will adopt.

Our SAA solution includes a LADAR system that is cued by EO cameras; data from a LADAR system is fused with the existing EO system. The main role of the LADAR system is to confirm the existence of a possible target, thus decreasing the false alarm rate. The LADAR system will also provide an accurate range to the target and track the target to determine its course.

The key aspects of this design include a telescope, transmitter/receiver switch, and beam scanner. The telescope consists of two lenses and is used for both transmission and reception of the laser signal. The transmitter/receiver switch provides detection for a long range signal and consists of an avalanche photodiode detector (APD) coupled with a time-to-digital (TDC) converter and a fiber laser. The accuracy of the LADAR system depends on the accuracy of both the beam scanner and the gimbal the system will be placed in. Our system is designed to have less than 1 foot accuracy at ranges approaching 10 km. Each component was tested and the system performance was validated with outdoor experiments to almost 8 km.

Committee / Advisors:
Joseph W. Haus, PhD (Committee Chair)
Edward Hovenak, MS (Committee Member)
Cong Deng, PhD (Committee Member)

The following list of LOCI students are either in the process of completing their degrees or they have left the program.

David Bricker

Degree: Master of Science (M.S.), University of Dayton, Electro-Optics, 2013 expected.

David Bricker is working in Dr. Vorontsov's group on issues related to Deep turbulence. He is a member of the AFOSR MURI Team.

Shane Gillespie

Degree: Master of Science (M.S.), University of Dayton, Electro-Optics, 2013 expected.

Shane was studying the phase noise effects of liquid crystal wave plates using a Mach-Zehnder interferometer set up that was designed to determine the I and Q signals in two polarizations, so that he can reconstruct the complex signal and extract the signal pahse. He has completed taking the data and is now writing the research up as a thesis.

Micah Gatz

Degree: Doctor of Philosophy in Electro-Optics (Ph.D.), University of Dayton, Electro-Optics. M.S. degree 2013.

Micah Gatz was working on beam propagation through a turbulent atmosphere. He is phasing multiple beams with a target-in-the-loop strategy.

Aaron Seidel

Degree: Master of Science (M.S.), University of Dayton, Electro-Optics, not completed.

Aaron Seidel, was supported by external funds from LOCI Industry Partners. He finished his coursework and the turbulence simulations for his thesis work, but did not complete writing his M.S. thesis. He has all the work done except for the writing of his thesis, but he has not contacted Dr. Haus or the Program since he left.

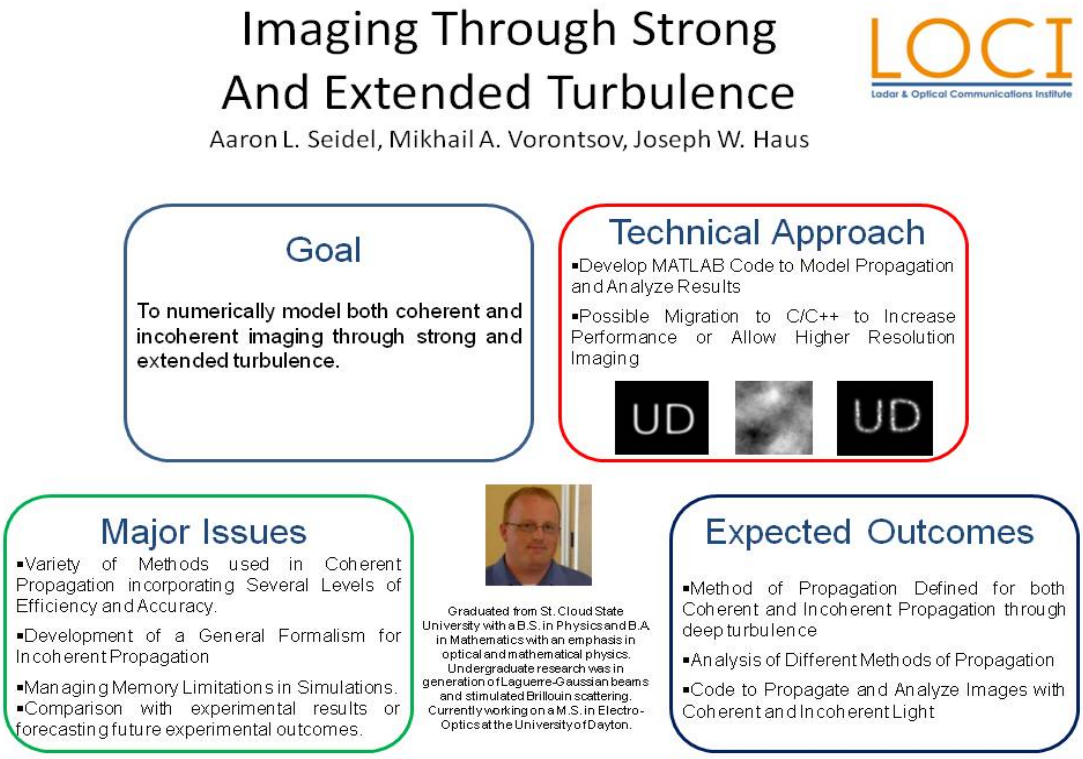

Brian Dolasinski

Degree: Doctor of Philosophy in Electro-Optics (Ph.D.), University of Dayton, Electro-Optics, degree expected 2014.

Brian Dolasinski is working on a project with AFRL/RX on non-destructive testing using THz signals. His THz laboratory is in LOCI space.

4.13 Endowed Professor Activities

Dr. Vorontsov has been an excellent addition to the University of Dayton. He has complemented the LADAR and optical communications center development in many ways. He is an expert in free space laser communications and he founded a company, Optonicus, to develop and commercialize his technology. His seminal paper showing a much larger beam at Mt. Haleakala than would be expected by classic turbulence theory was the inspiration for the AFOSR sponsored MURI won by Dr Vorontsov's group. LOCI has emphasized multi-aperture sensing systems. Dr Vorontsov's group has phased 7 lasers emitted from different sub-apertures over the 7 Km path to the VA center. His group has also phased 19 sub-apertures in the laboratory. The 19 sub-aperture system is shown in Figure 23.

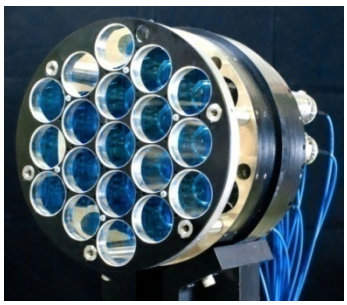

Figure 23: 19 Sub-Aperture System Built by Optonicus

As mentioned earlier, Mikhail Vorontsov's group has won an AFOSR MURI. The proposal was submitted to AFOSR, ONR BAA 11-26, Topic Number 12, "Deep Atmospheric Optical Turbulence Physics and Predictive Modeling,". Below is a more detailed description of that MURI.

Title: WAVE OPTICS OF DEEP ATMOSPHERIC TURBULENCE: FROM UNDERLYING PHYSICS TOWARDS PREDICTIVE MODELING, MITIGATION, AND EXPLOITATION.

Program Manager: Dr. Kent Miller.

Research Problem: In order to facilitate the development of future long-range optical systems there is a need for understanding the performance of optical wave propagation along various atmospheric paths that may cross several extended (deep) regions of the atmosphere with quite distinctive spatial structures and temporal dynamics. Currently, analyses are performed in the framework of classical "fully developed" Kolmogorov optical turbulence theory describing the atmosphere as three dimensional boundless, statistically homogeneous and isotropic random fields of refractive index fluctuations and thus neglecting the impact of boundary conditions imposed by terrain and hydro-thermodynamic processes as well as of gravity and solar radiation induced buoyancy and friction forces that lead to formation of distinct, nearly horizontally aligned atmospheric layers with a rich variety of large-scale self-organized spatio-temporal coherent atmospheric structures including gravity and rotary waves, rolls, Bernard cells, jets, stratified flows, instabilities, etc. – effects that can severely impact optical wave propagation over long distances.

Technical Approach: The research will focus on elaborating a foundation for the physics of atmospheric optics effects in deep turbulence by building bridges between meteorology, computational fluid dynamics, and statistical wave optics that take into account the large-scale structural complexity of the atmosphere and mean optical characteristics of layered structures.

The research team will develop a theoretical framework and the corresponding mathematical and numerical simulation tools that match small-scale meteorological features with optical wave propagation characteristics through high-resolution nested simulations and merge refractive and diffractive optics approaches in analysis of long-range propagation over the stratified atmosphere and highly anisotropic turbulence layers. For mitigation of atmospheric effects several new approaches will be evaluated: engineering of unconventional optical fields (e.g., with controllable space-varying coherence or dynamic phase and polarization patterns) and optical system architectures with reduced sensitivity to atmospheric distortions, including cascaded adaptive optics. The potential for exploitation of deep turbulence effects (e.g., optical wave-guiding or turbulence-induced diversity for compressive sensing/imaging) will be investigated.
Anticipated Outcome: The proposed research will provide a solid theoretical basis for optical wave propagation in deep turbulence conditions, lead to the development of practical computational tools for the realistic characterization assessment and prediction of beam projection and imaging over extended operational ranges, and provide an evaluation of approaches for mitigation and potential exploitation of deep-turbulence atmospheric effects.
Impact on DoD Capabilities: This basic research effort will facilitate tools and recommendations for optimal execution and efficiency improvement of Air Force missions such as directed energy, laser communications, and imaging/surveillance systems. The results will provide strategies for increasing Air Force optical system's effective ranges by accurately predicting and accounting for atmospheric conditions in potential fly zones.
Team: This program is a joint effort of the University of Dayton (Mikhail Vorontsov – Principal Investigator, Thomas Weyrauch, Ernst Polnau), the Air Force Institute of Technology (Steven Fiorino, Salvatore Cusumano), Michigan Technological University (Michael Roggemann), North Carolina State University (Sukanta Basu), University of Miami (Olga Korotkova), and New Mexico State University (David Voelz).
Funds Requested for MURI: 3-year base period: $4,499,525; 2-year option: $2,999,780; total: $7,499,305

4.14 LOCI Publications

4.14.1 Patent Disclosure

1. Title: Method for High Resolution Coherent Laser Radar Using Sparse Frequency Waveforms.
Inventors: Robert V. Chimenti, Matthew P. Dierking, Peter E. Powers, Joseph W. Haus,
disclosure date: 3/30/2009
2. Title: Terahertz source by difference frequency mixing,
Inventors: Dr. Joseph Haus/Dr. Peter Powers, disclosure date: 3/30/2009
3. Title: A Method for Multiple Aperture Coherent LADAR using Periodic Pseudo Noise Waveforms and Code Division Multiple Access Transmission and Reception
Inventors: Dr. Bradley Duncan, disclosure date: 5/15/2009
4. Title: Fiber Laser Generating Switchable Radially and Azimuthally Polarized Beams
Inventors: Dr. Joseph Haus/Dr. Peter Powers, disclosure date: 8/11/2009
5. Title: A Disk Laser Amplifier for Reduction of Transmit Power Loss in a Subaperture Based Laser System
Inventors: Dr. Peter Powers/Dr. Paul McManamon, disclosure date: 3/3/2010
6. Title: Increased Resolution Imaging
Inventor: Dr. Paul McManamon, disclosure date: 4/27/2010
7. Title: Multi-Transmitter Synthesis Techniques for Coherent LADAR
Inventor: Dr.Bradley Duncan, disclosure date: 6/6/2010
8. Title: Compact Narrow Band Width Tunable Source
Inventor: Dr. Peter Powers, disclosure date: 2/10/2011

4.14.2 Refereed Publications:

1. M.A. Greiner, B.D. Duncan and M.P. Dierking; “Bidirectional Scattering Distribution Functions of Maple and Cottonwood Leaves,” Applied Optics **46**, 6485-6494 (2007).
2. D.F. Jameson, M.P. Dierking and B.D. Duncan; “Effects of Spatial Modes on LADAR Vibration Signature Estimation,” Applied Optics **46**, 7365-7373 (2007).
3. J.D. Schmidt, M.E. Goda, and BD. Duncan; “Aberration Production Using a High-Resolution Liquid-Crystal Spatial Light Modulator,” Applied Optics **46**, 2423-2433 (2007).
4. J.L. Binford III, B.D. Duncan, J.H. Parker Jr., M.L. Delong and E. Beecher; “Imaging Diffractometer with Holographic Encoding Enhancements for Laser Sensing and Characterization,” Applied Optics **46**, 3518-3527 (2007).
5. N. J. Miller, M. P. Dierking and B. D. Duncan, "Optical sparse aperture imaging," Appl. Opt. **46**, 5933-5943 (2007).
6. Jason D. Schmidt, Matthew E. Goda and Bradley D. Duncan, "Aberration production using a high-resolution liquid-crystal spatial light modulator," Appl. Opt. **46**, 2423-2433 (2007).

7. W. Cheng, J. W. Haus and Q. Zhan, “Propagation of scalar and vector vortex beams through turbulent atmosphere,” Atmospheric Propagation of Electromagnetic Waves III. Edited by O. Korotkova. Proceedings of the SPIE **7200**, 720004-10 (2009).
8. R. V. Chimenti, M. P. Dierking, P. E. Powers and J. W. Haus, "Multiple chirp sparse frequency LFM LADAR signals", Proc. SPIE **7323**, 73230N (2009).
9. R. V. Chimenti, M. P. Dierking, P. E. Powers and J. W. Haus, "Sparse frequency LFM LADAR signals," Opt. Express **17**, 8302-8309 (2009).
10. M. A. Greiner, B. D. Duncan and M. P. Dierking, "Monte Carlo simulation of multiple photon scattering in sugar maple tree canopies," Appl. Opt. **48**, 6159-6171 (2009).
11. J. W. Stafford, B. D. Duncan and M.P. Dierking, Monte Carlo simulation of the effects of pulse and platform jitter on holographic aperture LADAR systems, Proc. SPIE, **7323**, 73230O (2009).
12. R. Zhou, B. Ibarra-Escamilla, J. W. Haus, P. E. Powers and Q. Zhan, “Fiber laser generating switchable radially and azimuthally polarized beams with 140 mW output power at 1.6 μm wavelength,” Appl. Phys. Lett. **95**, 191111 (2009).
13. X. Liu, J.W. Haus and , M. S. Shahriar, “Optical limiting in a periodic materials with relaxational nonlinearity,” Optics Express **17,** 2696-2706 **(**2009).
14. B. Ibarra-Escamilla, O. Pottiez, E.A, Kuzin EA and J.W. Haus, “All-fiber passive mode-locked laser to generate ps pulses based in a symmetrical NOLM,” Laser Physics **19,** 368-370 **(**2009).
15. W. Cheng, J. W. Haus and Q. Zhan, "Propagation of vector vortex beams through a turbulent atmosphere," Opt. Express **17**, 17829-17836 (2009).
16. A.R. Pandey, P. E. Powers and J. W. Haus, “Optical field measurements for accurate modeling of nonlinear parametric interactions,” J. Opt. Soc. Am. B**26**, 218-227 (2009).
17. A. J Stokes, B. D. Duncan and M. P. Dierking, Increasing mid-frequency contrast in sparse aperture optical imaging systems, Laser Radar Technology and Applications XIV, Monte D. Turner; G. W. Kamerman, Editors, SPIE Proceedings **7323**, 73230M (2009).
18. W. Han; J. W. Haus; P. McManamon; J. Heikenfeld; N. R. Smith; J. Yang, Beam steering performance of electrowetting microprism arrays, Enabling Photonics Technologies for Defense, Security, and Aerospace Applications V, M. J. Hayduk; P. J. Delfyett, Jr.; A. R. Pirich; E. J. Donkor, Editors, SPIE Proceedings **7339**, 73390J (2009).
19. P.F. McManamon, P. J. Bos, M. J. Escuti, J. Heikenfeld, S. Serati, H. Xie and Ed. A. Watson, “A Review of Phased Array Steering for Narrow-Band Electrooptical Systems,” Proceedings of the IEEE **97**, 1078 (2009). (invited review)
20. W. Cheng, J. W. Haus and Q. Zhan, “Propagation of scalar and vector vortex beams through turbulent atmosphere,” Atmospheric Propagation of Electromagnetic Waves III. Edited by O. Korotkova. SPIE Proceedings **7200**, 720004-10 (2009).
21. M. A. Vorontsov, Valeriy V. Kolosov, and Ernst Polnau, "Target-in-the-loop wavefront sensing and control with a Collett-Wolf beacon: speckle-average phase conjugation," Appl. Opt. **48**, A13-A29 (2009).

22. M. Vorontsov, J. Riker, G. Carhart, V. S. Rao Gudimetla, L. Beresnev, T. Weyrauch, and L. C. Roberts, Jr., "Deep turbulence effects compensation experiments with a cascaded adaptive optics system using a 3.63 m telescope," Appl. Opt. **48**, A47-A57 (2009).
23. M. A. Vorontsov, V. V. Kolosov, and E. Polnau, "Target-in-the-loop wavefront sensing and control with a Collett-Wolf beacon: speckle-average phase conjugation," Appl. Opt. **48**, A13-A29 (2009).
24. J. W. Stafford, B. D. Duncan, and M. P. Dierking, "Experimental demonstration of a stripmap holographic aperture LADAR system," Appl. Opt. **49**, 2262-2270 (2010).
25. W. Han, J. Haus, P. McManamon, J. Heikenfeld, N. Smith, J. Yang, Transmissive beam steering through electrowetting microprism arrays, *Optics Communications*, Volume 283, Issue 6, Pages 1174-1181 (2010).
26. A. J Stokes, B. D. Duncan, and M. P. Dierking, "Improving mid-frequency contrast in sparse aperture optical imaging systems based upon the Golay-9 array," Opt. Express **18**, 4417-4427 (2010).
27. M. P. Dierking and B. D. Duncan, "Periodic, pseudonoise waveforms for multifunction coherent LADAR," Appl. Opt. **49**, 1908-1922 (2010).
28. L. Shi, P. F. McManamon, D. Bryant, K. Zhang, and P. J. Bos, "Dynamics of a liquid-crystal variable optical prism based on Pancharatnam phase," Appl. Opt. **49**, 976-985 (2010).
29. L. Shi, J. Shi, P. F. McManamon, and P. J. Bos, "Design considerations for high efficiency liquid crystal decentered microlens arrays for steering light," Appl. Opt. **49**, 409-421 (2010).
30. Renjie Zhou, Joseph W. Haus, Peter E. Powers, and Qiwen Zhan, "Vectorial fiber laser using intracavity axial birefringence," Opt. Express **18**, 10839-10847 (2010).
31. R.V. Chimenti, M.P. Dierking, P.E. Powers and J.W. Haus, "Experimental verification of sparse frequency linearly frequency modulated LADAR signals modeling," Optics Express **18,** 15400-15407 **(**2010**).**
32. Nicholas J. Miller ; Joseph W. Haus ; Paul F. McManamon and David Shemano, "Multi-aperture coherent imaging", Proc. SPIE 8052, Acquisition, Tracking, Pointing, and Laser Systems Technologies XXV, 805207 (May 13, 2011). doi:10.1117/12.887351; http://dx.doi.org/10.1117/12.887351
33. Jeffrey Kraczek; Nicholas J. Miller; Paul McManamon; Joseph W. Haus and Joseph Marron, "Piston phase determination and its effect on multi-aperture image resolution recovery", Proc. SPIE 8037, Laser Radar Technology and Applications XVI, 80370T (June 08, 2011). doi:10.1117/12.883420;http://dx.doi.org/10.1117/12.883420
34. T. Weyrauch, M. A. Vorontsov, G. W. Carhart, L. A. Beresnev, A. P. Rostov, E. E. Polnau and J. J. Liu, "Experimental demonstration of coherent beam combining over a 7 Km propagation path," Opt. Lett. **36**, 4455-4457 (2011) . (Top ten download for November). http://www.opticsinfobase.org/ol/abstract.cfm?URI=ol-36-22-4455
35. Leonid A. Beresnev ; Mikhail A. Vorontsov ; Thomas Weyrauch ; Gary Carhart ; Svetlana L. Lachinova ; Jiang Liu; Experimental study of phase locking of fiber collimators using internal beam-tail interference. Proc. SPIE **7914**, Fiber Lasers VIII:

Technology, Systems, and Applications, 79142Z (February 21, 2011). doi:10.1117/12.877300.
36. Svetlana L. Lachinova ; Mikhail A. Vorontsov; Wavefront sensing and adaptive control in phased array of fiber collimators. Proc. SPIE **7924**, Atmospheric and Oceanic Propagation of Electromagnetic Waves V, 79240F (February 10, 2011). doi:10.1117/12.875943.
37. Nicholas J. Miller ; Joseph W. Haus ; Paul F. McManamon ; David Shemano; Multi-aperture coherent imaging. Proc. SPIE **8052**, Acquisition, Tracking, Pointing, and Laser Systems Technologies XXV, 805207 (May 13, 2011); doi:10.1117/12.887351.
38. Jeffrey Kraczek ; Nicholas J. Miller ; Paul McManamon ; Joseph W. Haus ; Joseph Marron; Piston phase determination and its effect on multi-aperture image resolution recovery. Proc. SPIE **8037**, Laser Radar Technology and Applications XVI, 80370T (June 08, 2011). doi:10.1117/12.883420.
39. T. Weyrauch, M. A. Vorontsov, G. W. Carhart, L. A. Beresnev, A. P. Rostov, E. E. Polnau and J. J. Liu, "Experimental demonstration of coherent beam combining over a 7 km propagation path," Opt. Lett. **36**, 4455-4457 (2011). (Top ten download for November). http://www.opticsinfobase.org/ol/abstract.cfm?URI=ol-36-22-4455
40. Bahadir K. Gunturk, Nicholas J. Miller, and Edward A. Watson, "Camera phasing in multi-aperture coherent imaging," Opt. Express **20**, 11796-11805 (2012). http://www.opticsinfobase.org/oe/abstract.cfm?URI=oe-20-11-11796
41. P. F. McManamon, “Review of LADAR: a historic, yet emerging, sensor technology with rich phenomenology,” Opt. Eng. **51**, 060901-1-060901-13 (2012). doi:10.1117/1.OE.51.6.060901. Listed as a top download on the SPIE website on August 20, 2012.
42. M. Aubailly, M. A. Vorontsov and J. Liu; “Scintillation-resistant wavefront sensing based on a multi-aperture phase reconstruction (MAPR) technique,” Proc. SPIE **8238**, High Energy/Average Power Lasers and Intense Beam Applications VI; Atmospheric and Oceanic Propagation of Electromagnetic Waves VI, 82380L (February 9, 2012). doi:10.1117/12.906080.
43. Nicholas J. Miller ; Jeffrey J. Widiker ; Paul F. McManamon ; Joseph W. Haus; “Active multi-aperture imaging through turbulence,” Proc. SPIE **8395**, Acquisition, Tracking, Pointing, and Laser Systems Technologies XXVI, 839504 (June 8, 2012). doi:10.1117/12.921160.
44. M. Aubailly ; M. A. Vorontsov ; G. Carhart ; J. Jiang Liu and R. Espinola; Content-dependent on-the-fly visual information fusion for battlefield scenarios. Proc. SPIE **8368**, Photonic Applications for Aerospace, Transportation, and Harsh Environment III, 83680J (May 1, 2012). doi:10.1117/12.918681.
45. G. M. Wu, N. J. Miller, P. F. McManamon, E. A. Watson and J. W. Haus; Wavefront control in a spatial heterodyne-based multi-aperture imager. Proc. SPIE **8395**, Acquisition, Tracking, Pointing, and Laser Systems Technologies XXVI, 839506 (June 8, 2012). doi:10.1117/12.920504.
46. Mathieu Aubailly and Mikhail A. Vorontsov, "Scintillation resistant wavefront sensing based on multi-aperture phase reconstruction technique," J. Opt. Soc. Am. A **29**, 1707-1716 (2012). http://www.opticsinfobase.org/josaa/abstract.cfm?URI=josaa-29-8-1707

47. Mikhail Vorontsov, Thomas Weyrauch, Svetlana Lachinova, Micah Gatz, and Gary Carhart, "Speckle-metric-optimization-based adaptive optics for laser beam projection and coherent beam combining," Opt. Lett. **37**, 2802-2804 (2012). http://www.opticsinfobase.org/ol/abstract.cfm?URI=ol-37-14-2802
48. Jean Minet, Mikhail A Vorontsov, Ernst Polnau, and Daniel Dolfi, "Enhanced correlation of received power-signal fluctuations in bidirectional optical links," Journal of Optics **15**, 022401 (2013).

4.14.3 Special Journal Issue

J. J. Dolne, M. A. Vorontsov, M. C. Roggemann, and B. L. Ellerbroek, "Wavefront Sensing, Imaging, and Image Enhancement: introduction to the feature issue," Appl. Opt. **48**, WFS1-WFS1 (2009).
http://www.opticsinfobase.org/ao/abstract.cfm?URI=ao-48-1-WFS1

Partha Banerjee, George Barbastathis, Myung Kim, and Nickolai Kukhtarev, "Digital holography and 3-D imaging," Appl. Opt. **50**, DH1-DH2 (2011).
http://www.opticsinfobase.org/ao/abstract.cfm?URI=ao-50-7-DH1

4.14.4 Invited Conference Presentations

1. R. V. Chimenti, M. P. Dierking, P. E. Powers and J. W. Haus, "Multiple chirp sparse frequency LFM LADAR signals", Proc. SPIE 7323, 73230N (2009).
2. R. V. Chimenti, E. S. Bailey, P. E. Powers, J. W. Haus, M. P. Dierking, "A review of sparse frequency linearly frequency modulated (SF-LFM) laser radar signal modeling with preliminary experimental results," 15th Laser Radar Conference, Toulouse, France, June 22-26, 2009.
3. E. S. Bailey, M. P. Dierking, P. E. Powers, and J. W. Haus, "Laser Radar Experiment Using a Signal with Three Sparse, Linearly Chirped Frequencies," in *Applications of Lasers for Sensing and Free Space Communications*, OSA Technical Digest Series (CD) (Optical Society of America, 2010), paper LSWB3. http://www.opticsinfobase.org/abstract.cfm?URI=LSC-2010-LSWB3
4. J. W. Haus, "LADAR and Laser Communications Center," Coherent Laser Radar Conference, Snowmass, CO, July 10, 2007.
5. B.D. Duncan and M.P. Dierking; "Stripmap Holographic Aperture LADAR," invited presentation delivered during the Aperture Synthesis Symposium of the 21st Annual Meeting of IEEE LEOS, Newport Beach, CA, November 12, 2008.
6. N.J. Miller, B.D. Duncan and M.P. Dierking; "Digital Holographic Image Synthesis," invited presentation delivered during the Aperture Synthesis Symposium of the 21st Annual Meeting of IEEE LEOS, Newport Beach, CA, November 12, 2008.
7. R. V. Chimenti, M. P. Dierking, P. E. Powers, J. W. Haus, and E. S. Bailey. *A Review of Sparse Frequency Linearly Frequency Modulated (SF-LFM) Laser Radar Signal Modeling with Preliminary Experimental Results*. Proc. of 15th Coherent Laser Radar Conference, Toulouse, France (2009).

8. M. Vorontsov, G. Carhart, T. Weyrauch, R. Gudimetla, S. Lachinova, L. Beresnev, "Coherent Optical Multi-Beam Atmospheric Transceiver (COMBAT): Deep Turbulence Effects Characterization & Mitigation over 149 km Propagation Path," Department of Theoretical and Applied Optics ONERA (Paris, France), Dec. 2009.
9. M. A. Vorontsov, T. Weyrauch, L. A. Beresnev, G. W. Carhart, L. Liu, and S. Lachinova, "Adaptive Complex Field Control with an Array of Phase-Locked Fiber Collimators," OSA Conference Frontiers in Optics 2009/Laser Science XXV, San Jose, CA, October 11 - 15, 2009.
10. Mi. A. Vorontsov, T. Weyrauch, L. A. Beresnev, G. W. Carhart, L. Liu, and K. Aschenbach, "Adaptive Array of Phase-Locked Fiber Collimators: Analysis and First Experimental Demonstration of Dynamic Phase Distortion Compensation," Directed Energy Systems Symposium, Monterey, California, 6-10 April, 2009.
11. M. Vorontsov, J. Riker, R. Gudimetla, G. Carhart, T. Weyrauch, L. Beresnev, K. Aschenbach and S. Lachinova, "Design of a Coherent Optical Multi-Beam Atmospheric Testbed (COMBAT) for Deep Turbulence Effects Characterization and Mitigation over 149 km Propagation Path," Directed Energy Systems Symposium, Monterey, California, 6-10 April, 2009.
12. M. Vorontsov, "Mitigation of Atmospheric Turbulence Effects in Laser Communication, Beam Projection & Imaging Systems," NATO SET-ET-061 meeting on "Adaptive Optics for Laser Beam Delivery and Passive and Active Imaging ," Paris, France (28-30 April, 2009).
13. M. A. Vorontsov, T. Weyrauch, L. A. Beresnev, Ga. W. Carhart, L. Liu, and K. Aschenbach, "Adaptive Array of Phase-Locked Fiber Collimators: Analysis and First Experimental Demonstration of Dynamic Phase Distortion Compensation," NATO SET-ET-061 meeting on "Adaptive Optics for Laser Beam Delivery and Passive and Active Imaging ," Paris, France (28-30 April, 2009).
14. M. Vorontsov, G. Carhart, V. S. Rao Gudimetla, T. Weyrauch, E. Stevenson, K. Rehder, J. Liu, L. Beresnev, S. Lachinova, I. Kemp and J. F. Riker, Characterization of Deep Turbulence over 149 km Propagation Path Using Multi-wavelength Laser Beacons. Invited Presentation, Advanced Maui Optical and Space Surveillance Technologies Conference (AMOS), Maui Hawaii, Sept. 14-16, 2010.
15. M. A. Vorontsov, Mathieu Aubailly, Michael T. Valley, Gary Carhart, and J. Jiang Liu, Atmospheric Effects Mitigation via Lucky Region Fusion ," Turbulence Workshop, CERDEC NVESD, Ft. Belvoir, VA August 10-11, 2010.
16. M. Vorontsov, Gary Carhart, V. S. Rao Gudimetla, Thomas Weyrauch, Eric Stevenson, Karl Rehder, Jiang Liu, Leonid Beresnev, Svetlana Lachinova, Izaak Kemp and Jim F. Riker, "Deep Turbulence Characterization over 149 km Propagation Path with Coherent Multi-Beam Atmospheric Transceiver (COMBAT) System ," International Workshop on Threat Warning and Tracking in Atmospheric Turbulence Baden-Baden, Germany, July 6-8, 2010.

17. M. A. Vorontsov, Ernst E. Polnau, Timothy J. Miller, and Michael T. Valley, "Atmospheric Laser Tracking System Using an Adaptive Fiber-Based Transceiver," International Workshop on Threat Warning and Tracking in Atmospheric Turbulence Baden-Baden, Germany, July 6-8, 2010.
18. M. Vorontsov, Thomas Weyrauch, Gary Carhart, Leonid Beresnev, Svetlana Lachinova, and Jiang Liu, "Adaptive Phase-locked Fiber-Collimator Array: Analysis and Experimental Demonstration**,"** XIV International Conference on "Laser Optics," St. Petersburg, Russia, 28 June – 2 July, 2010.
19. M. Vorontsov, "Intelligent Optics: How Atmospheric Turbulence Can Improve Optical System Performance," Ohio Innovation Summit, Dayton, OH, June 14, 2010
20. M. Vorontsov, Gary Carhart, V. S. Rao Gudimetla, Thomas Weyrauch, Eric Stevenson, Karl Rehder, Jiang Liu, Leonid Beresnev, Svetlana Lachinova, Izaak Kemp and Jim F. Riker, "Deep Turbulence Characterization over 149 km Propagation Path with Coherent Multi-Beam Atmospheric Transceiver (COMBAT) System," Directed Energy Systems Symposium, Monterey, California, 12-16 April, 2010.
21. M. Vorontsov, T. Weyrauch, G. Carhart, L. Beresnev, S. Lachinova, and J. Liu, "Target-in-the-Loop Beam Projection with Adaptive Phase-Locked Fiber Collimator Array: Analysis and Experimental Demonstration," Directed Energy Systems Symposium, Monterey, California, 12-16 April, 2010.
22. R. Zhou, Q. Zhan, P. E. Powers, B. Ibarra-Escamilla, and J. W. Haus, "A multi-fiber laser using a phase-locking Talbot self-imaging effect ," (Invited) Proc. SPIE Vol. **7839**, 78390M (2010).
23. Nicholas J. Miller ; Joseph W. Haus ; Paul F. McManamon and David Shemano, "Multi-aperture coherent imaging", Proc. SPIE **8052**, Acquisition, Tracking, Pointing, and Laser Systems Technologies XXV, 805207 (May 13, 2011).

4.14.5 Contributed Conference Presentations

1. N.J. Miller, B.D. Duncan and M.P. Dierking; "Resolution Enhanced Sparse Aperture Imaging," Proc. 2006 IEEE Aerospace Conference, paper #1406, Session 5.06: Novel Imaging Systems, Big Sky, Montana, March 4-11, 2006.
2. J.D. Schmidt, M.E. Goda and B.D. Duncan; "Emulating Bulk Turbulence with a Liquid Crystal Spatial Light Modulator" paper #6306-26, Advanced Wavefront Control IV, SPIE Optics & Photonics Symposium, San Diego, CA, August 13-17, 2006.
3. J.D. Schmidt, M.R. Whiteley, M.E. Goda and B.D. Duncan; "High-Resolution Liquid Crystal Spstial Light Modulators for Adaptive Optics," Proc. 2006 IEEE Aerospace Conference, paper #1367, Session 5.02: Photonic Technologies for Aerospace Applications, Big Sky, Montana, March 4-11, 2006.
4. J.D. Schmidt, M.E. Goda, J.S. Loomis and B.D. Duncan; "Aberration Production Using a High-Resolution Liquid Crystal Spatial Light Modulator," paper #6306-25, Advanced Wavefront Control IV, SPIE Optics & Photonics Symposium, San Diego, CA, August 13-17, 2006.

5. M.A. Greiner, B.D. Duncan, and Matthew P. Dierking; Monte Carlo Canopy Propagation Model, 14th Coherent Laser Radar Conference, Snowmass, CO, July 8-13, 2007.
6. D.F. Jameson, M.P. Dierking, and B.D. Duncan; Effects of Spatial Averaging on Coherent LADAR Pulse-Pair Vibration Measurements, 14th Coherent Laser Radar Conference, Snowmass, CO, July 8-13, 2007.
7. N.J. Miller, M.P. Dierking, and B.D. Duncan; Sparse Aperture Imaging, 14th Coherent Laser Radar Conference, Snowmass, CO, July 8-13, 2007.
8. J.D. Schmidt, M.E. Goda and B.D. Duncan; "Emulation of Optical Effects of Atmospheric Turbulence Using Two Liquid Crystal Spatial Light Modulators," Proc. of SPIE Vol. 6711, Advanced Wavefront Control: Methods, Devices, and Applications V, Richard A. Carreras, John D. Gonglewski, Troy A. Rhoadarmer, Editors, paper 67110M, 27 September 2007.
9. M. D. Cocuzzi, K. L. Schepler, P. E. Powers, and I. T. Lima, "Sub-Nanosecond Infrared Optical Parametric Pulse Generation in PPLN Pumped by a Seeded Fiber Amplifier," in *Advanced Solid-State Photonics*, OSA Technical Digest Series (CD) (Optical Society of America, 2008), paper WB30.
10. Mathieu Aubailly, Mikhail A. Vorontsov, Gary W. Carhart and Michael T. Valley, "Automated video enhancement from a stream of atmospherically-distorted images: the lucky-region fusion approach", Proc. SPIE 7463, 74630C (2009); doi:10.1117/12.828332
11. M. Aubailly, M. A. Vorontsov, G. W. Carhart, and M. T. Valley, "Video Enhancement through Automated Lucky-Region Fusion from a Stream of Atmospherically-Distorted Images," in *Computational Optical Sensing and Imaging*, OSA Technical Digest (CD) (Optical Society of America, 2009), paper CThC3. http://www.opticsinfobase.org/abstract.cfm?URI=COSI-2009-CThC3
12. Andrew J. Stokes ; Bradley D. Duncan ; Matthew P. Dierking ; Nicholas J. Miller; Increasing mid-frequency contrast in sparse aperture optical imaging systems. Proc. SPIE 7323, Laser Radar Technology and Applications XIV, 73230M (May 02, 2009); doi:10.1117/12.817837.
13. M. Vorontsov, T. Weyrauch, A. Beresnev, G. W. Carhart, L. Liu, and K. Aschenbach, "Adaptive Complex Field Control with an Array of Phase-Locked Fiber Collimators," in *Signal Recovery and Synthesis*, OSA Technical Digest (CD) (Optical Society of America, 2009), paper JWA4. http://www.opticsinfobase.org/abstract.cfm?URI=SRS-2009-JWA4
14. E. Watson, "Coarse-to-Fine: A Layered Sensing Approach to Situational Awareness," in *Conference on Lasers and Electro-Optics/International Quantum Electronics Conference*, OSA Technical Digest (CD) (Optical Society of America, 2009), paper PWA2.
15. B. Ibarra-Escamilla, O. Pottiez, E. A. Kuzin, J. W. Haus, M. A. Bello-Jiménez, and A. Flores-Rosas, "Wavelength-Tunable Figure-Eight Erbium-Doped Fiber Laser with a

Sagnac Fiber Filter," in *Frontiers in Optics*, OSA Technical Digest (CD) (Optical Society of America, 2009), paper FThD4.
16. E. S. Bailey, M. P. Dierking, P. E. Powers, and J. W. Haus, "Laser Radar Experiment Using a Signal with Three Sparse, Linearly Chirped Frequencies," in *Applications of Lasers for Sensing and Free Space Communications*, OSA Technical Digest Series (CD) (Optical Society of America, 2010), paper LSWB3.
17. R. W. Boyd, G. M. Gehring, M. A. Martinez Gamez, A. Schweinsberg, Z. Shi, J. E. Vornehm, Jr., E. A. Watson, and L. Barnes, "Phased-Array Laser Radar System Based on Slow Light," in *Applications of Lasers for Sensing and Free Space Communications*, OSA Technical Digest Series (CD) (Optical Society of America, 2010), paper LSWC3.
18. B. Javidi, E. A. Watson, and P. F. McManamon, "3-D Passive Sensing and Multiview Imaging," in *Applications of Lasers for Sensing and Free Space Communications*, OSA Technical Digest Series (CD) (Optical Society of America, 2010), paper LSWB2.
19. J. W. Evans, K. L. Schepler, P. E. Powers, and A. Sarangan, "A Novel Electro-Optic Beam Switch in 5mol% Magnesium-Oxide Doped Congruent Lithium Niobate," in *Frontiers in Optics*, OSA Technical Digest (CD) (Optical Society of America, 2010), paper FThV5.
20. M. A. Vorontsov, S. L. Lachinova, and J. Liu, **"**Wavefront Control Concept for Adaptive Phase-locked Fiber-Collimator Array**,"** Directed Energy Systems Symposium, Monterey, California, 12-16 April, 2010.
21. Mikhail A. Vorontsov, Thomas Weyrauch, Leonid A. Beresnev, Gary W. Carhart, Ernst Polnau, Svetlana Lachinova, and Jiang Liu,"Adaptive Optics for Free Space Laser Communications**,"** Invited Presentation at the OSA Optics and Photonics Congress, Applications of Lasers for Sensing and Free Space Communications (LS&C) Topical Meeting, San Diego, CA, January 31–February 3, 2010.
22. M. Vorontsov, T. Weyrauch, G. Carhart, and L. Beresnev, "Adaptive Optics for Free Space Laser Communications," in *Applications of Lasers for Sensing and Free Space Communications*, OSA Technical Digest Series (CD) (Optical Society of America, 2010), paper LSMA1.
23. Igor Anisimov ; Nicholas J. Miller ; Dave Shemano ; Paul F. McManamon ; Joseph W. Haus; Coherent high-resolution sparse aperture imaging testbed. Proc. SPIE 7684, Laser Radar Technology and Applications XV, 76840U (May 04, 2010); doi:10.1117/12.850221.
24. Jeffrey Kraczek ; Nicholas J. Miller ; Paul McManamon ; Joseph W. Haus ; Joseph Marron; Piston phase determination and its effect on multi-aperture image resolution recovery. Proc. SPIE 8037, Laser Radar Technology and Applications XVI, 80370T (June 08, 2011); doi:10.1117/12.883420.
25. L. A. Beresnev, M. A. Vorontsov, T. Weyrauch, G. Carhart, S. L. Lachinova and J. Liu, "Experimental study of phase locking of fiber collimators using internal beam-tail interference", Proc. SPIE 7914, 79142Z (2011); doi:10.1117/12.877300

26. S. L. Lachinova and M. A. Vorontsov, "Wavefront sensing and adaptive control in phased array of fiber collimators", Proc. SPIE 7924, 79240F (2011); doi:10.1117/12.875943
27. M. Vorontsov, V. Gudimetla, G. Carhart, T. Weyrauch, S. Lachinova, E. Polnau, J. Reierson, L. Beresnev, J. Liu and J. Riker, "Comparison of turbulence-induced scintillations for multi-wavelength laser beacons over tactical (7 km) and long (149 km) atmospheric propagation paths" Proceedings of the Advanced Maui Optical and Space Surveillance Technologies Conference, held in Wailea, Maui, Hawaii, September 13-16, 2011, Edited by S. Ryan, The Maui Economic Development Board, 2011., p.E37
28. R. Peterson, R. Feaver, and P. Powers, "Longwave-IR Optical Parametric Oscillator in Orientation-Patterned GaAs," in*Nonlinear Optics: Materials, Fundamentals and Applications*, OSA Technical Digest (CD) (Optical Society of America, 2011), paper NME7.
29. Mathieu Aubailly, Mikhail A. Vorontsov, Jiang Liu; "Scintillation-resistant wavefront sensing based on a multi-aperture phase reconstruction (MAPR) technique," Proc. SPIE 8238, High Energy/Average Power Lasers and Intense Beam Applications VI; Atmospheric and Oceanic Propagation of Electromagnetic Waves VI, 82380L (February 9, 2012); doi:10.1117/12.906080.
30. Mathieu Aubailly, Mikhail A. Vorontsov, Gary Carhart, J. Jiang Liu, Richard Espinola; "Content-dependent on-the-fly visual information fusion for battlefield scenarios," Proc. SPIE 8368, Photonic Applications for Aerospace, Transportation, and Harsh Environment III, 83680J (May 1, 2012); doi:10.1117/12.918681.
31. Nicholas J. Miller, Jeffrey J. Widiker, Paul F. McManamon, Joseph W. Haus; "Active multi-aperture imaging through turbulence," Proc. SPIE 8395, Acquisition, Tracking, Pointing, and Laser Systems Technologies XXVI, 839504 (June 8, 2012); doi:10.1117/12.921160.
32. Gui Min Wu ; Nicholas J. Miller ; Paul F. McManamon ; Edward A. Watson ; Joseph W. Haus; "Wavefront control in a spatial heterodyne-based multi-aperture imager," Proc. SPIE 8395, Acquisition, Tracking, Pointing, and Laser Systems Technologies XXVI, 839506 (June 8, 2012); doi:10.1117/12.920504.
33. Jeffrey J. Widiker, Nicholas J. Miller, Matthew R. Whiteley; "Real-time coherent phased array image synthesis and atmospheric compensation testing," Proc. SPIE 8395, Acquisition, Tracking, Pointing, and Laser Systems Technologies XXVI, 839505 (June 8, 2012); doi:10.1117/12.921892.
34. Erica M. Whitfield, Partha P. Banerjee, Joseph W. Haus, "Propagation of Gaussian beams through a modified von Karman phase screen," SPIE Optics and Photonics Conf, August 15 2012 Paper 8517-24.
35. Joseph W. Haus, Ben Dapore, Nicholas Miller, Partha Banerjee, Georges T. Nehmetallah, Peter Powers, Paul F. McManamon, "Instantaneously captured images using multiwavelength digital holography," SPIE Optics and Photonics Conf, August 15 2012 Paper 8493-34.
36. M.-T. Velluet; Mikhail Vorontsov; Piet Schwering; Gabriele Marchi; Stephane Nicolas; Jim Riker, "Turbulence characterization and image processing data sets from a

NATO RTO SET 165 trial in Dayton, Ohio, USA," Atmospheric Propagation IX, Linda M. Wasiczko Thomas; Earl J. Spillar, Editors, SPIE Proceedings Vol. 8380, 83800J (2012). doi: 10.1117/12.920657

37. A. Gonzalez Garcia, B. B. Ibarra Escamilla, E. A. Kuzin, O. M. Pottiez, M. Duran Sanchez, C. Deng, J. W. Haus, and P. E. Powers, "Q-switched Er/Yb Double Clad Single Mode Fiber Laser," in *Frontiers in Optics 2012/Laser Science XXVIII*, OSA Technical Digest (online) (Optical Society of America, 2012), paper FTu1G.2. http://www.opticsinfobase.org/abstract.cfm?URI=FiO-2012-FTu1G.2
38. Branden J. King; Ighodalo Idehenre; Peter E. Powers; Andrew M. Sarangan; Joseph W. Haus; Karolyn M. Hansen, "Tapered optical fibers for aqueous and gaseous phase biosensing applications," Frontiers in Biological Detection: From Nanosensors to Systems V, eds. Benjamin L. Miller; Philippe M. Fauchet, SPIE Proceedings 8570, (2013). doi: 10.1117/12.2004799
39. Jean Minet; Mikhail A. Vorontsov; Guimin Wu; Daniel Dolfi, "Efficiency comparison of spatial and spectral diversity techniques for fading mitigation in free-space optical communications over tactical-range distances," Free-Space Laser Communication and Atmospheric Propagation XXV, Hamid Hemmati; Don M. Boroson, Editors, SPIE Proceedings Vol. 8610, 86100X (2013). doi: 10.1117/12.200732
40. Branden J. King, Ighodalo Idehenre, Peter E. Powers, Andrew M. Sarangan, Joseph W. Haus, and Karolyn M. Hansen, "Tapered Optical Fibers for Biosensing Applications," 224th Electrochemical Society Meeting, Abstract #2662 (2013).
41. M. A. Vorontsov, "Conservation Laws for Counter-Propagating Optical Waves in Atmospheric Turbulence with Application to Directed Energy and Laser Communications," in *Imaging and Applied Optics*, J. Christou and D. Miller, eds., OSA Technical Digest (online) (Optical Society of America, 2013), paper PW3F.1. http://www.opticsinfobase.org/abstract.cfm?URI=pcDVT-2013-PW3F.1
42. C. Nunalee, J. Minet, S. Basu, and M. A. Vorontsov, "Atmospheric Refractivity Anomalies Induced by Mesoscale von K& aacute;rm& aacute;n Vortex Streets," in *Imaging and Applied Optics*, J. Christou and D. Miller, eds., OSA Technical Digest (online) (Optical Society of America, 2013), paper PW3F.2. http://www.opticsinfobase.org/abstract.cfm?URI=pcDVT-2013-PW3F.2
43. J. Minet, C. Nunalee, M. A. Vorontsov, and S. Basu, "Optical Wave Propagation through von Karman Vortex Streets," in *Imaging and Applied Optics*, J. Christou and D. Miller, eds., OSA Technical Digest (online) (Optical Society of America, 2013), paper PW3F.3. http://www.opticsinfobase.org/abstract.cfm?URI=pcDVT-2013-PW3F.3

5.0 Conclusions

5.1 Management

Dr. Haus is the founding director of LOCI and has served in that role for the past six years. Dr. Edward Watson was assigned as the AFRL liaison to LOCI. He spent much of his time over the following years working in LOCI with faculty and students. Dr. Watson was actively engaged in developing LOCI's research portfolio and created several student projects in that period. He has Graduate Faculty status which allows him to be the major advisor for graduate students at UD. In 2008 Dr. Paul McManamon was hired to be the half time technical director for LOCI. Dr. Haus oversaw the construction of the 10,000 sq. ft. LOCI facility and the purchase of equipment, such as optical tables, optical components, lasers and required electronics. The facility celebrated construction completion with an open house in March 2008, which was about 17 months after the announcement of the LOCI Center of Excellence Cooperative Agreement.

Dr. Haus hired Nicholas Miller to serve as the LOCI Lab Manager and to organize the laboratory equipment and to work on research projects. He also hired Dr. Igor Anisimov to lead and plan the construction of a multi-aperture testbed and to conduct experiments to test multi-aperture imaging concepts. Mr. Dave Shemano was hired by Dr. Anisimov to work on electronic and programming aspects of the testbed project.

Regular (almost weekly) meetings were organized and held on every aspect of the testbed design. Preliminary designs and experiments were fabricated and conducted. The analysis of those results led to the final improved design that is presented in Appendix A. Dr. Paul McManamon was a prime force in keeping the testbed project on-track and provided expertise in managing the project and meeting goals set by the project group.

Additional funds originally planned for the project did not materialize in the second and third year; this squeezed the rapid development of the testbed. Igor Anisimov was laid off in Spring 2010 and Dr. McManamon took over the primary job of managing the testbed and Mr. Miller was the senior technologist on the project. LOCI partnered with MZA in the final year of the project to Final experiments were conducted with a seven sub-aperture system and MZA processed the data using newly adapted algorithms based on imaging metrics. Nick Miller took a position at MZA in October 2012; a big loss for LOCI, since he was a driving force behind the testbed experiments. Dr. Haus hired Cullen Bradley as the replacement Lab Manager and he was tasked with getting the equipment ready to be returned to AFRL at the end of the contract.

Three phases of LOCI's development trajectory were identified by Mr. Gregory Rubertus over a 15 year span; they were designed to guide LOCI. LOCI will need to grow future funding to sustain and grow. However, the Cooperative Agreement funding was clearly ending after seven yearts, so the old plans had to be scrapped and a new one developed in its place.

LOCI decided on a future technology roadmap based on its customers and its local optics expertise. The plan was marketed to funding agencies and other DoD organizations. The LOCI members advertised projects activities and results by regularly presenting results at conferences and visiting agencies, organizations to stakeholders to promote its capabilities. LOCI continues to build credibility within the broader DoD community by performing on design, fabrication and testing projects that have a much shorter time span and is tied to customer needs.

5.2 Strategic Plan

The Strategic Plan was commissioned by AFRL as part of a Federal Appropriation. The funds were part of a subcontract from Wright Brothers Institute (WBI) and interim reports and a final report were delivered as part of that project. The committee was convened under the leadership of Dr. Haus to develop the LOCI Strategic Plan. A group of related Centers of Excellence, culled from documentation of their operations, was identified and their reported experiences were used to formulate a strategic plan. The committee consisted of members appointed from the LOCI Board of Governors, government representatives, and academic members. They deliberated with biweekly meetings conducted over one. The document identifies four Objectives and five Strategies to achieve the objectives.

The four objectives are designed to guide LOCI in achieving its mission and to address major hurdles it is facing. The LOCI Objectives identified in the Strategic plan are:

O1. Develop a Showcase Facility
O2. Attract the Best Students in the World
O3. Attract and Retain the Best Researchers in the World
O4. Develop and Build Broad Collaborations

Most Objectives are broad goals that LOCI wanted to reach while the first one is a short range goal. Five strategies were proposed to reach the goals expressed in the Objectives. The LOCI Strategies enable each of the LOCI Objectives to be accomplished. From a list of concepts the committee distilled the number to five statements. The five LOCI Strategies are:

S1. Accomplish Great Research;
S2. Build the Leaders of LADAR's Future;
S3. Solve the Needs of the Collaborative LADAR Community;
S4. Generate Collaborative Proposals;
S5. Have a Steady, Repeatable Presence in the Public LADAR Community;

The Strategies are periodically reexamined by collecting data and analyzing the results as planning for LOCI demands further reaction to the external and internal changes in its situation. The relationship between the Strategies and the Objectives is generally a many to one function. They are a springboard for deeper ideas to be examined and implemented.

A huge step forward for LOCI was the establishment of a WBI LOCI endowed Chair, as detailed in Section 4.13. It fulfilled a component of the third Objective and propelled LOCI to greater public recognition. T the same time his activities contribute to all five of the LOCI Strategies. Dr. Mikhail Vorontsov joined UD in September 2009 and was the result of a plan that took shape in the initial months of LOCI's establishment and of hard work from LOCI stakeholders. The fundraising effort for the Chair is creating an endowment of $1.75 million based on contributions from LOCI Industry Partners and UD. The Ohio Research Scholars Program contributed another $1.5 million to capital funds, and UD contributed another $410k in startup funds.

5.3 Leadership

As LOCI Director Dr. Haus was responsible for providing leadership, managing the LOCI assets and implementing a sustainment plan. Dr. Watson, as liaison between AFRL and LOCI, was

highly engaged in LOCI research and teaching and provided excellent advice to sustain an important connection to AFRL groups. Dr. Paul McManamon worked diligently to develop proposal concepts and he visited agencies to promote the concepts and organized researchers to write proposals for submission to targeted agencies.

There are many examples of leadership that could be mentioned. The all LOCI faculty have been very engaged in the international optics community. Drs. McManamon and Watson Co-Chair the OSA Topical Meeting on Remote Sensing (2009, 2011) and Dr. McMananon chairs and organizes sessions for the SPIE DSS conference. Dr. Banerjee has served as Chair and Program Committee member for the OSA Digital Holography conference. Dr. Haus has co-founded and chaired the Nanotechnology Technical Area for OSA and Co-chaired the International Conference on Nanophotonics (ICNP) for six out of seven years; ICNP has been held yearly in China and Japan. Dr. McManamon has co-chaired several high profile studies for the National Academy of Sciences. He was vice chairman of the NAS study called "Seeing Photons" and co-chair of the NAS 'Harnessing Light 2" study. Dr. Haus is Associate editor for the Journal of the European Optical Society; he is an Associate Editor-in-chief of Chinese Optics Letters and has served on the editorial board for Optics Communications.

Dr. Vorontsov boosted the acitvities and the reputation of LOCI in the community. Since he was hired in 2009 his group has grown from two staff to include visitors from Germany and France; he has established a company called Optonicus to commercialize the technology that his group has invented. Vorontsov has been active in a NATO project on adaptive optics and atmospheric turbulence for several years. He is the Team Leader of a deep turbulence MURI supported by AFOSR that was awarded in Spring 2012. The MURI project has experts from AFIT, University of Miami, Michigan Technological University, North Carolina State University and New Mexico State University. More details about this MURI can be found in Section 4.13.

Appendix A: Innovative Multi-Aperture Gimbal-less Electro-optical (IMAGE)

The IMAGE testbed was designed and developed by LOCI as a research tool in support of multiple sub-aperture based EO systems. The IMAGE testbed was conceived: 1. to test phasing algorithms that provide near diffraction limited resolution associated with array dimensions, to test required spatial sampling issues; 2. to test phasing approaches that also involve array motion; and 3. to provide a means of testing components associated with multi-sub-aperture based imaging. Carrier to noise ratio issues and atmosphere effects were investigated.

A secondary purpose of the testbed that we envisioned was to support directed energy weapon development using a similar architecture for Acquisition, Pointing, and Tracking (APT) and for the weapon itself. A tertiary purpose was to develop novel free space laser communication systems. It was envisioned that the development of the IMAGE testbed would be a strong enabler to allow development of conformal EO imaging and laser weapon system s, as well as an eventual enabler for space based active imaging and space based laser weapons.

The Initial sub-aperture optical system design comprised an afocal beam reducing telescope and a pupil relay telescope; see Fig. 24. The total length of the system was one meter. The beam reduction ratio is 8:1; thus, it reduced the receiving aperture from 5 cm to 6.25 mm (slightly undersized with respect to the camera active area). The 1:1 pupil relay telescope provides additional space (i.e., eye relief) for the insertion of local oscillator beam splitter and other optics, as required (e.g., beam steering or laser transmitter).

The testbed prototype system was envisioned to be a flexible experimental platform that can accommodate different imaging modalities. The beam reducing telescope can be adjusted to match different camera sizes; the succeeding optics can be changed to convert from pupil relay to imaging over various fields of view. Relatively large spaces between components allow for experimentation. Simple focus adjustments permit operation at the visible or NIR wavelengths and geometric effects of the finite range hall distance can be nullified by refocus and offset adjustments. (Simulating the far field character of longer ranges requires a collimator.).

To achieve this flexibility and to reduce costs of both the optics and the mechanical mounts, the design was constrained to use Commercial Off The Shelf (COTS) components and to be easy to construct and align. These constraints resulted in use of larger diameter lenses than necessary and increased length.

For example, the first lens of the beam reducing telescope is 75 mm diameter with 500 mm focal length. It is straightforward to design, specify, and procure a custom lens of reduced diameter (e.g., 62 mm) to achieve a 1.6:1 sub-aperture to sub-aperture mechanical spacing ratio. This ratio could be reduced further, possibly to as low as 1.3:1, by more complex optical component and mount design or by staggering the sub-aperture longitudinally and taking advantage of the hex-arrangement of adjacent sub-apertures. In addition, the optics in the two telescopes are fairly slow (i.e., working at f/10 and f/16, respectively). The focal lengths could be halved, reducing the overall length from one meter to about one-half meter. The eye relief would also be halved (from ~200 mm to ~100 mm), but would still be adequate for the insertion of the required heterodyne splitters and interface to the camera. The increased alignment sensitivities can be accommodated with achievable opto-mechanical tolerances. Further shortening of the system is also possible by folding the optical system and considering a more integrated opto-

mechanical design approach. Such optimizations and design studies were deferred until a later stage of the project.

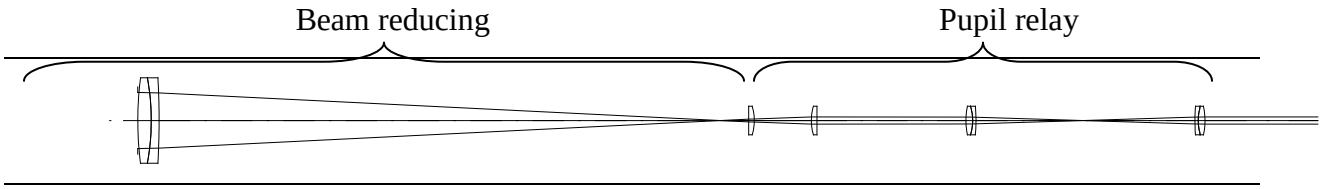

Figure 24: Sub-Aperture Receiver Optics (Range Left, Camera Right)

The mechanical design of this prototype will be based on using half inch aluminum plates mounted along a 1X4 foot breadboard. Each plate will have holes cut off for placement of the apertures in an appropriate configuration. Standard kinematic stops will be mounted on each plate for apertures alignment. A three aperture version of this initial testbed prototype is shown in Figure 25.

All costs of fabricating the prototype system were covered by the IDCAST capital equipment fund. The prototype system provided multi-aperture data for high resolution image reconstruction using an image sharpening metric.

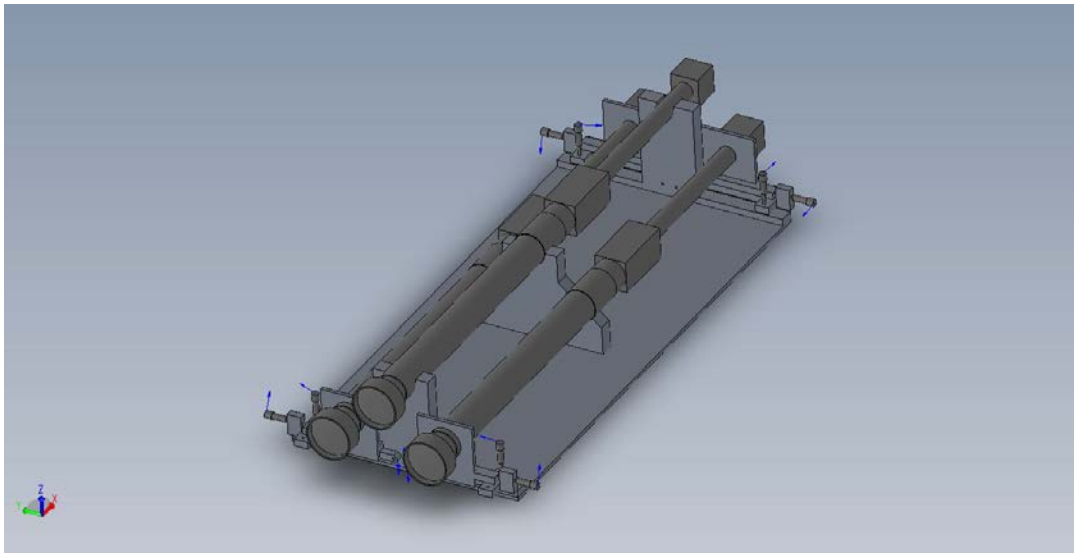

Figure 25: Three sub-aperture testbed design using in the first prototype IMAGE system.

The second IMAGE testbed design was made to increase the number of sub-apertures and use a support assembly that could be reconfigured. However, it became apparent that using beam splitter elements, would make the testbed unwieldy, as shown on the left in Figure 26. The major problem with the design is the LO assemblies on the back end of the telescope shown in the right in Figure 26. The sub-aperture \assembly and housing had many fixtures that took up too much space and required additional optical components. It was complicated and expensive. We needed a better solution!

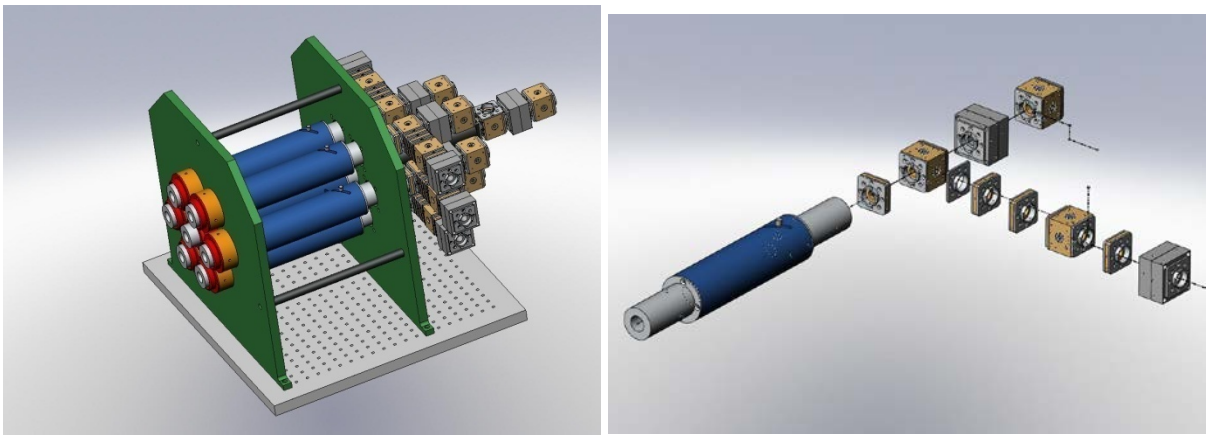

Figure 26: Initial Mechanical Design of the IMAGE Testbed

Our discussions on the need for simplification and cost cutting led us to the current and very novel mechanical design of the IMAGE testbed, which is shown in Figure 27. It has holes to accommodate up to 23 sub-apertures and four plates to hold the sub-Aperture telescopes. The first plate holds the 2" aperture lenses and the last plate attaches the firewire cameras to the end of the telescope. The design allows up a hex 19 sub-aperture system to be implemented, with the 5 sub-apertures usually shown across a hex 19 in the vertical direction. A picture showing the front view of the system is shown on the left in Figure 28. The LOs are on and the imager of the central sub-aperture of our hex 7 is illuminated. The off-axis LO's were positioned on a second face plate with a preset angular offset. We used a 1x8 multiplexer (also seem on the bottom of the image) to deliver the LO beams to each sub-aperture. No beam cubes were required in the system which produces a very efficient design with no spurious reflections from optical components.

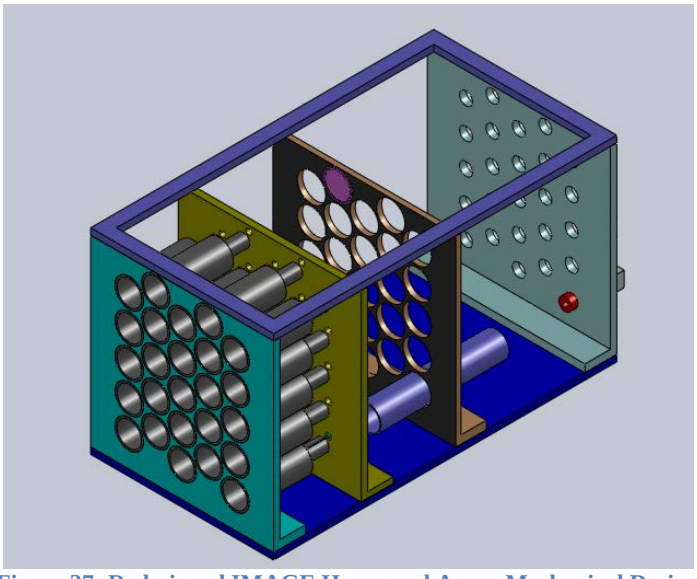

Figure 27: Redesigned IMAGE Hexagonal Array Mechanical Design

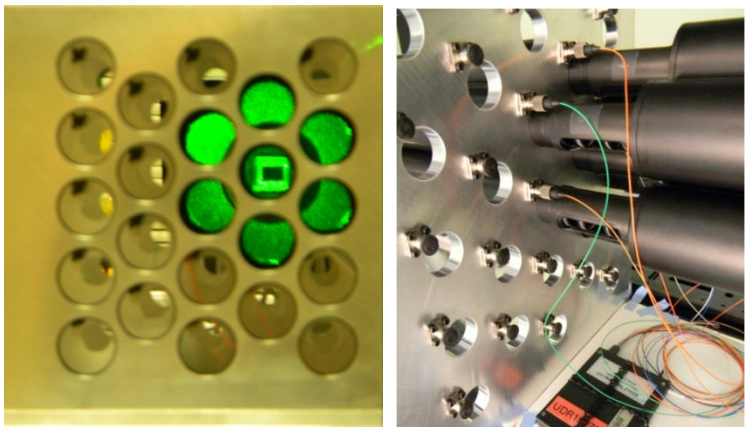

Figure 28: (left) LOCI Testbed End View and (right) Alternate View

The reason we implemented the hex 19 architecture with 5 sub-apertures in the vertical direction is for potential future use with 5 vertical sub-apertures being moved in the azimuthal direction. This is a future potential implementation of a synthetic aperture LADAR.

The optics in each telescope consisted of 5 lenses. Figure 29 has two ray diagrams of the telescope design from Zemax. On the left showing the reduction of the beam and focusing element. On the right the five lenses are indicated and the details of the lens designs are provided in Table 7. All our lenses are off-the-shelf components.

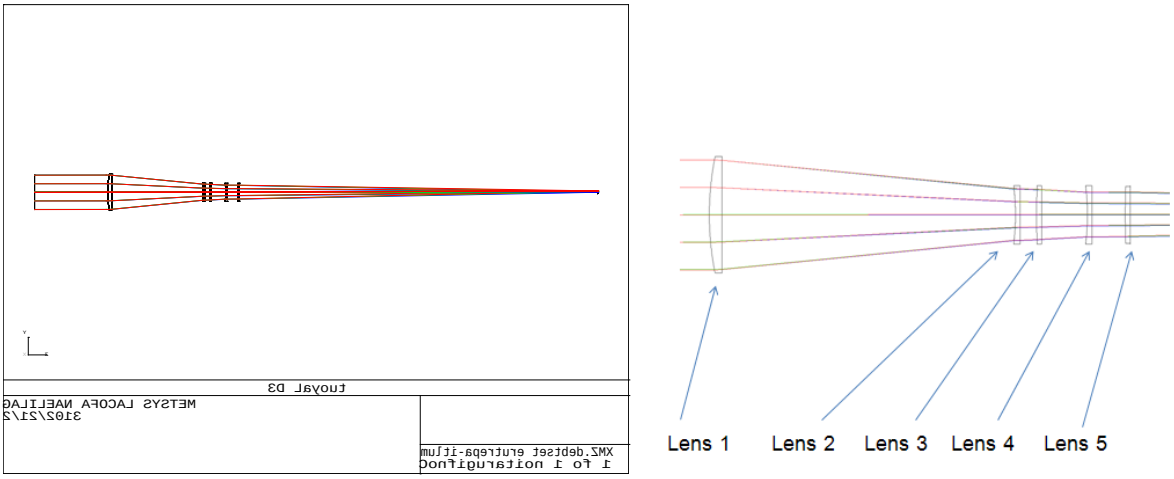

Figure 29: (Left) Zemax Layout of the Afocal Galillean Telescope (Right) Five Lenses Used

Lens Nos.	Lens Part No.	Manufacturer	url
1	LA1301	Thorlabs	http://www.thorlabs.com/thorproduct.cfm?partnumber=LA1301
2	OptoSigma 015-0350	Optosigma	http://www.optosigma.com/products/optical-components/spherical-lenses/bk-7-plano-concave-lenses/015-0350
3 & 5	LA1978	Thorlabs	http://www.thorlabs.com/thorproduct.cfm?partnumber=LA1978-A
4	LPK-25.4-103.7-C	CVI Melles Griot	https://www.cvimellesgriot.com/Products/Documents/Catalog/LPK.pdf

Table 7: List of the Five Lenses Used in the Telescope Design

The modulation transfer function (MTF) taken from Zemax for our telescope design is shown on the left in Figure 30. On the right is the spot diagram for on-axis and off-axis far-field point sources. Our telescopes as designed achieve diffraction limited imaging as shown in Figure 31. We designed and made 8 telescope assemblies. The experimental MTF for four of our telescopes are shown. The dotted line give the calculated MTF from Zemax for comparison.

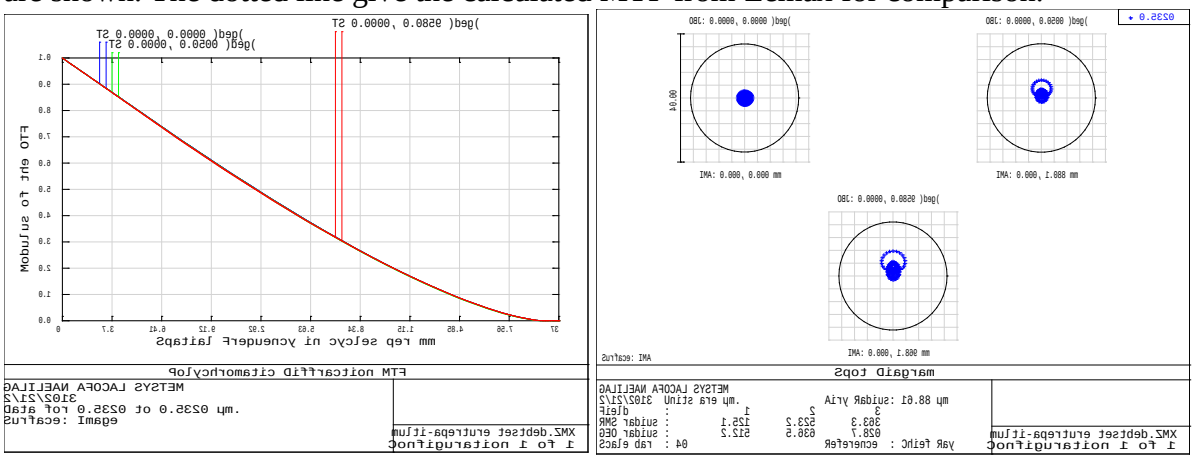

Figure 30: (Left) MTF of the Telescopes. (Right) Spot Diagrams of the Focused Collimated Beam

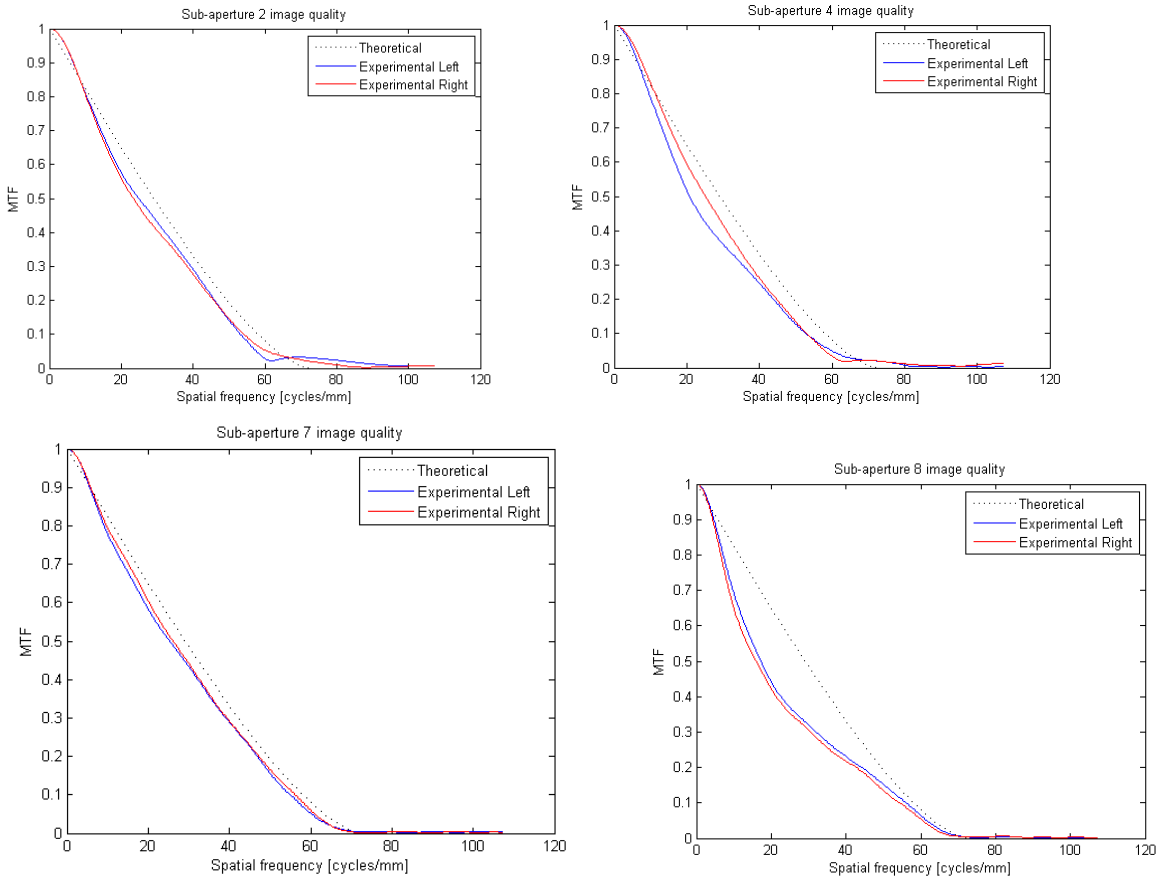

Figure 31: Measured MTF Data for Four Sub-Apertures

Figure 32 is a photographic image revealing the cameras and telescopes placed in the IMAGE system, and a view showing the fiber optics and the shields that protect each aperture

from cross talk with another aperture. Figure 30 is a side view picture of the testbed with the black tubes for isolating each sub-aperture and seven cameras placed in the focal plane at the rear of the structure.

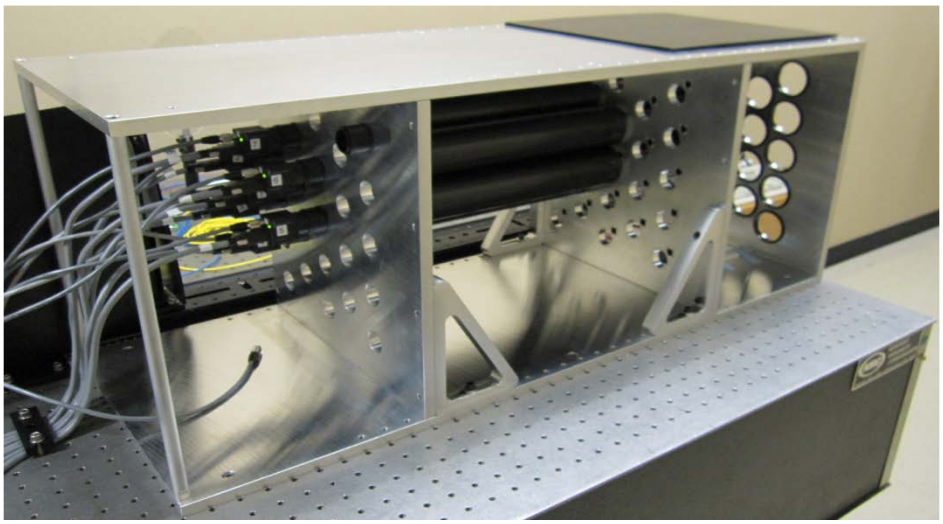

Figure 32: LOCI Testbed Side View

Figure 33 is an illustrative diagram of a single sub-aperture implemented in the image plane mode. A sample of the Illumination laser is split off and sent to become the local oscillator for the imager. The LO illuminates the image plane from an off axis position that is near the edge of the focusing lens before the image plane. As shown in the discussion on spatial heterodyne the off-axis LO creates a fringe pattern when beat against the return signal, assuming the coherence length of the illuminating laser is long enough for the round trip distance, or a sample of the outgoing laser is delayed, in which case the coherence length only needs to be as long as the depth of the object being imaged.

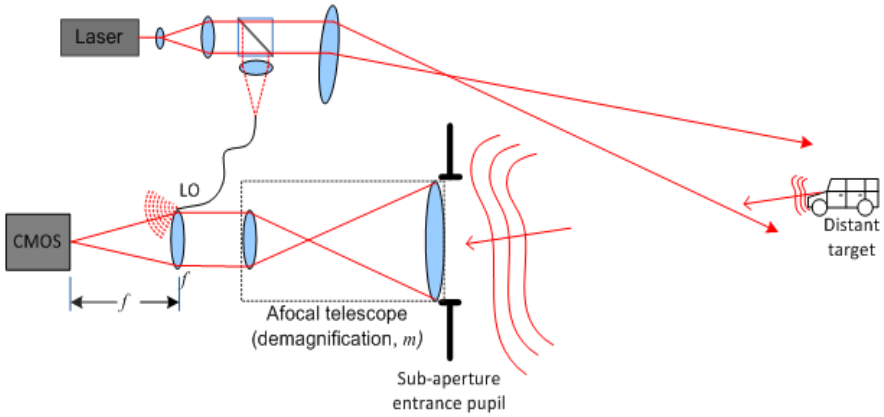

Figure 33: LOCI Testbed Single Aperture Conceptual Diagram

In Figure 34 the IMAGE testbed is illustrated as being conceptually integrated in the compact range, using two phase screens. The illumination laser directly illuminates the target to be imaged in the compact range. Light scatters off the target and passes through the phase screens, and then to a lens in the telescope, which expands the beam to use the large mirror of the

compact range. Light reflects off our large mirror and portions of the phase front are captured by the sub-apertures. The cameras are ganged together so that images in the seven cameras can be simultaneously captured.

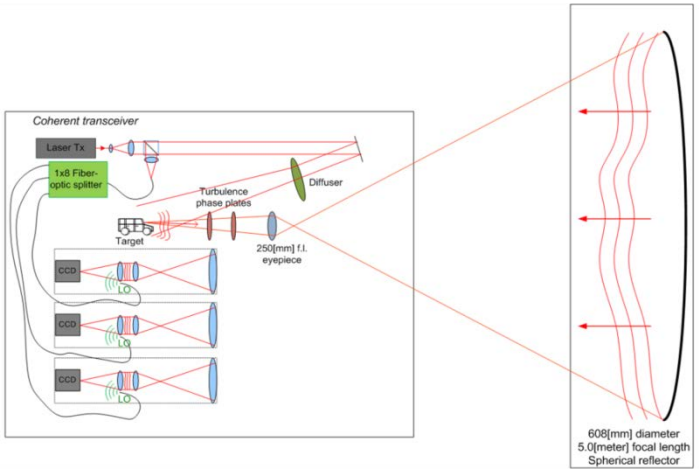

Figure 34: Concept for 3 Sub-Apertures Viewing the Mirror in the Compact Range

The target image reflected from the mirror and the IMAGE system is translationally offset from the center of the mirror as Figure 35 shows. Here we illustrate the IMAGE system with only a hex 7 filled. The compact range has an obscuration in the middle of the large mirror.

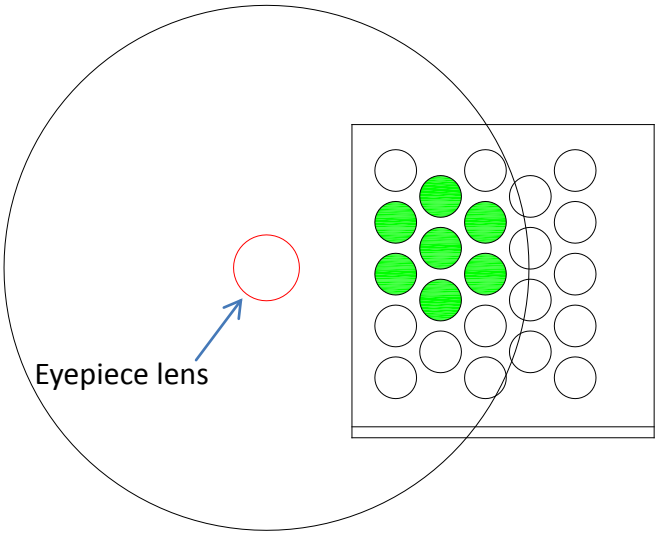

Figure 35: Hex 7 Imaging in the Compact Range

It is possible to simulate a continuous set of phase screens, the classic deep turbulence problem, using two phase screens at know positions between the object plane and the pupil plane. Figure 36 illustrates the distributed turbulence is replaced by a set of thin phase screens which integrate the phase effects of turbulence over a prescribed depth.

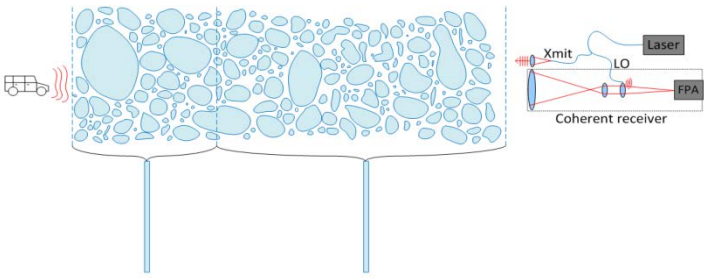

Figure 36: Using LOCI Testbed with Multiple Phase Screens

A view of the optical table holding the IMAGE system and showing an illuminated target through the compact range's pupil is shown on the left in Figure 37. On the right in Figure 37 we illustrate the compact range and the placement of an atmospheric phase plate at different distances from the pupil.

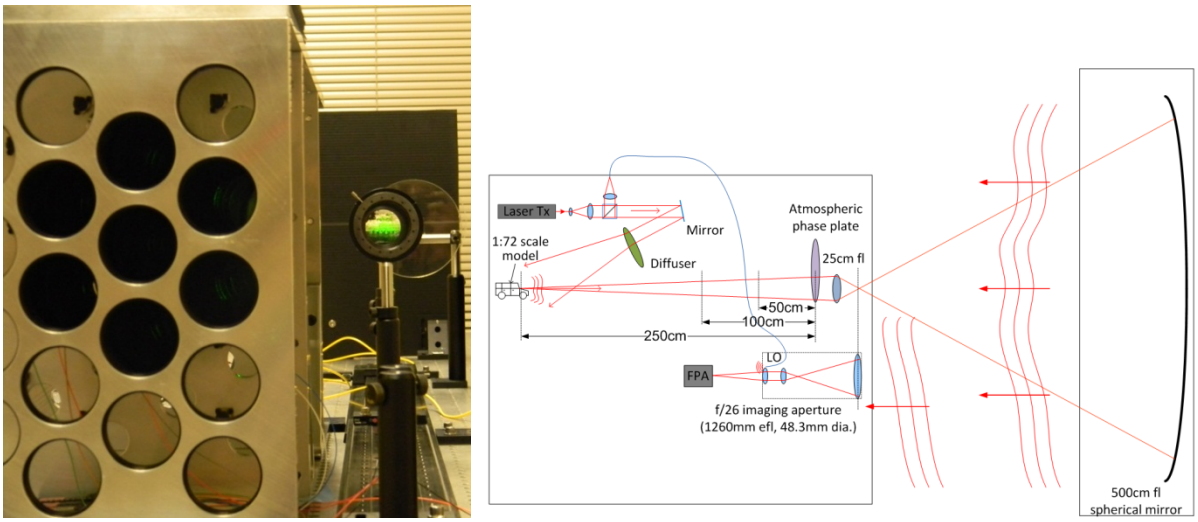

Figure 37: (left) Phase Plate Inserted in the path Between the Conjugate Plane and the Target. (right) Schematic View

Figure 38 has three examples of the same target taken in our compact range with one sub-aperture. The images are speckle averaged. The image on the left was the target shown with no phase plate inserted in the compact range. The central image has the atmospheric phase plate inserted at the conjugate pupil plane, i.e. the plane that is imaged to the pupil plane of the telescopes. In this case the wave undergoes phase distortions only. Some features are lost, but they can be recovered by using a sharpening algorithm. The images are distorted by both amplitude and phase aberrations when the plate is inserted at some distance from the pupil plane. To demonstrate this we have an image on the right formed when the atmospheric phase plate is moved 50 cm from the pupil plane. The image not only loses small features, but also there are additional anisoplanatic distortions of the image. Restoring the original image in this case remains a research challenge.

Figure 38: IMAGE Testbed Speckle Averaged Images

((left) Image with no phase plate;(middle) image with phase plate at the conjugate plane; (right) Image with phase plate 50 cm from the conjugate plane.)

A.1 1.55 µm Receiver Design

The 1.55 µm wavelength is considered "eyesafe" and suitable for conventional glass optics and lenses. Significant investment on the part of the telecommunications industry has provided a wealth of knowledge and commercial components useful to LADAR imaging, as well as for free space laser communications. InGaAs is a semiconductor material that is sensitive from approximately 0.9 µm to 1.70 µm. InGaAs focal plane arrays operating at 1.55 µm do not require cooling to achieve acceptable SNR. InGaAs cameras can be made smaller, cheaper, and be designed to draw less power than previous IR imagers that requiring cooling. Like visible CCD cameras, InGaAs cameras are factory corrected for pixel non-uniformity and do not require periodic corrections during field usage. InGaAs is suitable for high-volume production and potential future cost reductions. The selection of COTS InGaAs focal plane arrays is quite limited. We selected a Goodrich Sensors Unlimited camera. The Sensors Unlimited camera was selected taking into account the pixel count required for the target and image distances specified for the testbed. A 320 x 256 pixel array exceeds the specifications. The SU320KTSX-1.7RT camera was the most sensitive InGaAs COTS camera that we found. Since we will be using mostly heterodyne approaches more sensitivity would not be of significant value anyway. A high local oscillator power will help overcome detector noise issues. This camera has a 25 µm pitch. Initially we bought 3 focal plane arrays, and fabricating 3 sub-apertures. This allowed testing prior to purchasing components for the full testbed. It has a standard 12-bit Camera Link data format which simplifies the image acquisition. Figure 39 lists some 1.55 µm camera features and Figure 38 shows the visible camera characteristics for the same testbed.
Figure 37 shows the specs for the near IR camera used in the early 3 camera version of the IMAGE testbed. We have 3 NIR cameras, which allows imaging with 3 sub-apertures in a row.

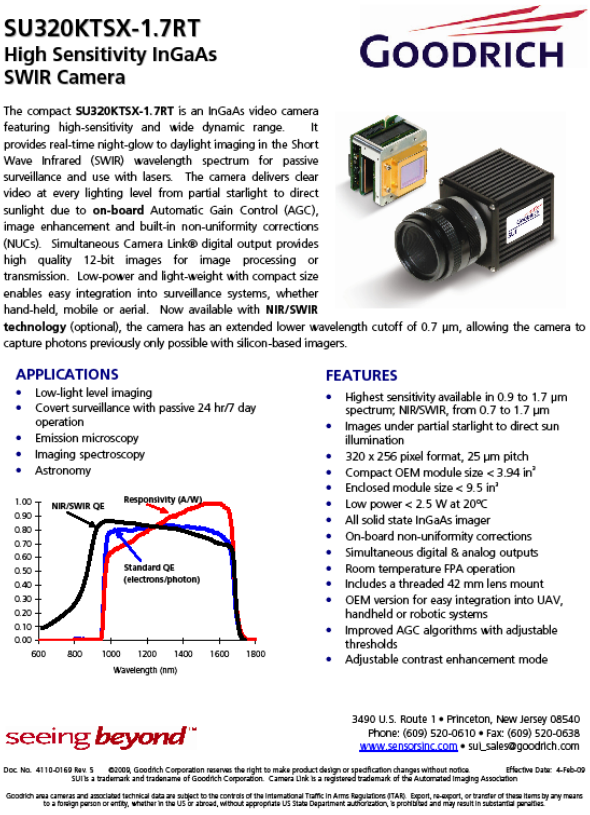

SU320KTSX-1.7RT
High Sensitivity InGaAs SWIR Camera

GOODRICH

The compact **SU320KTSX-1.7RT** is an InGaAs video camera featuring high-sensitivity and wide dynamic range. It provides real-time night-glow to daylight imaging in the Short Wave Infrared (SWIR) wavelength spectrum for passive surveillance and use with lasers. The camera delivers clear video at every lighting level from partial starlight to direct sunlight due to **on-board** Automatic Gain Control (AGC), image enhancement and built-in non-uniformity corrections (NUCs). Simultaneous Camera Link® digital output provides high quality 12-bit images for image processing or transmission. Low-power and light-weight with compact size enables easy integration into surveillance systems, whether hand-held, mobile or aerial. Now available with **NIR/SWIR technology** (optional), the camera has an extended lower wavelength cutoff of 0.7 µm, allowing the camera to capture photons previously only possible with silicon-based imagers.

APPLICATIONS

- Low-light level imaging
- Covert surveillance with passive 24 hr/7 day operation
- Emission microscopy
- Imaging spectroscopy
- Astronomy

FEATURES

- Highest sensitivity available in 0.9 to 1.7 µm spectrum; NIR/SWIR, from 0.7 to 1.7 µm
- Images under partial starlight to direct sun illumination
- 320 x 256 pixel format, 25 µm pitch
- Compact OEM module size < 3.94 in³
- Enclosed module size < 9.5 in³
- Low power < 2.5 W at 20ºC
- All solid state InGaAs imager
- On-board non-uniformity corrections
- Simultaneous digital & analog outputs
- Room temperature FPA operation
- Includes a threaded 42 mm lens mount
- OEM version for easy integration into UAV, handheld or robotic systems
- Improved AGC algorithms with adjustable thresholds
- Adjustable contrast enhancement mode

seeing beyond™

3490 U.S. Route 1 • Princeton, New Jersey 08540
Phone: (609) 520-0610 • Fax: (609) 520-0638
www.sensorsinc.com • sui_sales@goodrich.com

Figure 39: NIR cameras Specifications

The 1550nm wavelength was selected as one of the wavelengths for the testbed. 1550 nm will be the wavelength used for future outdoor "range" experiments. 1550nm is considered to be "eye safer" since the water in the eye absorbs at 1550 nm, preventing the light from reaching a focus. There are 1550nm lasers with coherence length up to 100Km. Long coherence length makes implementation of long range heterodyne detection much easier. With coherence length as long as the round trip to an object there are no issues in implementing heterodyne interference between the return signal and the local oscillator so long as neither the atmosphere nor the target or sensor motion blur the return signal phase. With moderate coherence length lasers heterodyne can still be implemented, but a sample of the outgoing laser pulse must be stored to act as the local oscillator or only relative phase is measured. For spatial heterodyne measuring relative phase is good enough. The coherence length must be at least as great as the depth of the object being imaged. Output of the 1550nm source can be amplified with an additional EDFA to the levels of 50-100W without changing the coherence length of the source. There are amplifiers available that will follow the master oscillator in frequency. It only needs money and some engineering to raise the laser output power levels. NP Photonics manufactures 1550nm fiber coupled lasers systems with up to 5W output with optional seed port that can be used as an amplifier input. LOCI has a NP Photonics laser model RFLSA-2000-1-1550-PM-S-UNL (output power 2W) as capital equipment using university funding. This laser could be used as the basic laser source for 1550 nm laser radar experiments indoor for a 3 sub-aperture experiment. The results of this study will be relevant for planning experiments over the 7 km

path. With the IR cameras we possess and the power of our laser we could reasonably attempt images over that distance with targets that are covered with 3M reflective materials.

A.2 532 nm Receiver Design

Multiple sub-aperture based array experiments were performed at 532 nm. Inexpensive focal plane arrays are readily available at this wavelength and optical alignments are more easily accomplished by students because light is visible at this wavelength. Numerous detector arrays with more than 1000 x 1000 pixel counts are available from many manufacturers. This format size easily exceeds our requirements. We selected a COTS Lumenera 120 board camera because of its easy PC compatibility via USB output, small package size, and high dynamic range. The specifications for the visible cameras are displayed in Figure 40.

Lumenera corporation

Lu120

1.3 Megapixel USB 2.0 Camera

Outline

Lumenera's Lu120 series of megapixel cameras are designed to be used in a wide variety of applications. Both color and monochrome product models are available.

With 1280x1024 resolution and on-board processing these cameras deliver great image quality and value for industrial and scientific imaging applications.

Electronic Global Shutter provides capabilities similar to a mechanical shutter, allowing simultaneous integration of the entire pixel array, and then stopping exposure while image data is read out. They are ideal for capturing objects in high-speed motion.

Uncompressed images in live streaming video and still image capture are provided across a USB 2.0 digital interface. No framegrabber is required. Advanced camera control is available through a complete Software Developer's Kit (SDK), with sample code available to quickly integrate camera functions into OEM applications.

Hardware and software based synchronization trigger is provided standard. Lu120 model cameras are offered in both enclosed and board-level form. Custom form factor (sizes) can be provided.

All Lumenera products are supported by an experienced team of software developers and application engineers. We understand your imaging needs and are here to help you with your integration and development. Products come with a full one (1) year warranty.

Performance Features

- **High dynamic range sensor using multi-slope integration**
- **Color or monochrome, progressive scan, 1.3 megapixel sensor**
- **High-speed USB 2.0 (480Mbits/sec)**
- **15 fps at full 1280x1024 resolution 60 fps 640x480**
- **Higher frame rate at lower resolution with full sub-window control**
- **Global and rolling electronic shutter**
- **GPI/Os for control of peripherals and synchronization of lighting (4in/4out)**
- **FCC Class B, CE Ready**
- **RGB Bayer video output**
- **Select 8 or 10-bit pixel data**
- **Simplified cabling - video, power and full camera control over a single USB cable**
- **C-Mount provided**
- **DirectShow compatible**
- **USB cameras are software compatible with Windows™ 98 SE, Windows ME, Windows 2K and Windows XP operating systems**
- **Complete SDK available**

Lumenera Corporation • 7 Capella Court, Ottawa, ON, Canada K2E 8A7 • (t) 1.613.736.4077 • (f) 1.613.736.4071 • www.lumenera.com

Figure 40: Visible Camera Description and Features

The 532nm laser system (JDSU M142H-532-400SF) is capable of 400mW output power and has a >100m coherence length. This laser was used for experiments in the compact range discussed earlier. This is not an eyesafe laser, so controls were required in the range hall while the laser was in use. The 532 nm laser was not used for outdoor tests, but if there is sufficient reason to do so arrangements could be made to use the WPAFB laser test range, while providing appropriate safety considerations. The 532 nm laser was used in the IMAGE testbed. We initially bought x cameras, and used them in the preliminary 3 sub-aperture tested. Then we bought y more cameras for the 7 sub-aperture test of the image testbed.

A.3 Integration Time and Vibrations

A long integration time is used with the cameras, so any motion of the object or the atmosphere can create blur. To phasing up multiple sub-apertures object motion must be kept less than 10 % of the wavelength, which is 532 nm for the visible wavelength laser. In the range hall we can limit integration time and still have plenty of energy for a measurement. Possible blur due to object motion will be discussed here. We can assume target oscillation is given simply by:

$$x = A\sin\left(\frac{2\pi t}{T}\right) \quad , \tag{22}$$

where T is the period of the vibration and A is the amplitude. The velocity is the derivative of the amplitude. The change of position for a time Δt is:

$$\Delta x = \frac{2\pi A \Delta t}{T}\cos\left(\frac{2\pi t}{T}\right) \tag{23}$$

From Eq. 23 we deduce that higher frequency vibration will cause more blur during a short integration time. Consider a 10 μs integration time and a 1 μm vibration for frequencies lower than 1000 Hz the integration time is much less than the period of oscillation at 1000 Hz. The maximum amplitude change (blur) in the period for 1000 Hz would be 6.28 nm. Lower frequencies would yield smaller blurs.

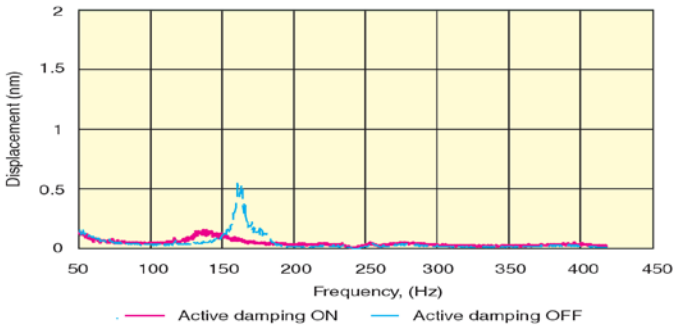

Figure 41: Displacement of a Newport ST-UT2 Series 8 inch Thick Table

Of course the maximum motion is the amplitude of the vibration, which occurs if a long enough sample time is used. The 1 μm amplitude is of course arbitrary. Higher frequency vibrations have much more impact and lower frequencies yield a smaller impact. Optical tables are very stiff and they tend to have much smaller amplitude vibrations. Figure 41 shows vibration for a Newport 8 inch thick table. The scale on the displacement is in nanometers.

A.4 S/N, range, and power consideration

The testbed was designed to operate against a large distributed, stationary, target. The current embodiment uses spatial heterodyne to measure the spatial complex field at each sub-aperture. We anticipate that image sharpening will be required on each sub-aperture image. Therefore, we need adequate S/N in each sub-aperture to obtain an image. This is not disadvantageous when viewing a large distributed object since the pixel area is larger for the small receive collection aperture. The larger pixel area makes up for the smaller aperture. S/N for point images will, in the future, be more challenging. Point target imaging could be addressed in the future. For the VA hospital at 7 Km each 5 cm sub-aperture will see a diffraction limited area of 21.7 x 21.7 cm.

A.4.1 Photon Link Budget

This section calculates the link budget for a NIR IMAGE testbed operating outdoor to the VA center, even though we did not get to outdoor operation. A Gaussian transmitter beam is defocused such that the spot at the target range (defined by the $1/e^2$ irradiance ring) equals the desired FOV. A target is placed on axis that is sufficiently small so that the irradiance across it is assumed to equal the Gaussian spot's peak irradiance. The number of photons returning to the receive aperture, *N*, can be calculated using the Laser Range Equation,

$$N = \eta_{sys}\eta_{atm}^2 E_{pulse} \frac{R_{target} A_{target}}{2 \cdot w_z^2 \cdot \Omega_{target}} \left(\frac{D_{rec}^2}{z^2} \right) \left(\frac{\lambda}{hc} \right) [photons] \tag{24}$$

where η_{sys} = Transceiver optical system efficiency
η_{atm} = Atmospheric absorption (one way)
E_{pulse} = Transmit pulse energy *[Joules]*
R_{target} = Target Reflectivity
A_{target} = Target area $[m^2]$
w_z = $1/e^2$ transmitter irradiance radius at the target range *[m]*
Ω_t = Target backscatter angle *[sr]*
D_{rec} = Receive aperture diameter *[m]*
z = Distance to range *[m]*
λ = Optical wavelength of transmitter beam *[m]*
h = Planck's constant *[ ]*
c = Vacuum speed of light *[m/s]*

We have neglected atmospheric turbulence so the received photon count is an average number. Next, we use the following values for each variable,

- η_{sys} **= 80%** The transceiver losses include the transmitter losses (primarily due to beam expander), and receiver losses (primarily due to the receiver telescope, and beamsplitter(s))
- $\eta_{atm} = e^{-\alpha z}$ where α **= 1 x 10^{-4} [m^{-1}]** Atmospheric attenuation estimate is based on previous study which measured the attenuation as,

  $\alpha \sim 7 \times 10^{-5}$ for 16 mile visual range*
  $\alpha \sim 4.4 \times 10^{-5}$ for 24 mile visual range*

* Date taken from : J. H. Taylor and H. W. Yates, "Atmospheric Transmission in Infrared" JOSA **47,** 223 (1957).

- E_{pulse} **= 2 [mJ]** Transmitter pulse energy is given by,
  2[W] CW laser at 1ms exposure time set by atmospheric coherence time.
- R_{target} **= VARIABLE,** for a Lambertian target (such as Spectralon) *R*= 90%, and for the *3M* retroreflective targets *R*= 23% and 60% respectively for 3M-900X and 3M-3000X.
- D_{rec} **= 5 [cm]**
- λ **= 1.55 [μm]**
- A_{target} **= (.037) [m^2]** The target is a 21.7cm diameter disk equaling the resolution spot size of a single 5cm sub-aperture at the z=7Km range,

$$A_{target} = \frac{\pi}{4}\left(\frac{\lambda z}{D_{rec}}\right)^2 \tag{25}$$

- $2 \cdot w_z$ = **5 [m]** for the 7Km target range
- Ω_t **= VARIABLE,** for the Lambertian target = π, for 3M-900X = 0.00080[ster.], and for the 3M-3000X = 0.00063[ster.]

  Figure 42 is a plot of the link budget for three different target scenarios. The Lambertian target returns the fewest number of photons to the receiver, as expected. At seven kilometers just a couple hundred photons would be expected to be recorded. For the 3M targets the return beam has much narrower angular spread which can return more than three orders of magnitude more photons to the receiver aperture. These artificial targets can make up for a lack of laser power in imaging at distances up to 7 km. Table 8 summarizes the expected number of received photons for the three target cases at 1, 2 and 7 km.

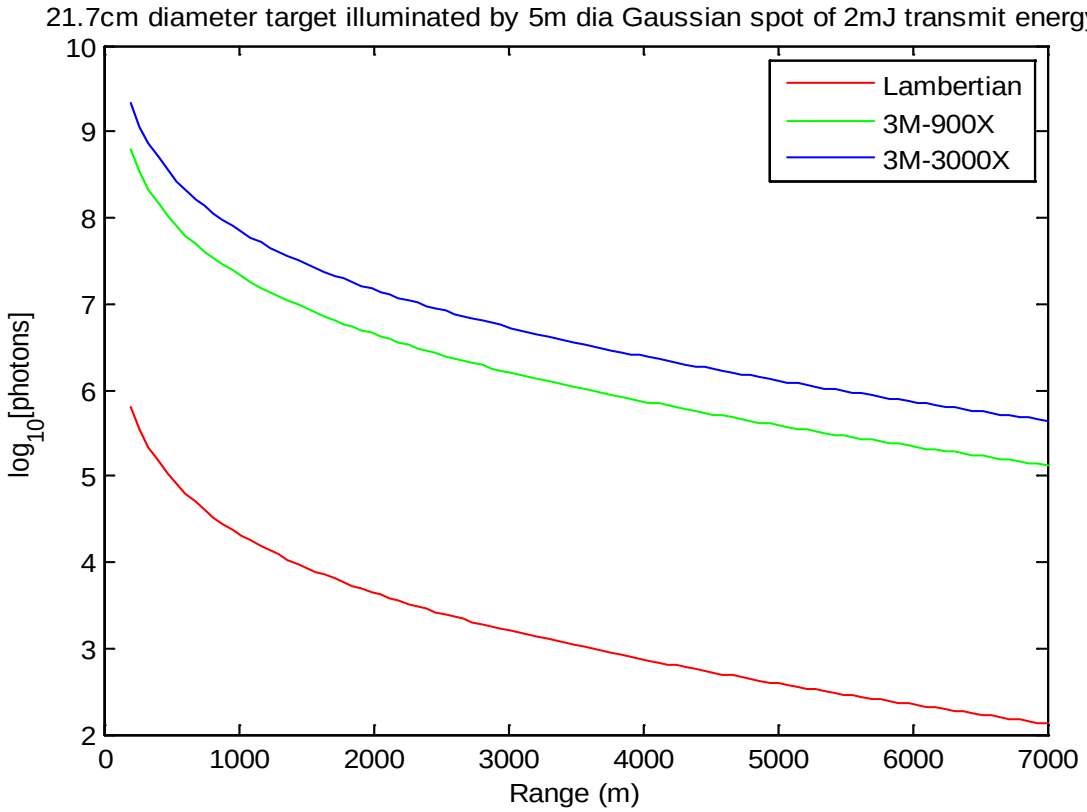

Figure 42: Theoretical Number of Return Photons for the Outdoor Range (Eq. 24)

Reflectivity and Backscatter angle	**1Km**	**2 Km**	**7Km**
R=90% $\Omega_{target} = \pi$ [ster.]	2.1 x 10^4 [photons]	4400 [photons]	130 [photons]
R=23% Ω_{target} = 0.80 [mster.]	2.2 x 10^7 [photons]	4.5 x 10^6 [photons]	1.3 x 10^5 [photons]

R=60% Ω_{target} = 0.63 [mster.]	7.2 x 10^7 [photons]	1.5 x 10^7 [photons]	4.4 x 10^5 [photons]

Table 8: Number of Expected Return Photons from Targets

A.5 Photons Required for Imaging

A.5.1 Coherent Detection in the Pupil Plane

The question of how many received photons are needed for imaging an object was also examined. An afocal telescope maps the entrance pupil, which coincides with the 5cm sub-aperture lens, onto the 6.4mm x 8.0mm camera detector array with no wasted signal using a magnification, $M = 8$.

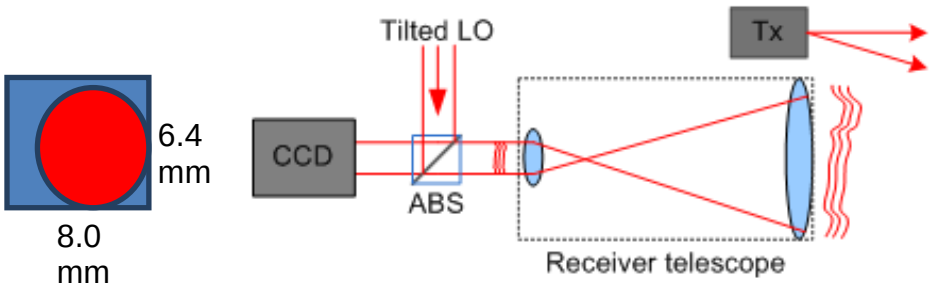

Figure 43: Single Aperture Diagram

In this imaging method, the pupil diameter determines the diffraction-limited spatial frequency resolution,

$$f_{cutoff} = \frac{D}{\lambda R} = 4.61[cycles/m] \tag{26}$$

where

$$D \equiv Subaperture\ diameter = 5cm$$

$$\lambda \equiv Wavelength = 1.55\mu m$$

$$R \equiv Range = 7Km$$

The detector array's pixel pitch determines the maximum alias-free *FOV*

$$FOV_{unaliased} = \frac{\lambda R}{2MP_x} = 27.1m \tag{27}$$

where

$$M \equiv Telescope\ magnification = 8X$$

$$P_x \equiv Camera\ \ pixel\ \ pitch = 25\mu m$$

The design FOV of the IMAGE testbed is 5m at the 7Km VA Hospital range. The FOV of the IMAGE testbed can be limited by any of three factors: 1. the illumination spot diameter in the target plane, 2. the telescope's optical field of view, and 3. the detector array's unaliased FOV derived above. The illumination spot should be the minimum that fully covers the target in order to maximize the CNR. The telescope's FOV should encompass the target. A narrow telescope FOV will reduce background light and a wider telescope FOV will ease the aiming tolerance. However, the telescope's FOV must be narrower than the detector array's un-aliased FOV.

A.5.2 Forming an Image from Pupil Plane Data

The number of photons incident on the receiver aperture can be calculated with the laser range equation for a given transmit power, target reflectance distribution function, and range. These signal photons are mixed with a relatively strong tilted LO beam as shown in Figure 45. The amplitude and phase of the field reflected off the object is encoded in the resulting spatial interference pattern that is recorded by the two-dimensional detector in the pupil plane. The complex field can then be extracted and numerically propagated via Fresnel transform to create a virtual focal plane image. The signal-to-noise ratio, SNR, of the resulting virtual image is dependent on the carrier-to-noise ratio, CNR, of the pupil plane interferogram. When the signal shot noise is the dominant noise source, the CNR is given by the expression below where N_{signal} is the number of signal photons, η_q is the detector quantum efficiency, η_h is the heterodyne efficiency, and F_h is the excess noise factor that accounts for noise sources beyond signal shot noise. Heterodyne efficiency, η_h is affected by factors such as atmospheric turbulence effects on the receive wavefront, depolarization of the signal wavefront by the target. The excess noise factor, F_h, is camera dependent.

$$CNR = \frac{\eta_q \eta_h}{F_n} N_{signal} \tag{28}$$

We have found it difficult to quantify the excess noise factor, F_h for our digital camera IR camera in pupil plane imaging mode. Manufacturers of IR cameras are primarily interested in optimizing the camera for use in low light conditions. However, in pupil plane imaging mode, the camera is flooded with a strong LO beam so that each pixel typically generates greater than half its well depth of photoelectrons during a short integration time. This strong LO beam provides coherent signal gain and makes signal shot noise the dominant noise source. Pixel photo-response non-uniformity, pixel crosstalk, and dark current non-uniformity are expected to have an equal or even greater negative impact on CNR than the noise sources typically specified by IR camera manufacturers. Therefore, the sensitivity of the IR camera was experimentally measured. The experiment is shown in Figure 44.

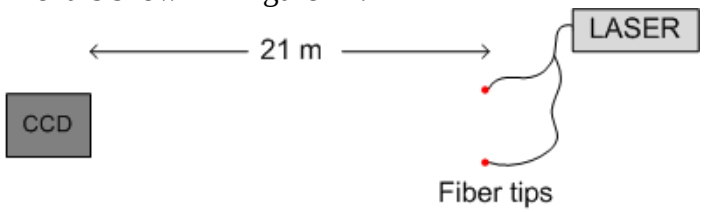

Figure 44: Camera Sensitivity Measurement Setup

The IR laser source is split and each fiber end is pointed over the 4.3m range toward the *Sensors Unlimited SU320KTSX* IR camera, or the TV camera, whichever is being measured. One fiber end is designated as the LO beam and its power is set so that each camera pixel generates just greater than half its well depth of photoelectrons during an integration time. The other fiber end is designated as the point object and its intensity is initially set at 5% of the LO power. The ~10μm diameter fiber ends approximate point sources over the 4.3m range and have like polarization so that a spatial sinusoidal intensity is recorded by the camera (Figure 45A) and via Fresnel transform an image of the point is formed in the upper left quadrant of Figure (45B). The upper 115 by 115 pixel portion of the upper left quadrant was defined as the FOV in order to avoid the energy near the DC peak. The "point" (located at pixel (row=94, column=94) is

clearly visible in this example where approximately 18,000 signal photons were incident across the entire sensor array.

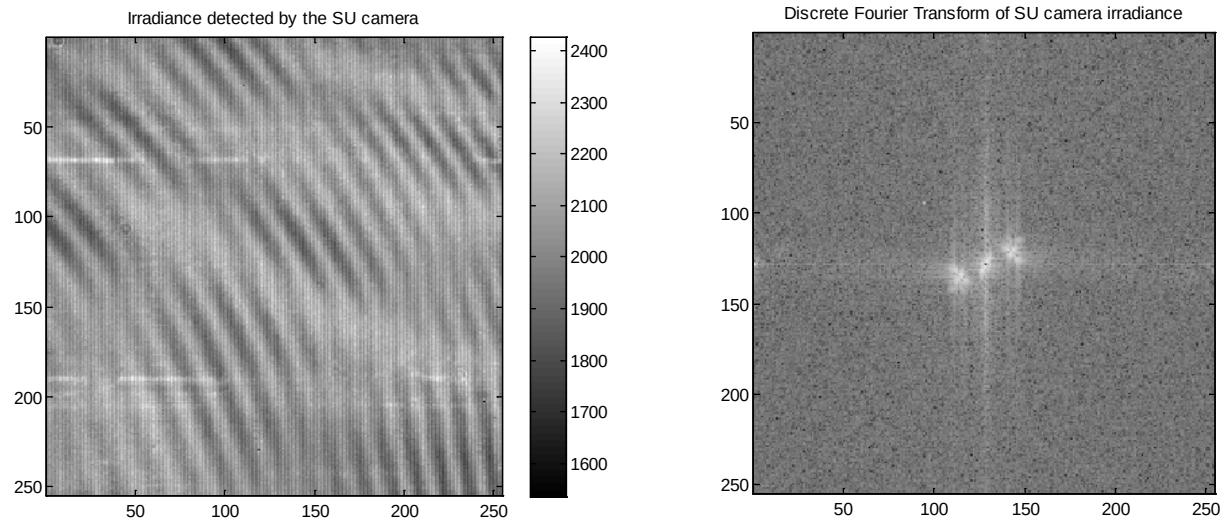

Figure 45: A and B Point Patterns Using the 1.5 µm Camera.

The intensity of the "point" in the FOV is measured are compared to the next highest pixel value in the FOV. The point is considered imaged successfully if it is the brightest pixel in the FOV. The power in the point object is reduced and the ratio of the pixel value of the "point" to the next brightest pixel in the FOV is compared. The successful detection of the "point" is limited by both deterministic and random noise sources. A fixed, deterministic noise source would include the low frequency fringes (probably due to reflections of the strong LO beam caused by the camera cover glass) visible in the detected irradiance. Fortunately, after discrete Fourier transform to the virtual focal plane, most of this energy appears in the discarded quadrants. Another method to eliminate the fixed, deterministic noise in the LO beam is to subtract an LO irradiance image from the image of the mixed signal and LO. The difference image is shown at the left in Figure 46 and its virtual focal plane image is shown to the right.

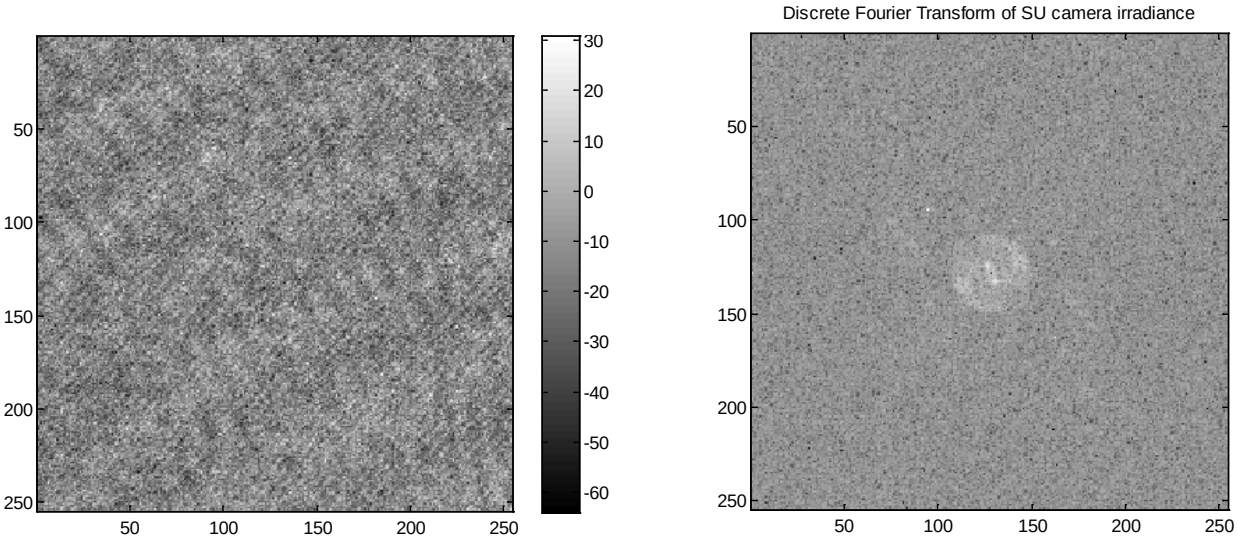

Figure 46: Transforms of the 1.5 µm Camera Images

A.5.3 Experimental results using the Sensors Unlimited camera

Multiple images were recorded. A virtual focal plane image was formed via Fourier transform and the pixel value at the known "point" location was measured and compared to all the other pixel values in the FOV. If the "point" was not successfully detected 5/5 times, we subtracted out an LO image before performing the Fourier transform to the virtual focal plane.

Number of signal photons	Successful "point" detection ratio	Successful "point" detection ratio after subtracting LO image
1500	5/5	N/A
720	2/5	20/20
360	0/5	16/20
123	0/5	5/20

Table 9: Results of Multiple Measurements and Extraction of a Point Source

A.5.4 Extrapolating Sensors Unlimited Experimental Results to Outdoor Use

The heterodyne efficiency, η_h of the experiment using the Sensors Unlimited camera is approximately 100%. We expect that for a diffuse target and effects of depolarization, the heterodyne efficiency will be much less, perhaps in the neighborhood of 30%. Therefore, coupling the experimental results using the Sensors Unlimited camera with a 2 watt cw laser, a 1 msec integration time, and the laser range data shown in Table 8, a 21.7cm diameter Lambertian target cannot be imaged at the 7KM distance. However, a similarly sized target of either retro reflective material might be imaged at this 7Km range.

A.5.5 Modeling Pupil Plane Detection

The irradiance across the pupil plane detector for two interfering beams is given by,

$$I(x,y) = I_{LO}(x,y) + I_s(x,y) + 2\sqrt{I_{LO}(x,y)I_s(x,y)}\cos[\phi_{LO}(x,y) - \phi_s(x,y)] \tag{29}$$

The LO beam is modeled as a plane wave with uniform amplitude and the signal beam is modeled as a distant, point source so that the signal beam is also approximated with a uniform amplitude plane wave. The LO plane wave has a linear tilt with respect to the object wave.

$$I_{LO}(x,y) = U_{LO}(x,y)\cdot U^*_{LO}(x,y) \quad where\ U_{LO}(x,y) = U_{LO}\exp[j2\pi(f_{spx}x + f_{spy}y) + \phi_{LO}] \tag{30}$$

$$I_s(x,y) = U_s(x,y)\cdot U^*_s(x,y) \quad where\ U_s(x,y) = U_s\exp[j\phi_s] \tag{31}$$

The LO plane wave can be back-propagated to a point source in the object plane. The spatial frequency of the tilt, f_{spx} and f_{spy} are related to the distance between the point object and back-propagated LO point,

$$f_{spx} = \frac{x_{object} - x_{BPLO}}{\lambda R} \tag{32}$$

and

$$f_{spy} = \frac{y_{object} - y_{BPLO}}{\lambda R} \tag{33}$$

Next, we wish to calculate the optical power incident on each pixel by integrating the intensity across the active area of each pixel. The pixel center coordinates are given by the vectors *X* and *Y* where P_x and P_y are the pixel pitches and *N* and *M* are the number of pixels along each axis.

$$\mathbf{X} = P_x \cdot \left\{ -N/2, -N/2+1, \ldots, -1, 0, 1, \ldots, N/2-2, N/2-1 \right\} \tag{34}$$

$$\mathbf{Y} = P_y \cdot \left\{ -M/2, -M/2+1, \ldots, -1, 0, 1, \ldots, M/2-2, M/2-1 \right\} \tag{35}$$

The active area of each pixel is Δx by Δy. Therefore, the power incident on a pixel centered at *(X,Y)* is,

$$P(X,Y) = \int_{Y-\frac{\Delta y}{2}}^{Y+\frac{\Delta y}{2}} \int_{X-\frac{\Delta x}{2}}^{X+\frac{\Delta x}{2}} I(x,y)\,dx\,dy \tag{36}$$

Assuming that $I_{LO}(x,y)$ and $I_s(x,y)$ are approximately uniform across a pixel extent, then spatial integration gives the power incident on a pixel,

$$P(X,Y) = \left(I_{LO}(X,Y) + I_s(X,Y)\right)\Delta x \Delta y + \frac{2\sqrt{I_{LO} I_s}}{\pi^2 f_{spx} f_{spy}} \sin(\pi f_{spx} \Delta x) \sin(\pi f_{spy} \Delta y) \cos\left[2\pi\left(f_{spx} X + f_{spy} Y\right)\right] \tag{37}$$

The Sensors Unlimited camera has square pixels with a 100% fill factor so that $\Delta x = \Delta y = P_x = P_y$ and the expression for the power on a pixel becomes.

$$P(X,Y) = \left(I_{LO}(X,Y) + I_s(X,Y)\right)P_x^2 + \frac{2\sqrt{I_{LO} I_s}}{\pi^2 f_{spx} f_{spy}} \sin(\pi f_{spx} P_x) \sin(\pi f_{spy} P_x) \cos\left[2\pi\left(f_{spx} X + f_{spy} Y\right)\right] \tag{38}$$

Using the semi- classical approach to photon detection, the mean number of photons, *NP*, generated per pixel during a camera integration time T_{int}, is proportional to the integrated intensity given by,

$$NP(X,Y) = \frac{\lambda T_{\text{int}}}{hc} P(X,Y) \tag{39}$$

$$NP(X,Y) = \frac{\lambda T_{\text{int}}}{hc} P_x^2 \left[\left(I_{LO}(X,Y) + I_s(X,Y)\right) + 2\sqrt{I_{LO} I_s}\,\text{sinc}(f_{spx} P_x)\,\text{sinc}(f_{spy} P_x) \cos\left[2\pi\left(f_{spx} X + f_{spy} Y\right)\right]\right] \tag{40}$$

The detection of photons by the Sensors Unlimited camera array is corrupted by noise. We will consider the following noise sources:

- Photon shot noise (We expect LO shot noise to be the dominant random, temporal noise source)
- Photo-response non-uniformity (Probable significant fixed, deterministic noise source)
- Pixel crosstalk (Will limit sensitivity to high spatial frequency irradiances)
- Dark current non-uniformity (Could be a significant fixed, deterministic noise source)
- Dark current shot noise (Probably insignificant compared to LO shot noise)
- Thermal noise (Probably insignificant compared to LO shot noise)
- Row noise (Fixed and temporal components exist)
- Column noise (Fixed and temporal components exist)
- Quantization noise

Presently fixed, deterministic noise sources (such as non-uniform LO illumination) limit camera sensitivity more than the noise sources described above. Additionally, most of the noise sources described above are not specified by Sensors Unlimited and will need to be experimentally measured. Only when the deterministic noise sources are eliminated and the SU camera characteristics measured and incorporated into the model can we hope to have experimental results that correlate with a theoretical model based on the noise sources described above.

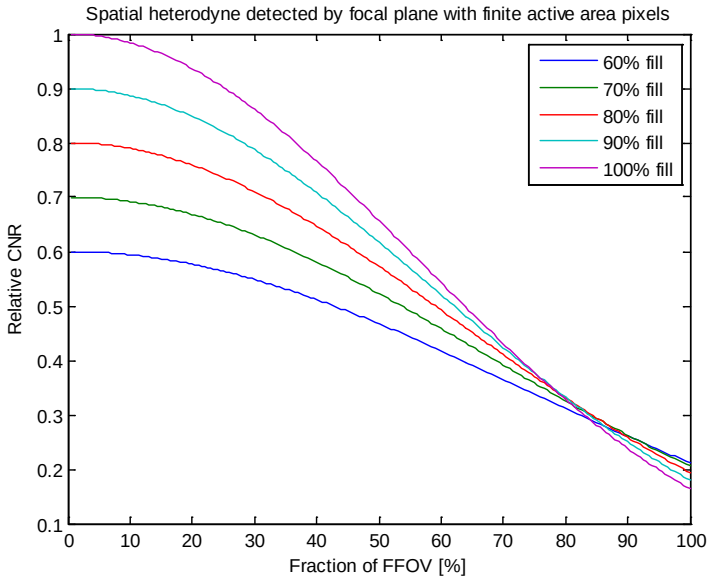

Figure 47: Relative CNR for Different Camera Fill Factors

A.6 Outdoor Range and Atmospheric Turbulence

Atmospheric turbulence can produce undesirable effects such as beam spreading, beam wander, loss of spatial coherence, temporal phase fluctuations, and scintillation. Because coherent detection is required for the IMAGE testbed synthesis algorithm, spatial beam coherence is especially important. Both spatial coherence and mean irradiance are second order moments of the optical field that can be derived in the cases of weak-fluctuation using the Rytov method. Analytical expressions for the spatial coherence diameter of both plane and spherical waves in the inertial sub-range are given by the expressions,

$$r_{0,plane} = 2.1\left(1.46C_n^2 k^2 L\right)^{-3/5} \tag{41}$$

$$r_{0,spherical} = 2.1\left(0.55C_n^2 k^2 L\right)^{-3/5} \tag{42}$$

where C_n^2 is the constant structure index, k is the wave number, and L is the propagation path length.

An analytical expression for the spatial coherence diameter of a collimated Gaussian beam wave valid for the inertial sub-range in the weak-fluctuation regime is given by,

$$r_{0,Gaussian,weak} = 2.1\left[\frac{8}{3\left(a + 0.618\Lambda^{11/6}\right)}\right]^{3/5}\left(0.55C_n^2 k^2 L\right)^{-3/5}, \tag{43}$$

where a is related to the Gaussian beam refraction parameter and Λ is the Gaussian beam diffraction parameter.

The path to the proposed 7Km range is a case of moderate-to-strong strong turbulence. The spatial coherence diameter of a collimated Gaussian beam in the strong fluctuation regime is greater than the coherence diameter of the same beam predicted using the weak fluctuation theory. Andrews and Phillips[36] derive the expression for the spatial coherence diameter of the collimated Gaussian beam using the techniques of effective beam parameters,

$$r_{0,Gaussian,strong} = 2.1\left[\frac{8}{3\left(a_e + 0.618\Lambda_e^{11/6}\right)}\right]^{3/5}\left(0.55C_n^2k^2L\right)^{-3/5}, \quad (44)$$

where a_e and Λ_ε are effective Gaussian beam parameters. The atmospheric coherence parameter, r_0 in the inertial sub-range for plane, spherical, and 7.6cm Gaussian beams for the proposed 7Km VA Hospital range path is plotted in Figure 48 below.

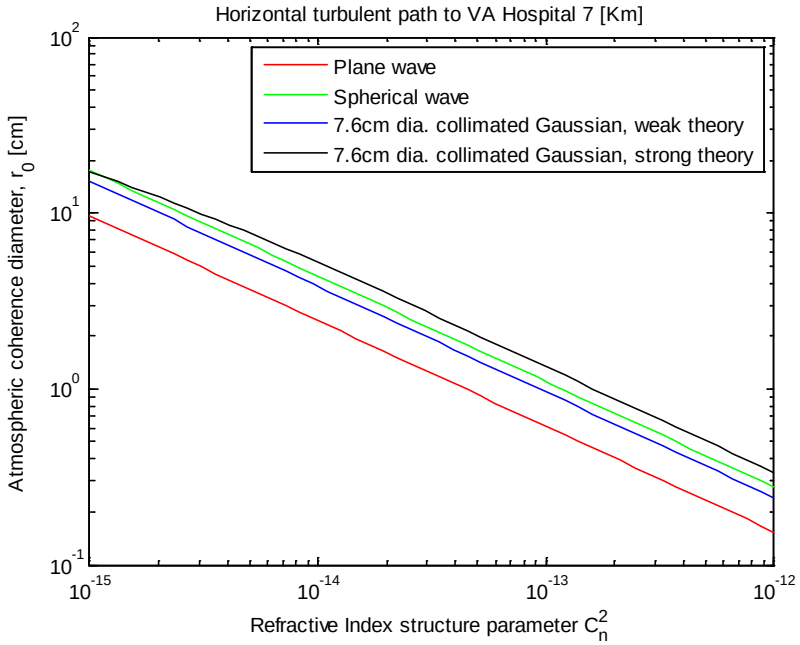

Figure 48: Atmospheric Coherent Diameter vs. Refractive Index Structure Parameter

In order to avoid the need for AO atmospheric compensation within a sub-aperture, the coherence diameter must be greater than the 5cm diameter of the sub-apertures. Assuming a spherical wave propagating back from the diffuse target, the coherence diameter exceeds the sub-aperture diameter when the path constant index structure parameter, $C_n^2 < 7\text{x}10^{-15}$.

Additionally, temporal phase fluctuations occur in the beam due to turbulence. Assuming a static target, these temporal phase fluctuations will limit the maximum temporal pulse width that can be used for the coherent field measurement required for aperture synthesis. The Greenwood time constant is the period over which atmospheric turbulence is essentially frozen and sets the limit on the maximum pulse width. The Greenwood time constant for an atmosphere with a uniform C_n^2 profile and constant crosswind velocity is given by[36],

$$\tau_0 = \frac{0.32r_0}{V_\perp} \quad (45)$$

where r_0 is the spatial coherence diameter and V_b is the crosswind velocity

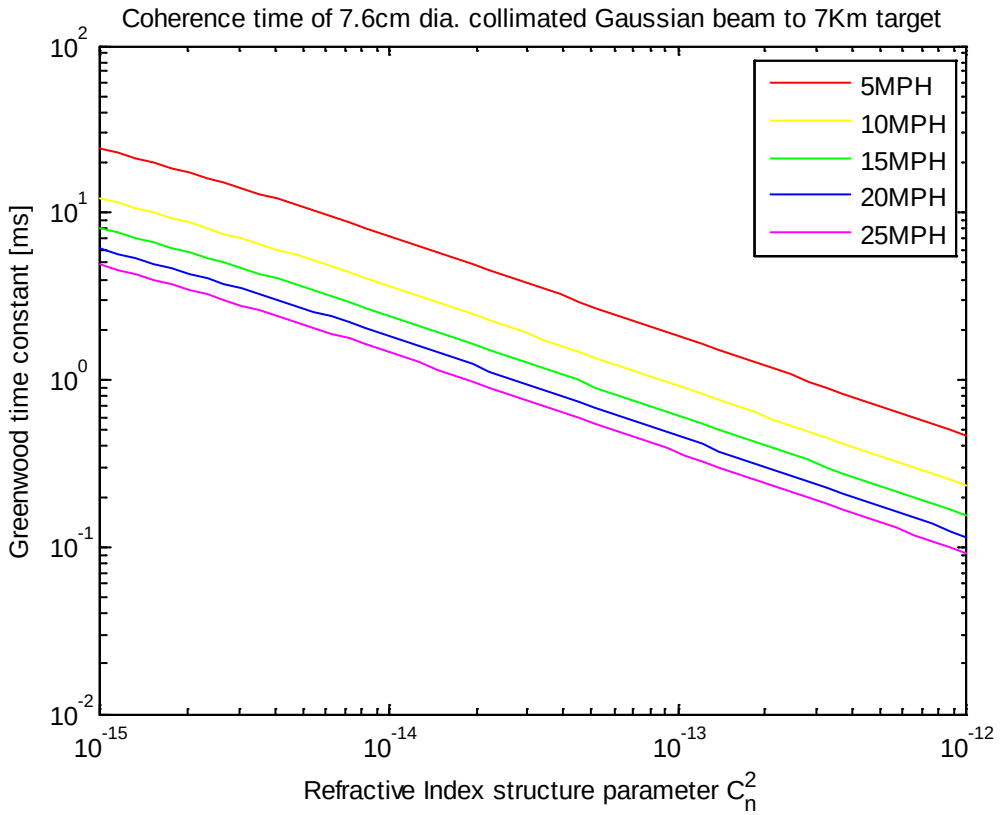

Figure 49: Greenwood Time Constant vs. Refractive Index Structure Parameter

The Greenwood time constant or a selection of wind velocities is plotted in Figure 49. If a continuous wave source is used, the Greenwood time constant limits the detector integration time. For the weak turbulence, $C_n^2 < 7x10^{-15}$, required for spatial coherence across a sub-aperture, the Greenwood time constant exceeds 1ms for winds up to 25MPH. Therefore, we expect that 1ms pulse widths will be sufficiently narrow for coherent field measurements.

The IMAGE testbed will illuminate the FOV in the target plane with a 3" diameter collimated Gaussian beam in a bi-static transmitter. Using the expression from Andrews and Phillips[36] for the long term spot size of a collimated Gaussian beam,

$$W_{LT} = W\sqrt{1+1.63\sigma_R^{\frac{12}{5}}\Lambda} \tag{46}$$

The atmospherically induced beam spread in weak turbulence, $C_n^2 < 7x10^{-15}$, is less than 50cm at the 7Km range. Therefore, the IMAGE testbed will be able to transmit a slightly diverging Gaussian beam to achieve the desired beam footprint.

A.7 Range Hall Collimator Design

The LOCI 61cm collimator that was characterized by Mr. Jan Servaites of AFRL. LOD took Mr. Servaites' parameters and inputted them into a Zemax optical design code. The wavefront errors are illustrated in Figure 50 on the left. For comparison a photo of the mirror is shown again on the right.

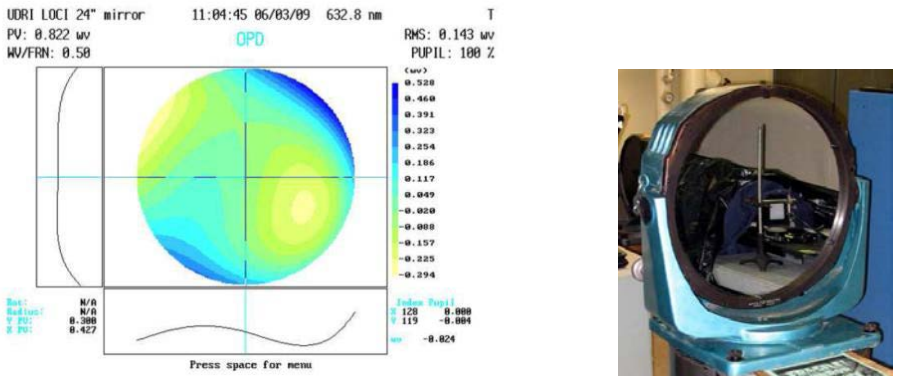

Figure 50: LOCI 61cm spherical collimator mirror and Wavefront Error

The specifications for this mirror in the Zermax layout are shown in Figure 51 below. The data from Mr. Servaites was inputted by LOD into the Zemax program. The wavfront errors and MTF for the mirror is shown in the figure.

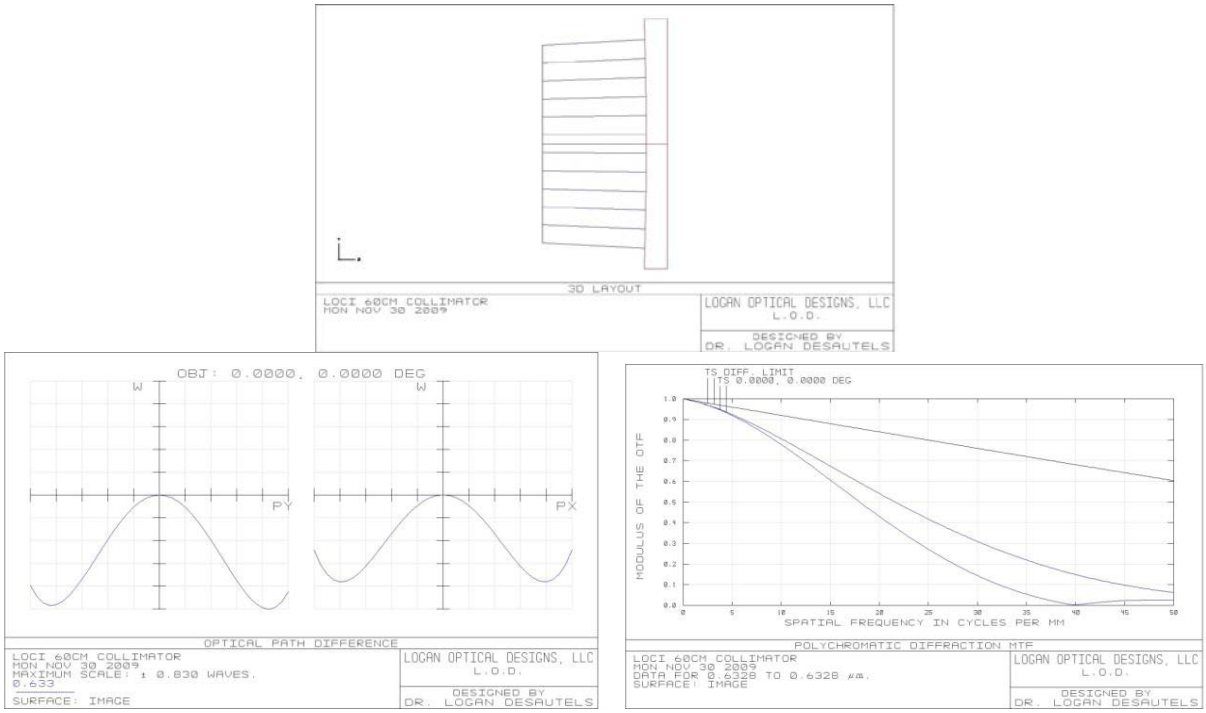

Figure 51: Collimator Optical Measurements

((top) Zemax Layout of the LOCI collimator, (bottom left) 61cm OPD that matches wavefront error, (bottom right) MTF plot of the 61cm mirror)

A.7.1 Collimator and Eyepiece Designs

The collimator model was next incorporated with multiple eyepiece designs. A custom eyepiece was first designed then LOD designed an off-shelf cost effective eyepiece. Both eyepieces are presented here, but only the cost effective eyepiece is shown in the collimator model.

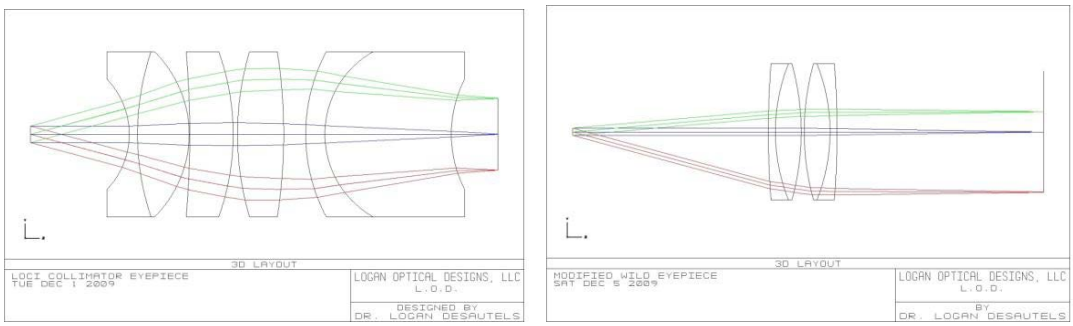

Figure 52: (left) Custom Eyepiece; (right) COTS Eyepiece from Newport

Figure 52 shows both of the LOD eyepiece designs. They are configured as a telecentric lens system, but can also be arranged to provide non-parallel rays at the image plane (to the right of each lens). This is better shown in the collimator-eyepiece design below. Dr. Ed Watson provided input that a larger scene (image plane) was needed thus the telecentric configuration was not desired. The amount of spread (or FOV) can be selected simply by moving the lens system closer or further from the stop (to the right of the lens).

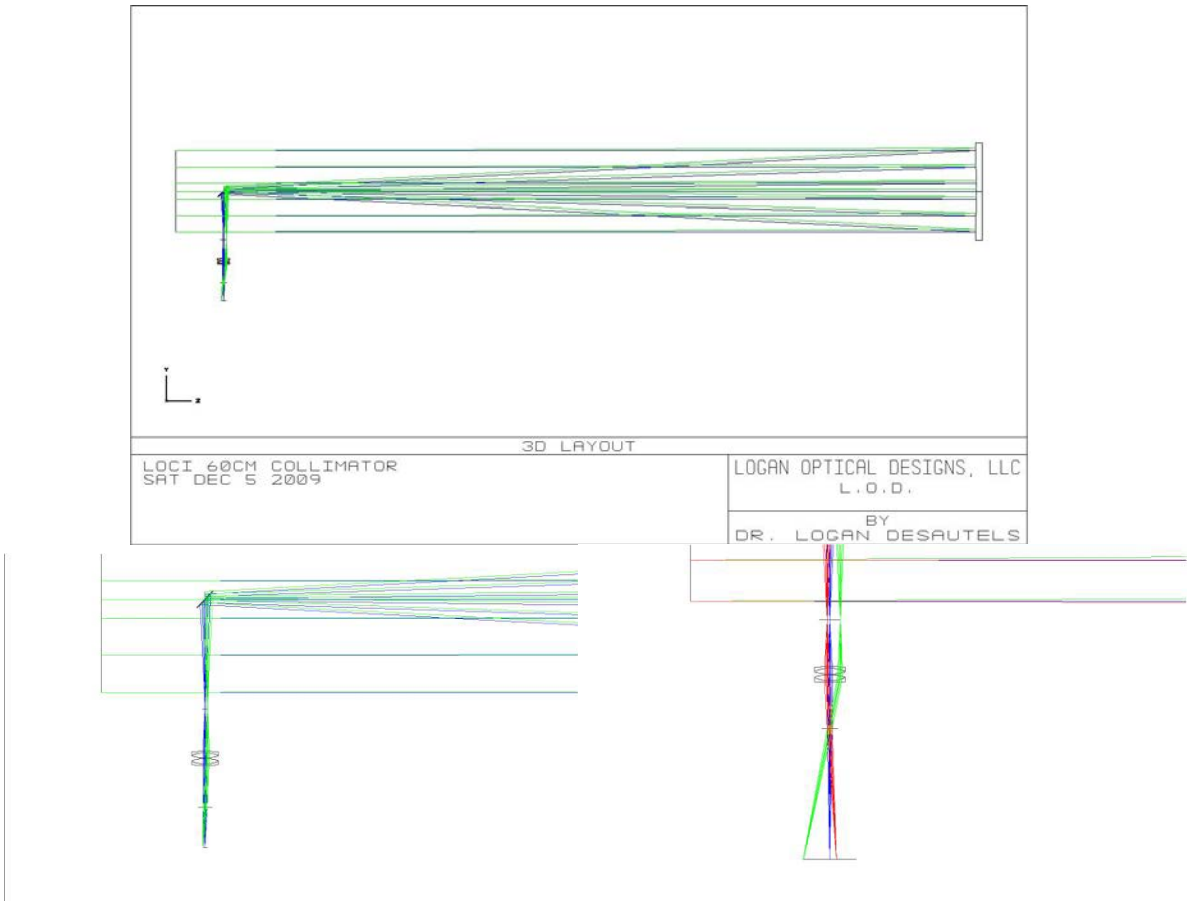

Figure 53: Collimator Optical Design with Eyepiece

((top) LOD collimator using the off-shelf eyepiece; (bottom left) Eyepiece telecentric configuration; (bottom right) Eyepiece in wide angle configuration.)

Lens Part No.	Manufacture	Focal Length	Thickness 1550nm	Thickness 532nm	Angle
LOCI 61cm Collimator	SOR	499.91cm	470cm	470cm	0°
4” Flat Mirror	TBD	Infinity	33.5cm can vary	33.5cm can vary	45°
PAC095	Newport	250mm	0.17cm	0.17cm	0°
PAC095	Newport	250mm	75.1cm varies with 33.5cm	73.5cm varies with 33.5cm	0°

Table 10: Collimator and COTS Eyepiece Specifications

The collimator with lens designs inserted is illustrated in a Zemax design in Figure 53. It can be used for 532nm or 1.55nm simply by adjusting the lens separation as shown in Table 10. The compact range is an alternative choice for making images over effective long ranges without requiring the laser power to image over those long ranges. Many scenarios for imaging and multiple receiver and transmitter design strategies could be explored using this much cheaper system.

Appendix B: LIST OF ACRONYMS, ABBREVIATIONS, AND SYMBOLS

AFIT = Air Force Institute of Technology
AFOSR = Air Force Office of Scientific Research
AOM = Acousto-Optic Modulator
BSDF = bidirectional scattering distribution function
cm = centimeters
CCD = Charge Coupled Device
COTS = Commercial Off the shelf
DAGSI = Dayton Area graduate Studies Institute
DH = Digital holography
DHI = digital holographic interferometry
DHM = digital holographic microscopy
DHT = digital holographic tomography
DRO = Doubly reflective Optics
EDFA = Erbium-doped Fiber Amplifier
EOBS = electro-optic beam switch
ErYb = Erbium/Ytterbium
FPA = Focal Plane Array
GHz = gigahertz
HAL = Holographic Aperture LADAR
Hex = Hexagon
HSLD = Highly Stable Laser Diode
IMAGE = Innovative Multi-Aperture Gimbal-less Electo-optical
InGaAs = Indium Gallium Arsenide
InSb = Indium Antimonide
ITAR = International Traffic in Arms Regulations
Km = kilometer
LADAR = Laser radar
LFM = Linear frequency modulation
Lidar = Light detection and ranging
LO = Local oscillator
LOCI = LADAR and Optical Communications Institute
LWIR = Long wave Infrared
MFSP = Multi-frequency Stretched Processing
MHz = megahertz
μJ = microJoule
mm = millimeter
μm = micrometer
ms = millisecond
MTF = Modulation Transfer Function
mW = Milliwatt
MWIR = Mid wave Infrared
nm = namometer
ns = nanosecond
OPA = Optical Parametric Amplifier

OPG = Optical Parametric Generation
OPGaAs = Orientationally Patterned Gallium Arsenide
OPO = optical parametric oscillation
OSH = Optical scanning holography
PC = Personal Computer
PPLN = periodically-poled lithium niobate
PSLR = Peak-to-side-lobe ratio
Radar = Radio detection and ranging
Rx = Receiver
SAR = Synthetic Aperture LADAR
SF-LFM = Sparse Frequency - Linear frequency modulation
SIMS = secondary ion mass spectrometry
SNR = Signal to Noise Ratio
SP = Stretch Processing
SRO = Singly reflective Optics
Sq. ft. = square feet or square foot
THz = Terahertz
Tm,Ho:YLF = Thulium, Holmium doped Lithium Yttrium Fluoride
Tx = Transmitter
UD = University of Dayton
USB = Universal Serial Bus
VAMC = Veterans Administration Medical Center
VF = Variable frequency
YAG = Yttrium Aluminum Garnet

References

[1] http://en.wikipedia.org/wiki/Aperture_synthesis, downloaded July 10, 2012
[2] P. F. McManamon and W. Thompson, " Phased Array of Phased Arrays (PAPA) Laser Systems Architecture, IEEE Aerospace refereed conference, March 2002.
[3] P. F. McManamon and W. Thompson," Phased Array of Phased Arrays (PAPA) Laser Systems Architecture", Fiber and Integrated Optics **22**, 79-88 (2003).
[4] P.F. McManamon, "A Review of LADAR – A Historic, yet Emerging, Sensor Technology with Rich Phenomenology", Optical Engineering, June, 2012.
[5] J. C. Marron and R. L. Kendrick, "Distributed aperture active imaging," Proceedings of SPIE **6550**, 65500A-7 (2007).
[6] D. Gabor, "A new microscopic principle," Nature 161, 777 (1948).
[7] T. H. Maiman, "Stimulated Optical Radiation in Ruby," Nature **187**, 493 (1960).
[8] A. White and J. Rigden, "Continuous gas maser operation in the visible," Proc. IRE **50**, 1697 (1962).
[9] E. N. Leith and J. Upatnieks, "Wavefront reconstruction with diffused illumination and three-dimensional objects," JOSA 54, 1295 (1964).
[10] E. N. Leith and J. Upatnieks, "Reconstructed Wavefronts and Communication Theory," Journal of the Optical Society of America **52**, 1123 (1962).
[11] E. N. Leith and J. Upatnieks, "Wavefront Reconstruction with Continuous-Tone Objects," Journal of the Optical Society of America **53**, 1377 (1963).
[12] J. W. Goodman, "Digital Image Formation From Electronically Detected Holograms," Applied Physics Letters **11**, 77 (1967).
[13] T. S. Huang, "Digital holography for quantitative phase-contrast imaging," Optics Letters **59**, 1335 (1971).
[14] J. Rigden and E. Gordon, "The granularity of scattered optical maser light," in Proc of the Institute of Radio Engineers **133**, 2367-2368 (1962).
[15] S. Lowenthal and H. Arsenault, "Image Formation for Coherent Diffuse Objects: Statistical Properties," Journal of the Optical Society of America **60**, 1478 (1970).
[16] R. A. Muller and A. Buffington, "Real-time correction of atmospherically degraded telescope images through image sharpening," Journal of the Optical Society of America **64**, 1200 (1974).
[17] J. C. Paxman, RG and J. C. Marron, "Aberration correction of speckled imagery with an image-sharpness criterion," Proc. of SPIE Statistical Optics. **976**, 37 (1988).
[18] D. Rabb, D. Jameson, A. Stokes, and J. Stafford, "Distributed aperture synthesis," Optics Express, **18**, 10334 (2010).
[19] N. J. Miller, J. W. Haus, P. F. McManamon, and D. Shemano, "Multi-aperture coherent imaging," in Defense, Security and Sensing, Proc. SPIE 8052, (2011).
[20] N. J. Miller, J. W. Haus, P. F. McManamon, and D. Shemano," Multli-aperture coherent imaging" Acquisition, Tracking, Pointing, and Laser Systems Technologies XXV Proc. Of SPIE **8052**, 805207 (2011)
[21] J.C. Marron and R.L. Kendrick; "Distributed Aperture Active Imaging," Laser Radar Technology and Applications XII, edited by Monte D. Turner and Gary W. Kamerman, Proc. of SPIE **6550**, 65500A (2007).
[22] http://en.wikipedia.org/wiki/File:Shack_Hartmann_WFS_lensletarray.svg, downloaded July 26, 2012.

[23] B. C.Platt and R. Shack, "History and Principles of Shack-Hartmann Wavefront Sensing". Journal of Refractive Surgery 17 (5). PMID 11583233 (October 2001).
[24] R. V. Shack, "Production and use of a lenticular Hartmann screen". Journal of the Optical Society of America **61**, 656 (1971).
[25] R. V. Chimenti, M. P. Dierking, P. E. Powers and J. W. Haus, "Multiple chirp sparse frequency LFM LADAR signals", Proc. SPIE **7323**, 73230N (2009). http://dx.doi.org/10.1117/12.817865
[26] N. Levanon and E. Mozeson. *Radar Signals* . (John Wiley & Sons, Hoboken, NJ, 2004).
[27] R. V. Chimenti, M. P. Dierking, P. E. Powers, and J. W. Haus, "Sparse frequency LFM LADAR signals," Opt. Express **17**, 8302 (2009).
[28] R. V. Chimenti, M. P. Dierking, P. E. Powers, J. W. Haus, and E. S. Bailey, "Experimental verification of sparse frequency linearly frequency modulated LADAR signals modeling," Opt. Express **18**, 15400 (2010).
[29] M. Skolnik, *Radar Handbook*, Third Edition. New York: McGraw-Hill (2008).
[30] M.-C. Amann, T. Bosch, R. Myllylä, and M. Rioux, "Laser ranging: a critical review of usual techniques for distance measurement," Opt. Eng. **40**, 10 (2001).
[31] Z. W. Barber, W. R. Babbitt, B. Kaylor, R. R. Reibel, and P. A. Roos, "Accuracy of active chirp linearization for broadband frequency modulated continuous wave LADAR," Appl. Opt. **49**(2), 213 (2010).
[32] K. W. Holman, D. G. Kocher, and S. Kaushik, "MIT/LL development of broadband linear frequency chirp for high-resolution LADAR," Proc. SPIE 6572, 65720J.8 (2007).
[33] A. Vasilyev, N. Satyan, S. Xu, G. Rakuljic, and A. Yariv, "Multiple source frequency-modulated continuous wave optical reflectometry: theory and experiment," Appl. Opt. **49**, 1932 (2010).
[34] R. Schneider, P. Thurmel, and M. Stockmann, "Distance measurement of moving objects by frequency modulated laser radar," Opt. Eng. **40**, 33 (2001).
[35] M. Umar Piracha, D. Nguyen, D. Mandridis, T. Yilmaz, I. Ozdur, S. Ozharar, and P. J. Delfyett, "Range resolved lidar for long distance ranging with sub-millimeter resolution," Opt. Express **18**, 7184 (2010) http://www.opticsinfobase.org/oe/abstract.cfm?URI=oe-18-7-7184
[36] L. C. Andrews and R. L. Phillips, *Laser beam propagation through random media,* (SPIE Press, Bellingham, Washington, 1998).